UNIVERSIDAD DE VALLADOLID

ESCUELA DE INGENIERIAS INDUSTRIALES

Grado en Ingeniería Mecánica

THE POTENTIAL OF HARVESTING ENERGY FROM MALTESE ROADS USING TEG MODULES

Autor:

Martínez Arranz, Jaime

Responsable de Intercambio en la Uva:

Francisco Javier Rey Martínez

University of Malta

Valladolid, Junio 2021.

TFG REALIZADO EN PROGRAMA DE INTERCAMBIO

TÍTULO: The potential of harvesting energy from Maltese roads using TEG modules

ALUMNO: Jaime Martínez Arranz

FECHA: 02/07/2021

CENTRO: Institute for sustainable energy

UNIVERSIDAD: University of Malta

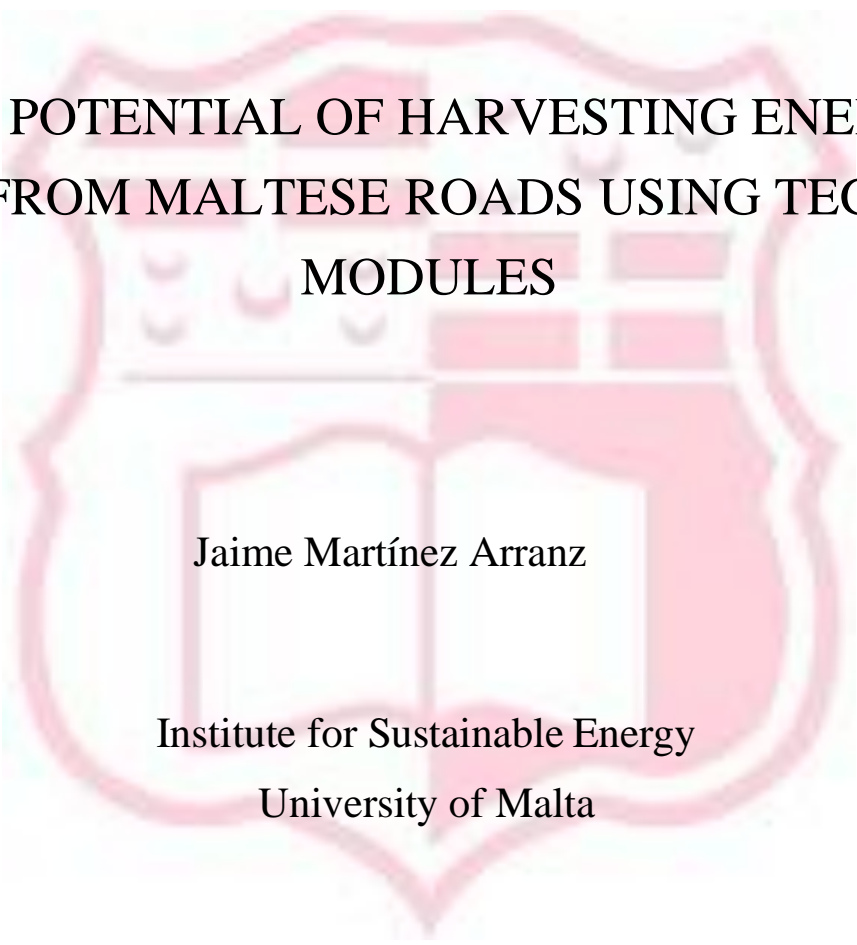TUTOR: Charles Yousif

RESUMEN:

Las economías mundiales son dependientes del precio y disponibilidad de los combustibles fósiles. Con este contexto, los países deben buscar nuevas alternativas para generar electricidad y así reducir la contaminación que conlleva esta situación.

El objetivo de este trabajo de final de grado es evaluar el potencial de los generadores termoeléctricos (TEGs) en tres diferentes materiales: asfalto, hormigón y caliza. Para ello, dos set ups fueron construidos para testear los módulos TEG bajo las condiciones establecidas en el laboratorio.

La parte final del proyecto analiza la factibilidad de estos módulos en Malta.

PALABRAS CLAVE:

TEG, Harvesting, Temperature difference, Energy, Modules

THE POTENTIAL OF HARVESTING ENERGY FROM MALTESE ROADS USING TEG MODULES

Jaime Martínez Arranz

Institute for Sustainable Energy

University of Malta

THE POTENTIAL OF HARVESTING ENERGY FROM MALTESE ROADS USING TEG MODULES

Jaime Martínez Arranz

A dissertation presented at the

Institute for Sustainable Energy of the University of Malta,

in partial fulfilment of the requirements for the degree of

Bachelor of Mechanical Engineering

at the

Universidad de Valladolid, Spain,

under the Erasmus Plus Student Exchange Programme 2020/21

DECLARATION

No portion of the work referred to in the dissertation has been submitted in support of

an application for another degree or qualification of this or any other university or other

institute of learning.

Signature of Student   Name of Student

_____   __Jaime Martínez Arranz__

June 2021

COPYRIGHT NOTICE

ABSTRACT

World economies are dependent on the cost and availability of fuel because the 85% of the electrical energy generation comes from fossil fuel combustion. Besides, on yearly basis the world's energy demand is gradually increasing. This context leads countries to find new ways of generating electrical energy to reduce the climate change repercussions this situation is carrying. Renewable energies are the best choice to achieve this objective. In the case of Malta, its Mediterranean climatic conditions allow for the exposure of long hours of sunlight, which should be taken into advantage. Thermoelectric generators (TEGs) are devices based on the Seebeck effect technology that benefit from solar heat to generate electricity. These modules convert heat directly into electricity. The bigger the temperature difference is between the surfaces of the TEG the more power is generated.

The purpose of this dissertation is evaluating the power generation of TEG modules in asphalt, concrete and limestone for a possible application in built up areas to power up information booths, which can be used to nudge people for sustainable mobility, and, analyse the possible temperature difference that can be created during the months of March, April and May in Malta.

Two different setups were built to test the performance of two TEG modules under the conditions set in the laboratory. Different resistances were applied in the setups to test which perform better. Data from other setups is provided in the literature review and compared with the results obtained in Chapter 4.

Furthermore, an analysis of the temperature data recordings from the three materials is shown in the results and analysis Chapter. The results obtained were satisfactory although the modules generated electricity for only a few hours during the day.

TABLE OF CONTENTS

ACKNOWLEDGEMENTS

LIST OF FIGURES

LIST OF TABLES

LIST OF ABREVIATIONS

ΔT   Temperature difference

EU   European Union

P   Power generated

PV   Photovoltaic

RTG   Radioisotope Thermoelectric Generator

TEG   Thermoelectric generator

TRL   Technology Level Readiness

U   Generated Voltage

CHAPTER 1. INTRODUCTION

The growing demand for energy and the resulting pollution emissions are two major problems the world is facing in the 21st century. In order to achieve the objective of reducing greenhouse gas emissions set by the European Union (EU), the transition towards decarbonization of the energy model in developed countries will be necessary.

Moreover, the yearly demand of the world's energy keeps increasing with 75% of the energy produced coming from burning oil, gas and coal. In 2040, according to the International Energy Agency, the energy demand will increase by 30% from 2017 [1]. Figure 1 shows the evolution of the world's energy consumption by energy source between 1990 and 2040.
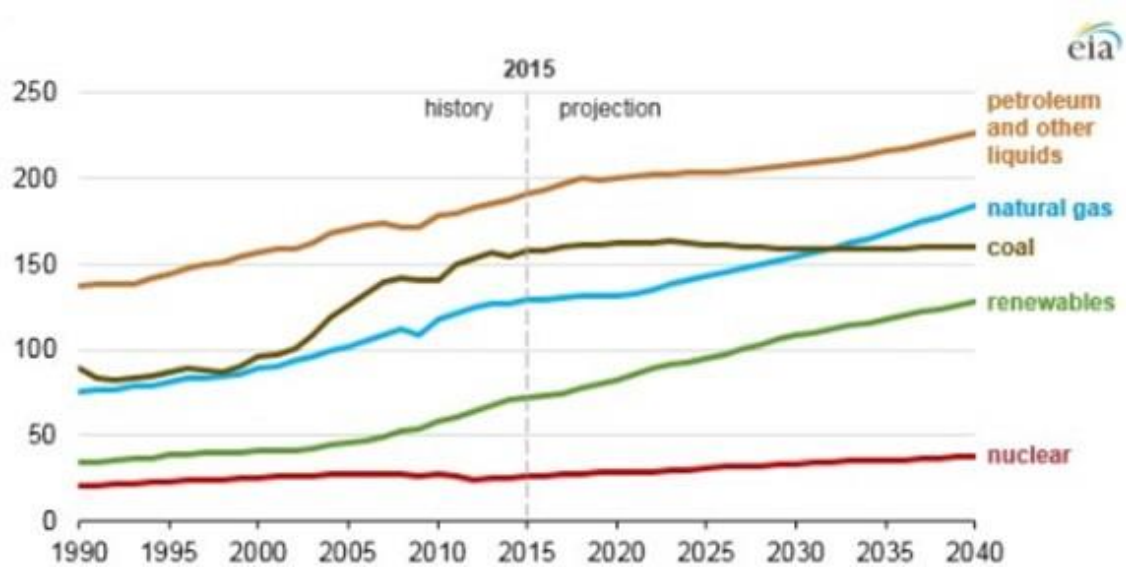
Figure 1. World energy consumption by energy source (1990-2040) in quadrillion British thermal units [2]

This global situation leads to the search for new ways to generate energy in a renewable and environmentally-benign way. In fact, a demonstration project has just been announced, whereby at a new pavement in Rabat (Malta) will be used to generate electricity through embedded flat photovoltaic modules [3].

This dissertation focuses on the function that the road infrastructure can play besides being used by vehicles and pedestrians. For instance, pavements which are normally used

only for walking can contribute to clean generation of electricity through solar photovoltaics or thermal to electric modules, thanks to their prolonged exposure to sunlight. The electricity generated by this technology can be used to power information booths that would nudge people for sustainable mobility encouraging them to use more frequently public transport or cycling and also, walking as an active way of moving.

The principal goal of this dissertation is to analyze the performance of the thermoelectric generator (TEG) modules and check their potential applications on the roads.

The objectives of the dissertation are:

- Investigate the potential of power generation from a sample TEG module at Proof-of-Concept level in the laboratory, which is equivalent to Technology Level Readiness (TRL 3).
- Identify the issues concerning with large-scale deployment of TEG modules on the road.
- Analyse the temperature levels of three typical pavement materials (asphalt, concrete, limestone), as well as the top surface and below surface -temperature gradients.

The dissertation consists of five chapters. Chapter 1 set the scene for the project and provides the aims and objectives of the dissertation. In Chapter 2, a literature review is carried out on the thermoelectric effect technology, past experiments based on pavements and current applications of this technology. Chapter 3, presents in detail the methodology used for the experiments that have been carried out in the laboratory. Chapter 4 includes the results and analysis of the laboratory simulations as well as the temperature data obtained from the Institute for Sustainable Energy. Finally, Chapter 5 incudes the conclusions of the results obtained. In addition, recommendations for additional research are given.

CHAPTER 2. LITERATURE REVIEW

Currently, 85.45% of the electrical energy generated comes from fossil fuel combustion, which makes world economies significantly dependent on fuel availability and costs [4]. This is also leading to irreversible climate change repercussions as evidence by extensive polar ice melting and the gradual rise of the sea level. In addition, extreme weather events such as flash floods, heat waves and drought are becoming more frequent [5].

Figure 2 represents the global temperature increase over the last century, which is a direct consequence of the greenhouse gases that are emitted when fossil fuels are burnt.
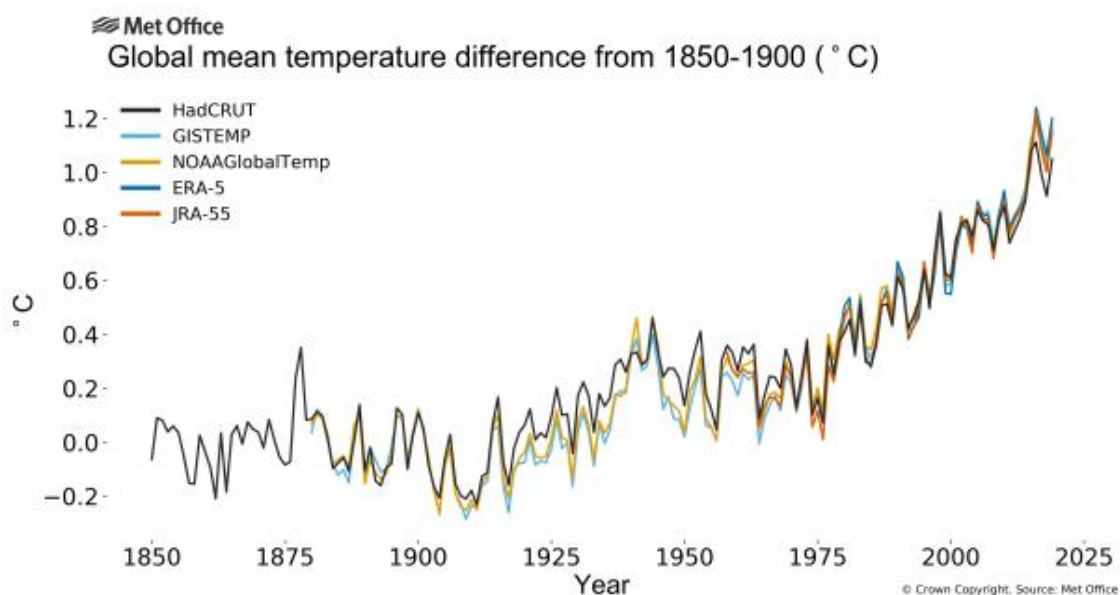
Figure 2. Global Average Temperature from 1850-1900 to 2025. Source: HadCRUT, GISTEMP, NOAAGlobalTemp, ERA-5, JRA-55 [6]

As a response to reducing global warming, year on year renewable energies are becoming more popular. As an example, solar energy is a good alternative compared to energy generated by fossil fuels for electricity generation.

Governments are trying to find different ways of creating a sustainable economy to reduce the irreversible environmental damage. In the case of Malta and as requested by the EU, a national energy and climate plan for 2030 has been devised [7]. The objectives that have been proposed to reduce climate change are the following:

- Achieve a diversification in ways of producing energy to reduce the dependence on the importation of oil.

- Increase the use of renewable sources and natural gas to reduce greenhouse gas emissions and carbon footprint in Malta.

- Improve and strengthen Malta´s security of supply and back up fuel storage capacity.

- With the aid of incentives stimulate investment in renewable energy sources.

- Enhance Malta´s generation capacity to achieve a higher efficiency while investing in natural gas infrastructures.

Increasing the use of renewable energy sources is one of the main objectives that Malta´s plan has [7], and with that, it is also intended to encourage sustainable mobility which refers to any means of transport that has a low impact on the environment. In fact, in 2016 Transport Malta (the regulator) published the National Transport Strategy and Masterplan [8].

Solar photovoltaics and wind energy are the most popular ways to generate renewable energy, which many countries are already adopting. However, one renewable way of obtaining energy, which is still at its infancy, is with thermoelectric generators (TEGs) which are based on the thermoelectric effect. These devices benefit from solar heat to generate electricity and can be used in built-up areas.

Urban areas attract populations, which need mobility, as a result the road system involves complex networks. For instance, Malta, in 2015, had a 40% of its land built up according to Times of Malta [9]. Figure 3 shows an aerial photo of mainland Malta with the built-up area being concentrated mostly to the eastern side of the island, where the majority of the Maltese population is concentrated. [10].

Figure 3. An aerial image of mainland Malta [11]

The purpose of this technology, with the TEG modules, is to take advantage of that built up area, particularly the pavements. Many different technologies have been tested in pavements such as piezoelectric, photovoltaic, TEG, hydraulic and electromechanical [12]. However, in the literature review, a deep research will be done about different experiments that have been carried out in the past using the TEG technology. These modules can have many different applications, but the research will be focused on the harvesting energy from pavements. At the end of the review of experiments, all the information collected will be studied and concluded to prepare the methodology for the experimental part of this project.

2.1 The Thermoelectric Effect

The thermoelectric process covers two effects that were discovered separately, the Seebeck effect and Peltier effect [13].

The Seebeck effect (Figure 4) was discovered in 1834 by a French physicist after the discovery of a German physicist in 1821, who observed that in a circuit formed by two different conductors, whose welded joints are in a media with different temperatures, a potential difference appears between them. This potential difference is a function of the nature of the conductors and the difference in temperatures. The greater the temperature gradient, the more is the energy generated. This is the phenomenon that we are going to focus on during this project.

The Peltier effect, which is basically the opposite of the Seebeck effect, consists of passing a continuous source of electrical energy, through a circuit formed by two different semiconductor N and P, heat will be generated at one junction while the other junction would cool down, as shown in Figure 5.
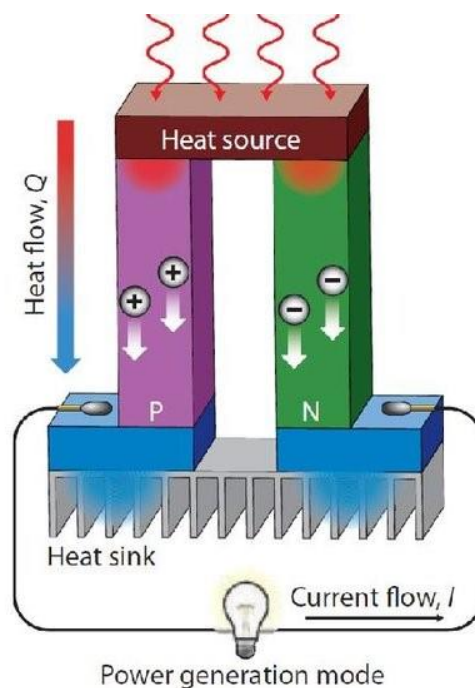
Figure 4. Seebeck effect. Power generation mode [14]

6
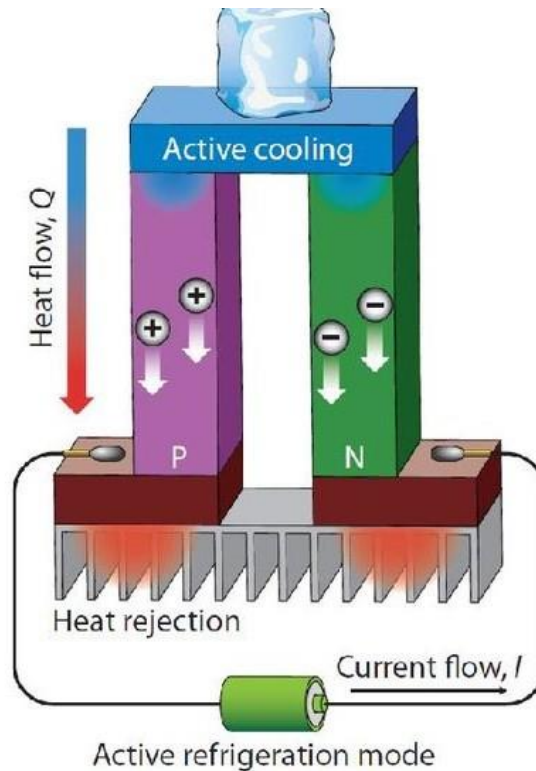
Figure 5. Peltier effect. Refrigeration mode [14]

2.2 Thermoelectric generators (TEGs)

The thermoelectric generators (Figure 6) are based on the Seebeck effect. They convert heat directly into electricity. Heat induces the circulation of an electrical current. To generate electricity through the thermoelectric effect a thermoelectric module and a temperature difference between both sides of the module are necessary. Since the circulation of current also generates heat migration, hot and cold sources must continuously supply and dissipate heat to maintain that difference [15]. Semiconductors are the materials most used for thermoelectric devices due to the higher efficiency they have compared to metals.
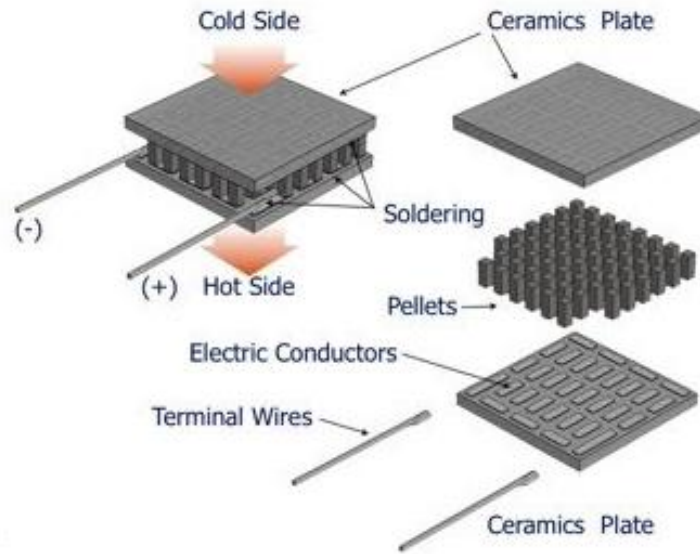
Figure 6. TEG parts [16]

The most common alloy used commercially are silicon germanium (SiGe), bismuth telluride (Bi₂Te₃) and lead telluride (PbTe) [17]. Recently, new material compositions have been investigated. Figure 7 shows a graphical abstract with different materials tested and its merit ZT, which is a way of evaluating the efficiency. These new materials that have been tested have a better efficiency but for higher temperature differences.
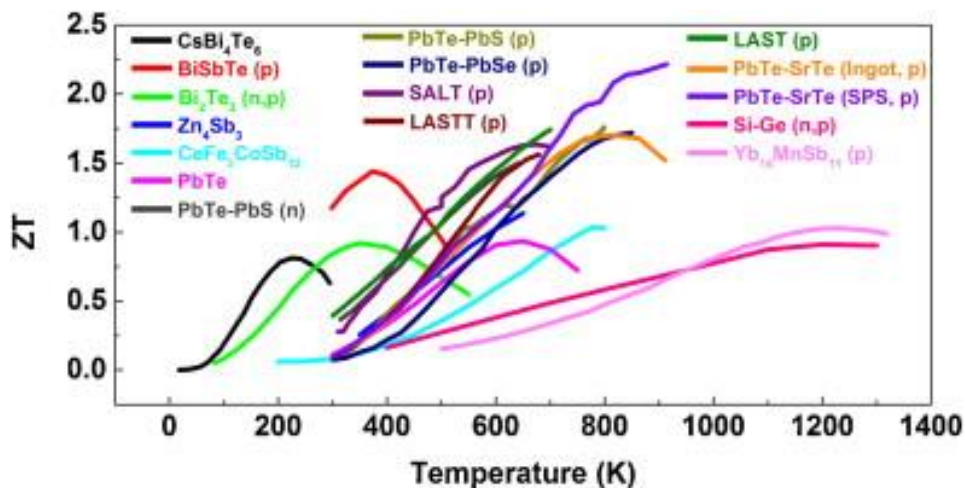
Figure 7. Graphical abstract of Merit ZT and Temperature [18]

8

Even so, the problem with the TEG modules is that they still have a very low conversion efficiency. The next formulae represent how to calculate the conversion efficiency of TEGs [19].

$$\mu_{max} = \frac{(T_H - T_C)}{T_H} \frac{\sqrt{1+(zT)_{avg}} - 1}{\sqrt{1+(zT)_{avg}} + (\frac{T_C}{T_H})} \qquad (1)$$

where - T_H is the hot side temperature (K)

- T_C is the cold side temperature (K)

- zT_{avg} is the average thermoelectric materials figure of merit.

Depending on the materials that the TEG has the zT_{avg} change [15].

$$zT_{avg} = \frac{\sigma S^2}{k} T \qquad (2)$$

where - σ is the electrical conductivity

- S or α is the Seebeck coefficient

- k is the total thermal conductivity (including electronic, lattice and bipolar)

- T is the absolute temperature which is calculated as $(T_H + T_C)/2$ (K)

It is also important to know the voltage that each TEG module will generate. This is called Seebeck voltage, which is defined as the open circuit voltage when there is no current flowing. When a junction of two dissimilar conductors is maintained at two different temperatures T_H and T_C, an open circuit voltage is developed [15]:

$$V_{OC} = \alpha_{p,n}(T_H - T_C) \qquad (3)$$

Where $\alpha_{p,n}$ is the Seebeck coefficient.

9

The Seebeck coefficient of the junction between two materials (p-type and n-type) is the same as the difference between the two absolute coefficients [15]:

$$\alpha_{p,n} \; = \; \alpha_p - \alpha_n \qquad\qquad (\,4)$$

2.3 A review of experiments

This section covers a review of past experiments focused on harvesting energy from pavements.

Most of the research on energy harvesting from road pavement has focused on three different technologies:

1) **Piezoelectric technology.** Piezoelectric materials are made up of multiple solid-state materials, which can generate electricity from mechanical vibrations that are cause by cars or persons passing over them. The problem described with this technology is the poor durability of the materials used when they are under repeated traffic load due to the mismatch in stiffness between the pavement and the piezoelectric materials [12]. For this reason, obtaining a high voltage is complicated. Nevertheless, many experiments have been carried out with this technology. In 2010, Zhao H, Yu J and Ling J [20] studied the application of cymbal piezoelectric transducers on road pavements, which generated 1.2 mW at 20 Hz from one vehicle passage. One year later, in 2011 Wischke M, Masur M Kroer M and Woias P [21], after a study on the application of piezoelectric modules in road pavements in tunnels, concluded that due to the vehicles suspensions, the vibrations generated were very low. In 2014, Hill D, Agarwal A and Tong N [22] studied the data provided by two companies, Innowattech and Genziko. The first company, presented a module with an energy generation of 5.76 J per vehicle, while Genziko presented an energy generation of 40 J. However, it was concluded that none of these companies had enough real-environmental validations.

2) **Photovoltaic technology.** This implies the replacement of traditional asphalt and concrete by solar panels on paved roads (which is similar to the case study in Rabat, Malta [3]). This way, they absorb the solar radiation and convert it into electricity. The main difficulties for solar panels are the necessity for developing a new solar panel with new requirements for use in road surface. It was concluded that due to the thin-film that solar cells are made of, these devices would be conditioned by external factors such as mechanical load and environmental conditions. Even so, in 2015 Julie and Scott Brusaw patented a design of a solar collector system to replace the upper layer of the road pavement. Each panel had an installed power of 36 W and measured 0.37 m^2. In fact, the creators assure an efficiency of the system of 11.2%, a value that has still to be confirmed scientifically [23].

3) **Thermoelectric technology.** By using thermoelectric generators (TEGs) on the pavement surface, part of the thermal energy is absorbed and converted into electricity. The main challenge of this technology is the low efficiency of power generation, that is dependent on the temperature difference between the surfaces of the TEG modules [12].

Despite, the different challenges that these technologies must face, the thermoelectric technology compared with piezoelectric and photoelectric modes, has more success in pavements. The electric energy can be directly converted from the thermal energy absorbed by road surface without changing pavement materials and structures [12].

The key to improving the efficiency of TEGs in the road is to maintain the highest temperature gradient possible. In the city of Xi'an, China in 2016 an experiment was conducted where the temperature was collected in two different seasons. The first one, in winter, December 8th and the second one, in summer, August 16th. In the next two Figures (8 and 9), the data obtained during these days is presented.
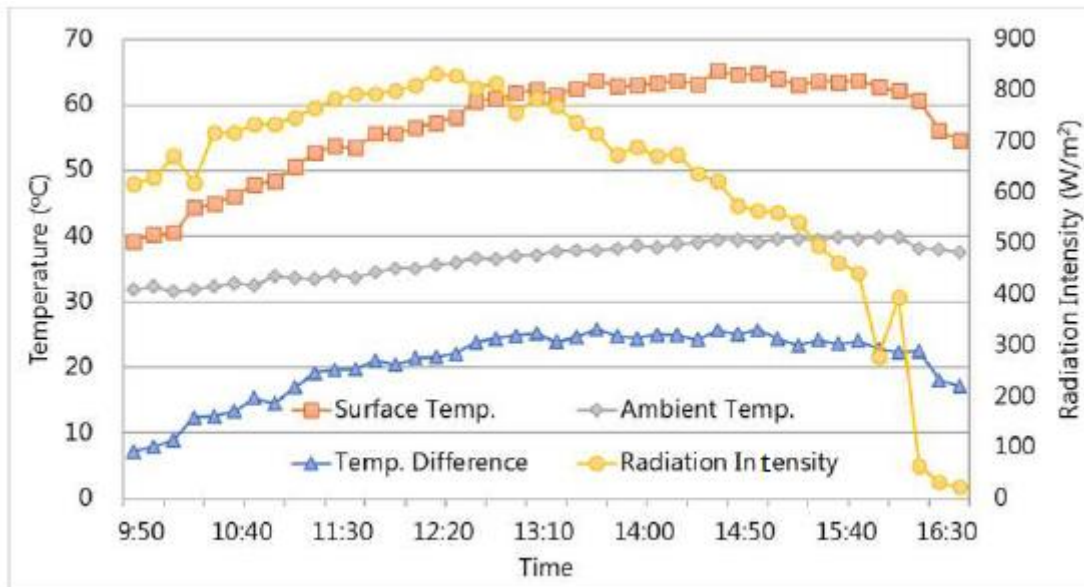
Figure 8. Display August 16th [12]
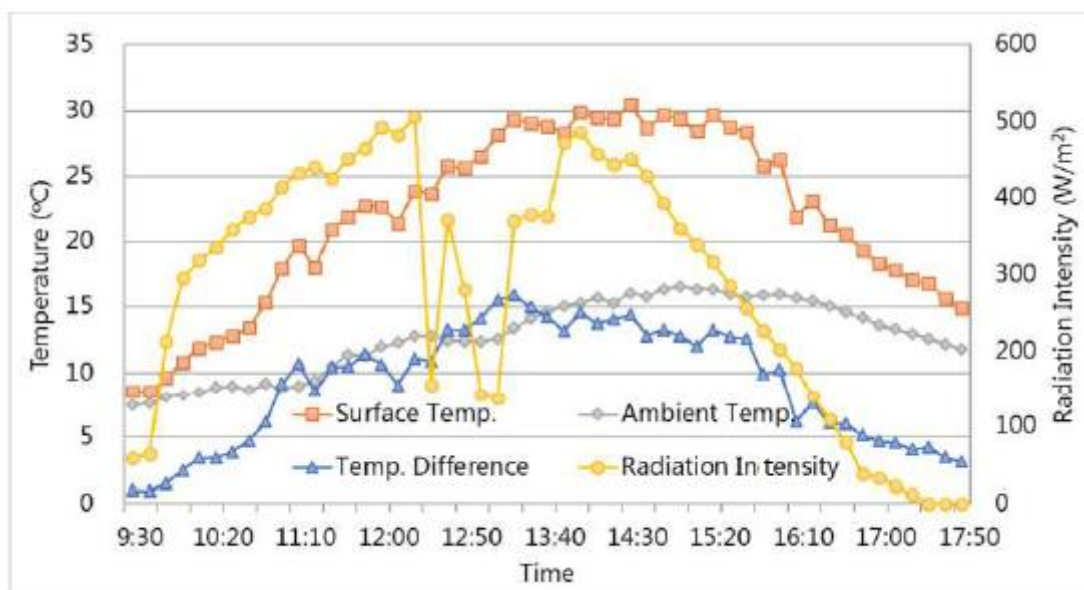
Figure 9. Display December 8th [12]

As illustrated in Figures 8 and 9, the different colors present the surface temperature, ambient temperature, temperature difference and radiation intensity, the highest ΔT registered between the surface and the ambient air is in August with around 25°C. In winter, the maximum ΔT registered was 16°C. Thus, it can be concluded that due to the

endothermic effect of asphalt pavement a ΔT will be present during a significant amount of time during the day regardless of the season [12].

Besides, this city of China with average ambient temperature of 14ºC is not located in the best climate zone. Conversely, Malta has an average temperature of 19ºC [24], and being situated at 36ºN of the Equator, its conditions are more suitable for the application of pavement thermoelectric technology.
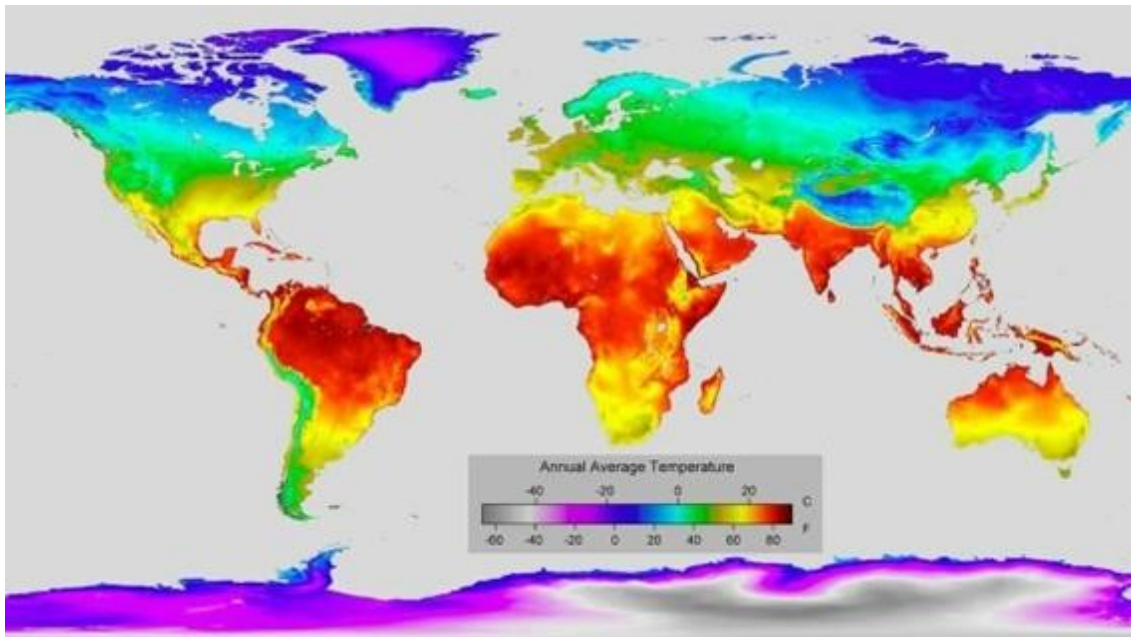
Figure 10. World map of annual average temperature [25]

Jiang, W, Yuan, D, Xu, S et al. (2017) created a slab made of asphalt to have an idea of the ΔT underneath the road surface. The dimensions of the slab were 300 mm x 300 mm x 100 mm. A total of 18 sensors were placed at different depths of the specimen. Figure 11 shows a scheme with the sensors and the slab experiment [12].
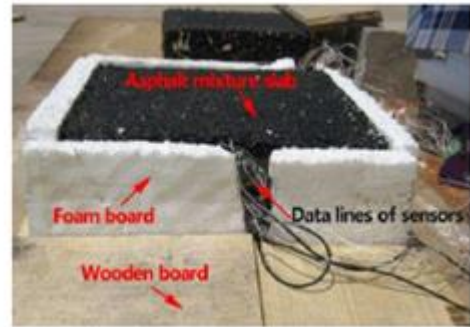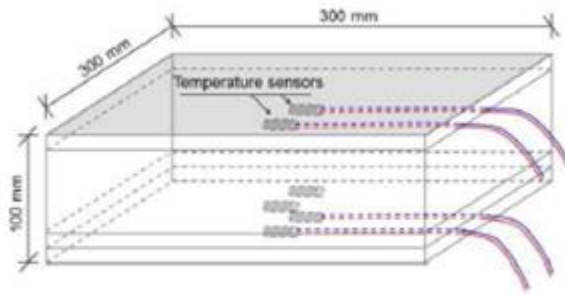
Figure 11. Placement of temperature sensor in the slab specimen [12]

The experiments were carried out on August 23rd and December 27th of 2017. Figures 12 and 13 shows the generated displays.
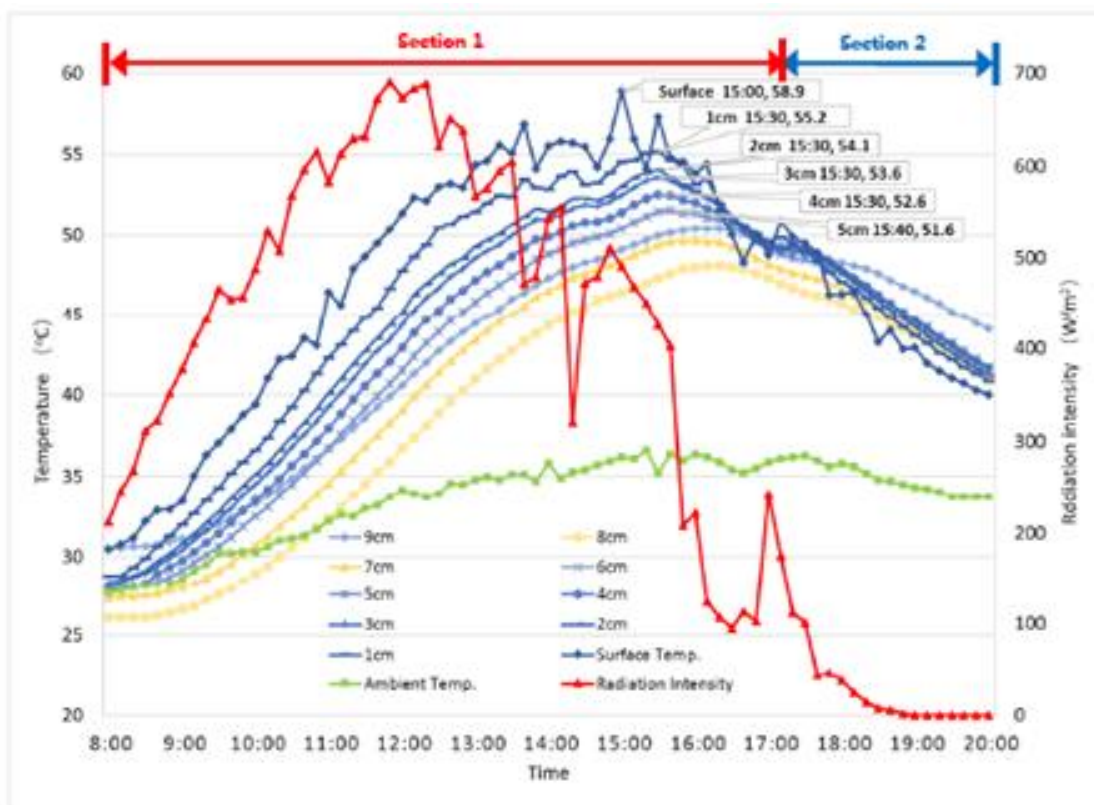
Figure 12. August 23rd data collection [12]
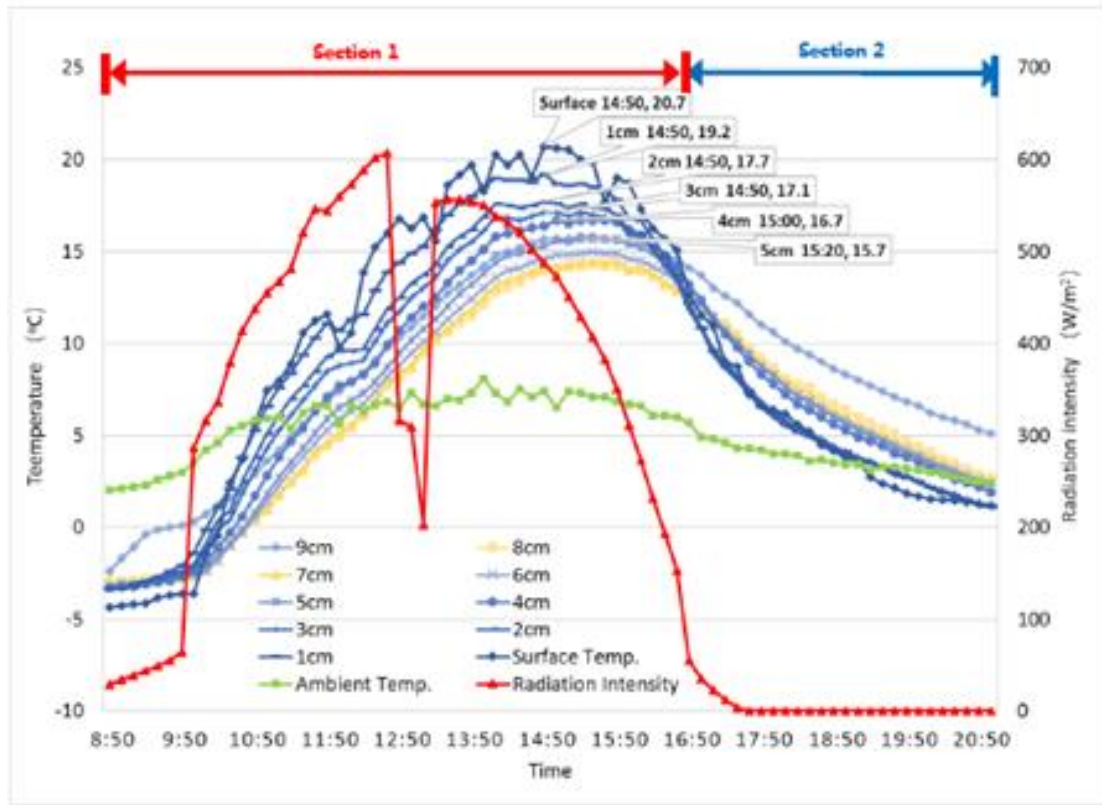
Figure 13. December 27th data collection [12]

In both scenarios it was observed that during the day the surface temperature is higher than the ones that are underneath. Conversely, during the evening and night the temperature of the surface was less than the underneath temperatures. In summer, the peak value of the asphalt surface was 58.9 $^{\circ}$C and in winter the peak was of 20.7 $^{\circ}$C [12].

With all the analyzed information they decided to create a prototype called RTEGs, which is described as the application of TEGs in the road. The main goal was to extract the maximum heat from the road surface with the help of vapor chambers that were placed at 20 mm to 30 mm of depth of the road. One side of the vapor chamber was embedded in the pavement and the other side stuck to the hot side of the TEGs. Figure 14 shows a schematic of the top view prototype.
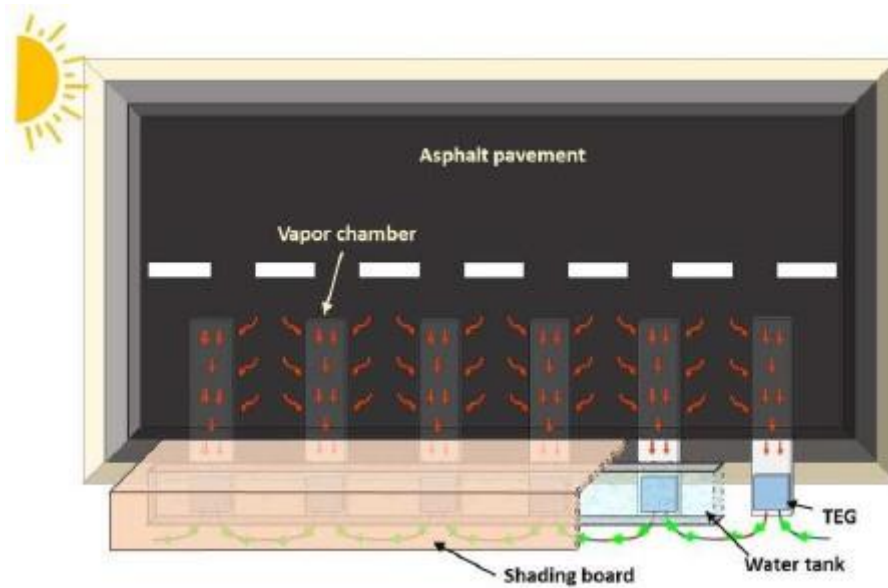
Figure 14. Schematic of RTEGs [12]

The cold side of the TEGs were also connected to vapor chambers that were in contact with a water tank. This way, the temperature gradient would be incremented. For covering the tank, a shading board was also installed. Figure 15 shows a side view of the experiment.
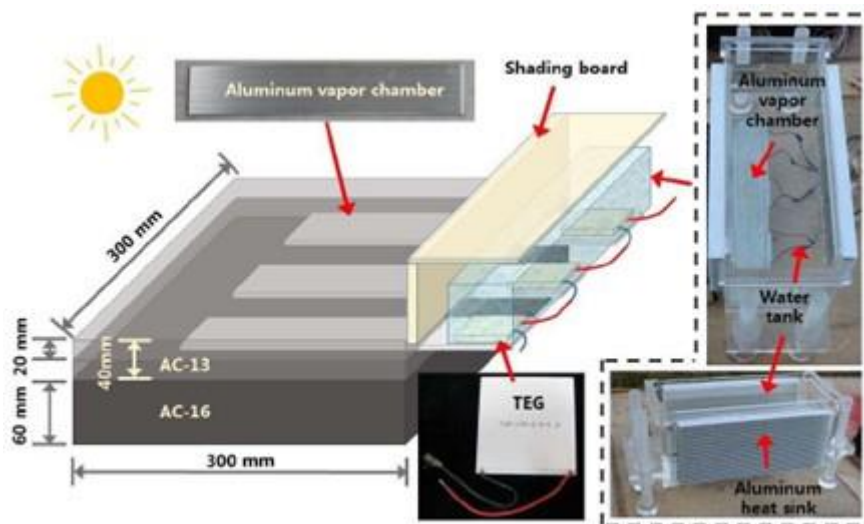
Figure 15. Side view of RTEG experiment [12]

The test methods used for this experiment were two:

1) **Indoor testing**. To simulate the solar radiation and heat a 500-Watt iodine-tungsten lamp was used.

2) **Outdoor testing.** The specimens were put in a natural environment. In this way, they were subjected to different factors such as wind, rain, radiation intensity or heat.

For both experiments, three TEGs modules connected in series were used. The commercial name is TEG-199 and its dimensions are 62 x 62 x 4 mm.

The results obtained in the different experiments were the following:

1) **Output voltage indoor test.**

Figure 16 shows that depending on the heating or cooling process, the voltage generated is different. This is because the temperatures were measured at the slab surface and water, which are different from the surfaces of the TEG modules. This means that the data recorded is approximated and so the voltage generated.
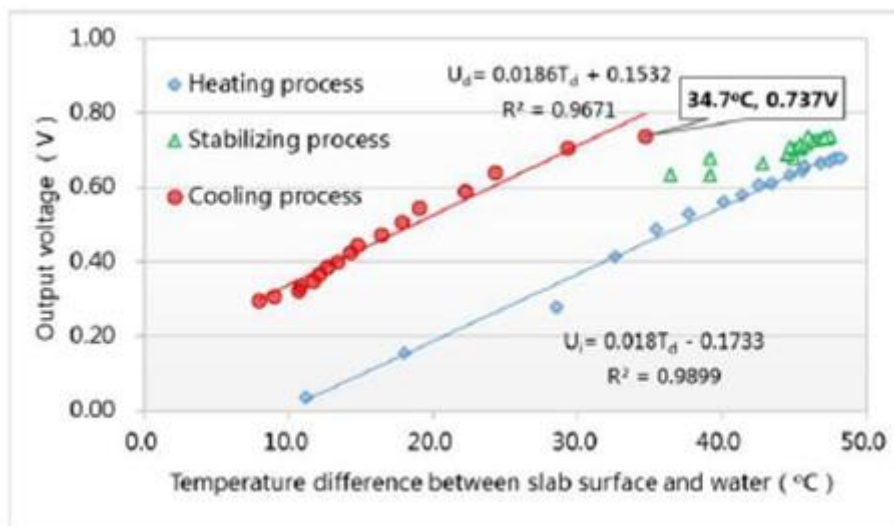
Figure 16. Graphic of the RTEGs by indoor test [12]

The maximum output voltage obtained during the simulation was of 0.737 V when the temperature difference between the water tank and slab surface was of 34.7ºC [12].

2) Output voltage of outdoor test.

The outdoor simulation took place in Chang´an University, Xi´an on October 31st of 2017. Because it was autumn, the day temperatures were low. A considerable amount of output voltage, however, was generated compared with the temperature difference. The peak ΔT was 16.56 °C and generating 0.41 V. The same situation as in the indoor test happened, which occurred because of the sensors that were placed in the slab surface and the water of the tank, the heating and cooling process results were different (Figure 17) [12].
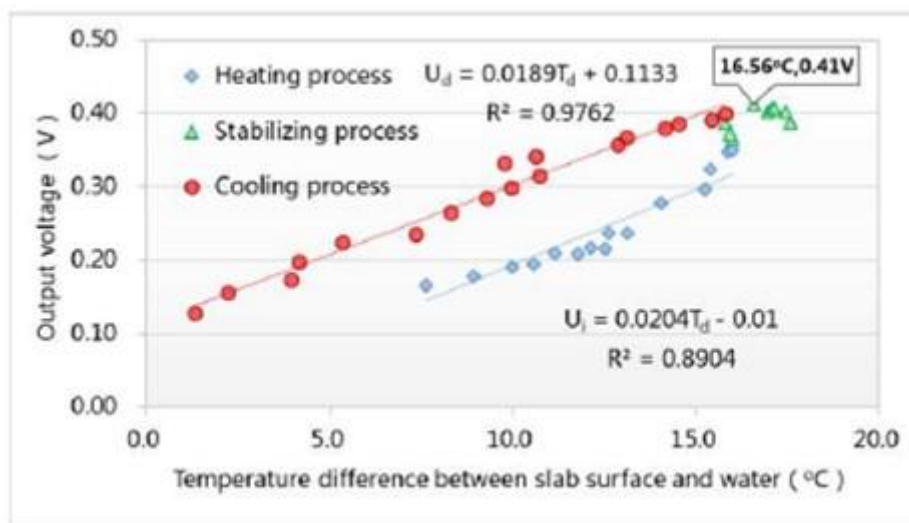
Figure 17. Graphic of the RTEGs by outdoor test [12]

A similar experiment was carried out in 2016 by the Department of Civil Engineering of Nitte Meenakshi Institute of Technology, in Bangalore, India. Four different case studies were carried out during this experiment. The equipment used were an Arduino board used for collecting the output voltage, GSM module, a TEG, adaptors and a heat sink [26].

1) **Placing copper plate directly on the existing pavement and laying a layer of pavement above it.**

A copper plate was placed at the bottom of the set-up in contact with the TEG module. Afterwards, it was covered with a layer of asphalt and an insulation box. The voltage obtained in this experiment was not satisfactory because the copper plate did not reach a sufficiently high temperature.

Figure 18. Setup of first experiment [26]

2) **Excavating a part of the pavement surface and placing a single TEG on the copper plate and another TEG on the pavement surface.**

The TEG module was placed in the asphalt over the copper plate. Also, a heat sink was placed on the hot side of the TEG module. The result obtained was not as expected because no voltage was generated; the heat sink was not effective being exposed directly to the sun.

3) **Copper board embedded in between the pavement layer.**

The copper plate was placed at the top of the surface of the pavement and the TEG module under it. For this last experiment, three different TEG modules were connected in series. The results obtained were better as expected due to the improved layout. The voltage fluctuated between 0 and 5V during the experiments depending on the climate conditions at every instant. Enough voltage was generated to be able to power an Arduino board because its maximum input is 5V [26]. Figure 19 shows an illustration of the setup and Figure 20 represents the average voltage compared with the time during this experiment.

Figure 19. Copper board embedded in pavement [26]
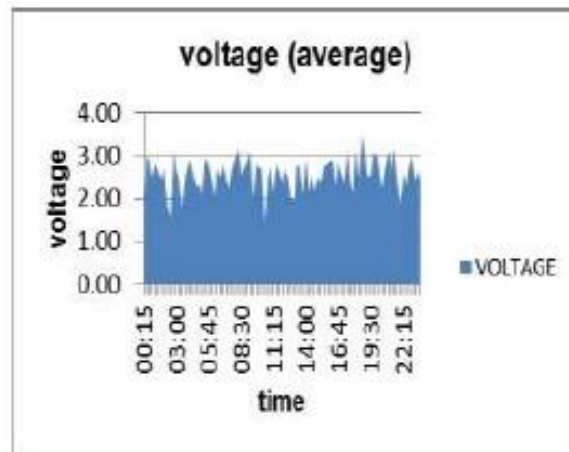
Figure 20. Average voltage vs Time [26]

Something that had never been investigated before is the performance of the TEG modules depending on the combination: series, parallel, parallel-series or series-parallel. Therefore, in 2014, the Department of Electrical Engineering of the Faculty of Engineering at Sriracha, in Thailand decided to carry out an experiment about it [15].

For this experiment, an experimental box was built to control the ΔT. The bottom side of the box was heated with a heater which in turn was controlled by a microcontroller. The top side was cooled down using dry ice and a fan. Four TEG modules were placed in the middle. The measures of each module were 40 x 40 x 3.3 mm; its commercial name was TEC1-12710. The system was able to collect the voltage and temperature every 2 seconds. The current (I) and the power generated (P) was calculated applying a resistance load that

could vary between 0.1 ohm and 10 ohms [15]. Figure 21 represents the schematic of the four experiments carried out.
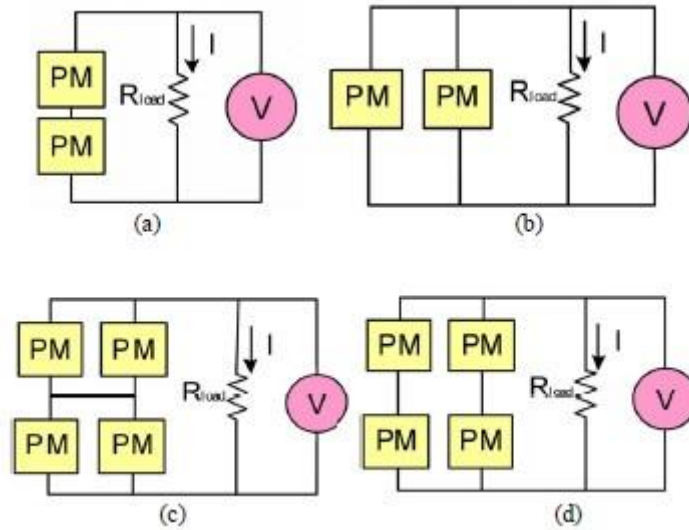
Figure 21. Experiments carried out: a) Series combination b) Parallel combination c) Parallel-series combination d) Series-parallel combination [15]

The results for each combination were the following:

a) Series combination.

For this combination, three different tests, were carried out. The tests were conducted with a single module, with 2 modules and 4 modules in series. The temperature difference was all the time constant at 10 °C.
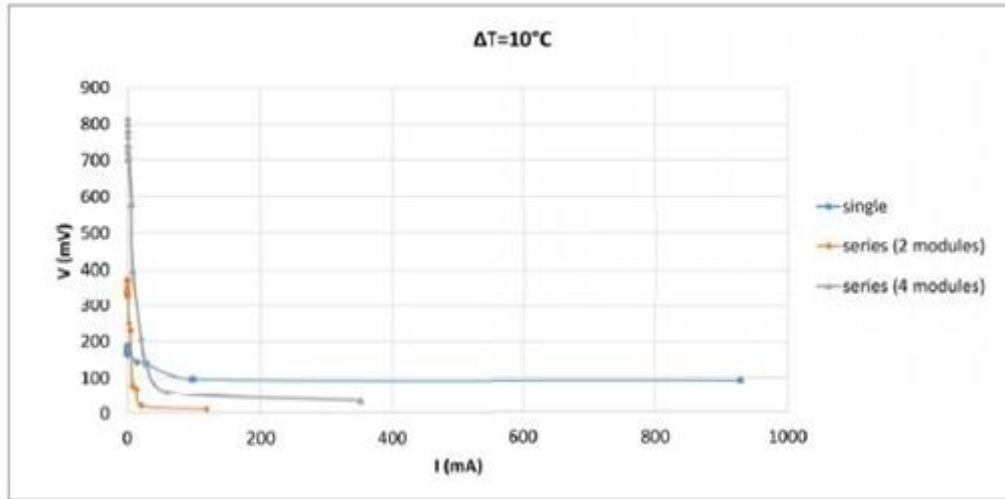
Figure 22. Series combination. Voltage vs current [15]
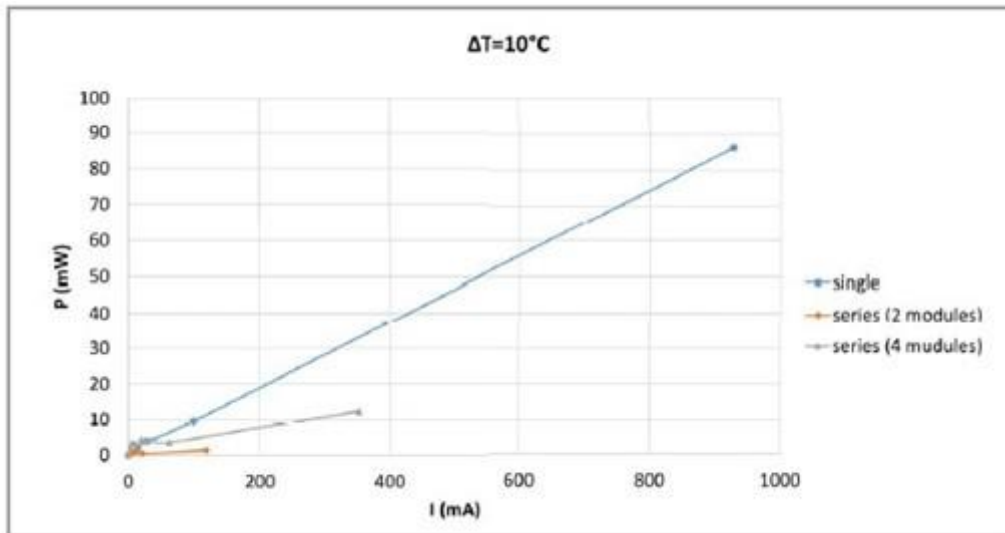
Figure 23. Series combination. Power vs Current [15]

Figure 22 shows that the voltage increases twice or even 4 times more compared to the single module but the current at the same time decreases twice or four times. It was also found that connecting more than one module in series decreases the power generated as shown in Figure 23.

b) Parallel combination.

Figure 24 represents the graphs of the voltage generated and as it can be observed the maximum voltage and current is obtained with the 4 modules in parallel.
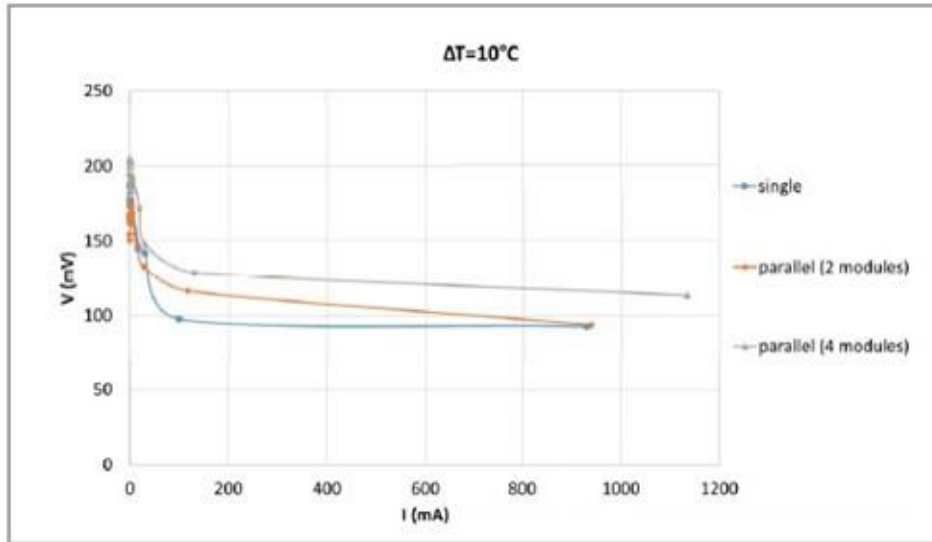
Figure 24. Parallel combination. Voltage vs current [15]

Figure 2.25 represents the power generated. The highest amount obtained was with the 4 TEG modules configuration in parallel.
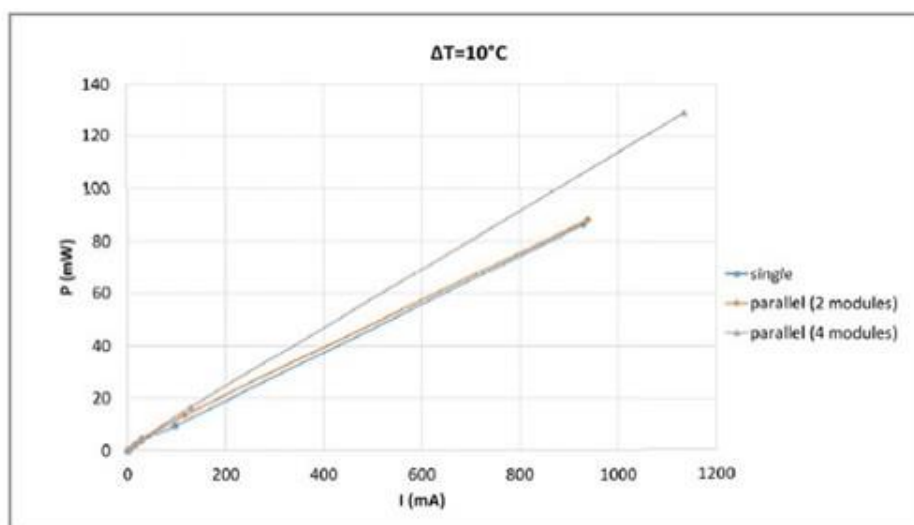
Figure 25. Parallel combination. Power vs Current [15]

c) Parallel-series / Series-parallel combination.

The last two combinations were compared in the same graphs as shown in Figure 26 and Figure 27.
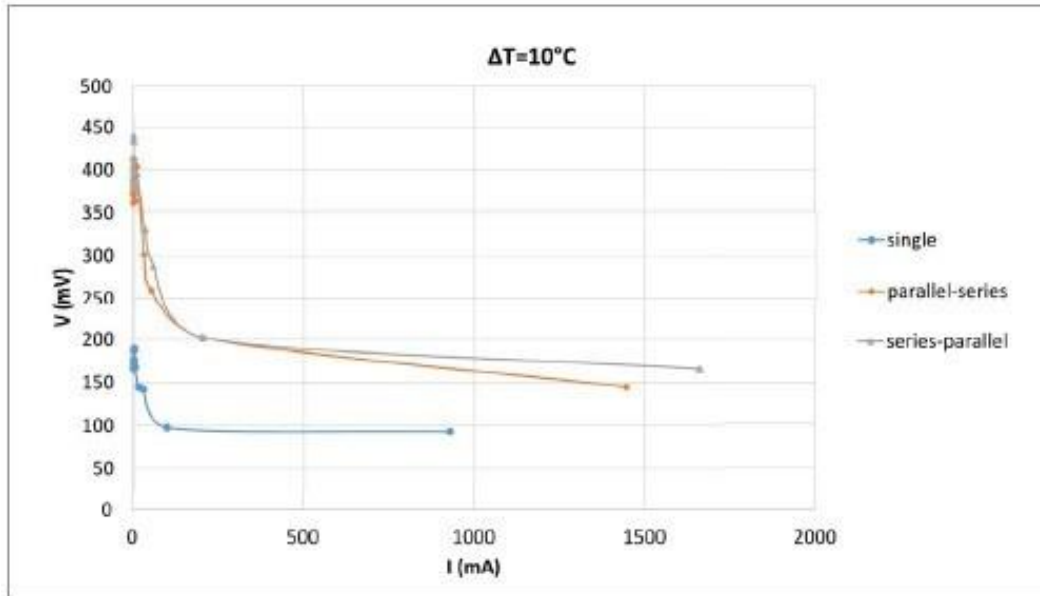
Figure 26. Parallel-series/ series-parallel combination. Voltage vs current [15]
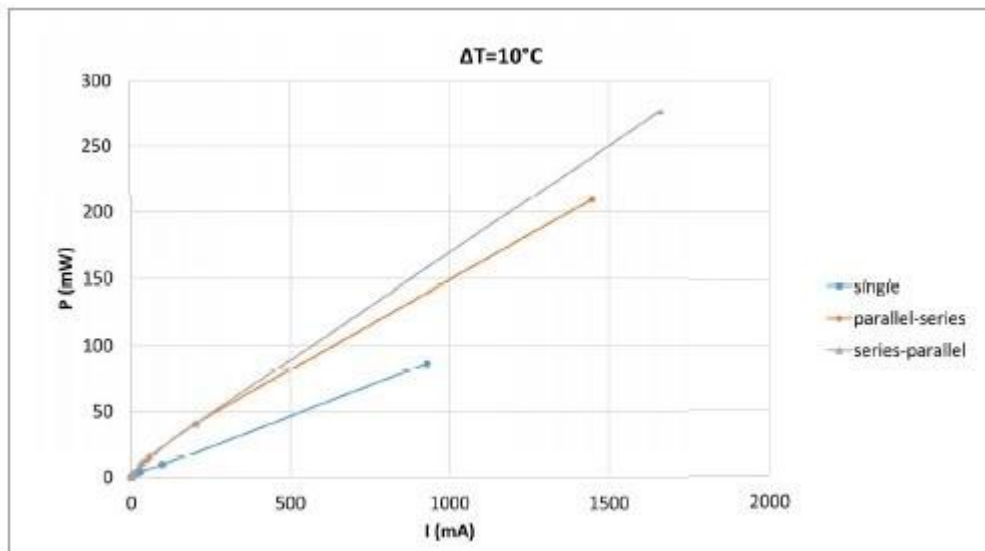
Figure 27. Parallel-series/ series-parallel combination. Power vs current [15]

The best performance was obtained for the combination of series-parallel of the four modules. The current and power peak was of 1.66 A and 276 mW at a 0.1

ohms load. In conclusion, the best circuit combination with the best electric efficiency is for the series-parallel [15].

Amid, Gholikhani and Dessouky (2020), investigated energy harvesting for roadway sustainability. In order to create a prototype, they used previous research, where they concluded that heat sinks were not being correctly used because the surrounding area and the cold side of the module did not have enough insulation, and they also criticized the use of water or soil to cool the heat sinks despite their low thermal storage capacity. For this reason, a new prototype shown in Figure 28 was created without the use of water or soil as a way of refrigeration [27].
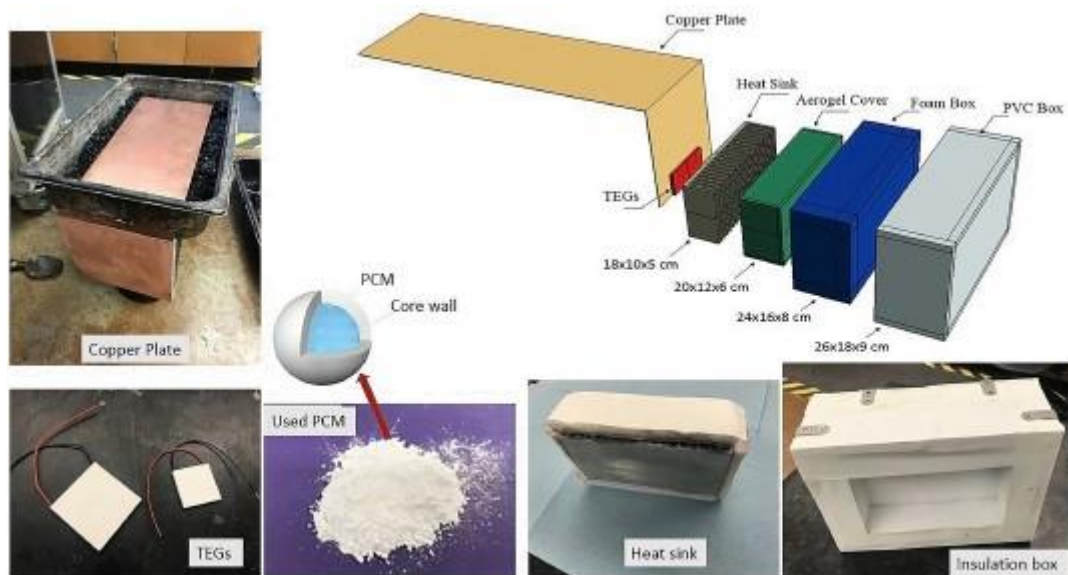
Figure 28. Prototype and components used [27]

The prototype main elements were the TEG modules, a copper plate for collecting the heat, an insulation box and an aluminum heat sink. The copper plate was composed of two segments, the first one, with a length of 50 cm and the second of 20 cm. The width is 20 cm. The main objective of the plate was to collect as much heat as possible from the road surface to heat up the hot side of the TEG module. Two different type of modules were used in the experiment, a 40 x 40 mm TEG named TXL-199-02Q (199 thermocouples) and a 62 x 62 mm TEG named TXL.287-03Z (287 thermocouples). The heat sink of aluminum was placed on the cold side of the TEG module to dissipate the

maximum possible heat. Its dimensions were of 18 x 10 x 5 cm. To substitute the water or soil that was usually being used in other experiments, PCM material was used. This material, known as phase change material, is generally used in air conditioning because of its ability to store energy through their change of state, in the form of latent heat. The operation temperature was of 18ºC, which means that, when the temperature rises the material changes from solid to liquid maintaining the temperature constant. To cover the heat sink, as shown in Figure 28, an aerogel cover, foam box and PVC box were used. These three materials are very low conductive materials with a high insulation capacity [27].

The experimental set-up is shown in Figure 29. A representation of how the prototype would be embedded in the road surface is shown in Figure 29a. A simulation of a real pavement was created as indicated in the set-up in Figure 29b and 29c.
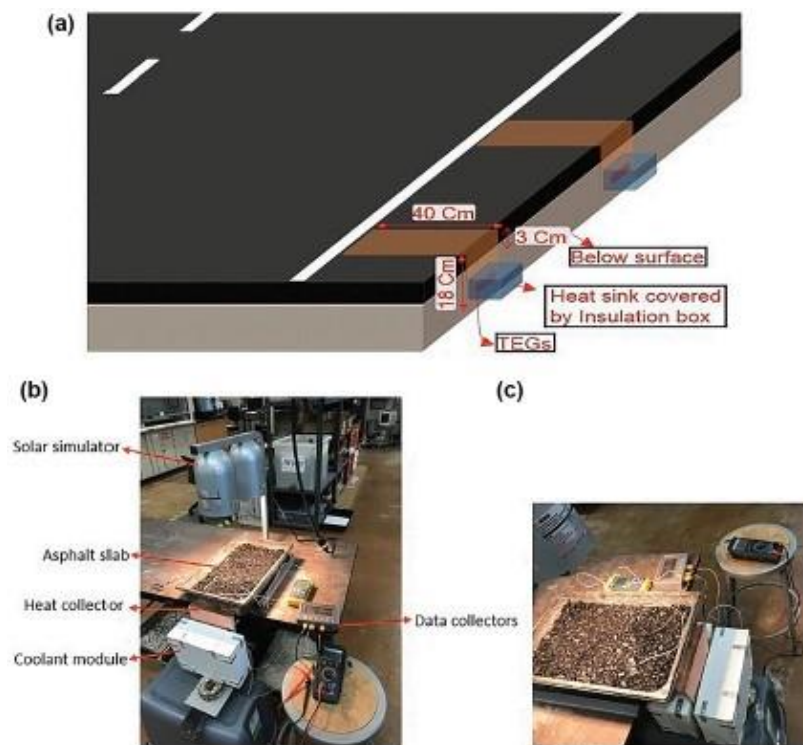
Figure 29. a) Prototype embedded in the pavement. b) Set-up right side view c) Set-up left side view [27]

For the set-up an asphalt slab with dimensions of 70 x 30 x 10 cm was used to simulate the pavement. An incandescent lamp simulated the solar radiation and heat was applied to the slab surface. Five different spots were selected to measure temperature: surface of

the asphalt slab, 30 mm below the surface, ambient air, bottom of the copper plate and the heat sink. Table 1 shows the different simulations that were conducted during this experiment. The range of temperatures was between 45ºC and 65ºC.

Table 1. Simulations conducted in the experiment [27]

Prototype	Number of TEGs	Size of TEG	Sides of attachment
1 TEG (4-1 side)	1	4 × 4 cm	1
2 TEG (4-1 side)	2	4 × 4 cm	1
3 TEG (4-1 side)	3	4 × 4 cm	1
4 TEG (4-1 side)	4	4 × 4 cm	1
4 TEG (4-2 side)	4	4 × 4 cm	2
1 TEG (6.2-1 side)	1	6.2 × 6.2 cm	1
2 TEG (6.2-1 side)	2	6.2 × 6.2 cm	1
3 TEG (6.2-1 side)	3	6.2 × 6.2 cm	1
4 TEG (6.2-2 side)	4	6.2 × 6.2 cm	2

Before starting with the simulations, a finite element analysis was carried out to check the impact of the TEG combinations efficiency. The program used to analyze the data was called ABAQUS. The input data was collected from three depths (3 cm, 15cm and 20 cm) during five days in the state of Texas, USA. Figure 30 shows the 5 different combinations that were tested to see the efficiency [27].
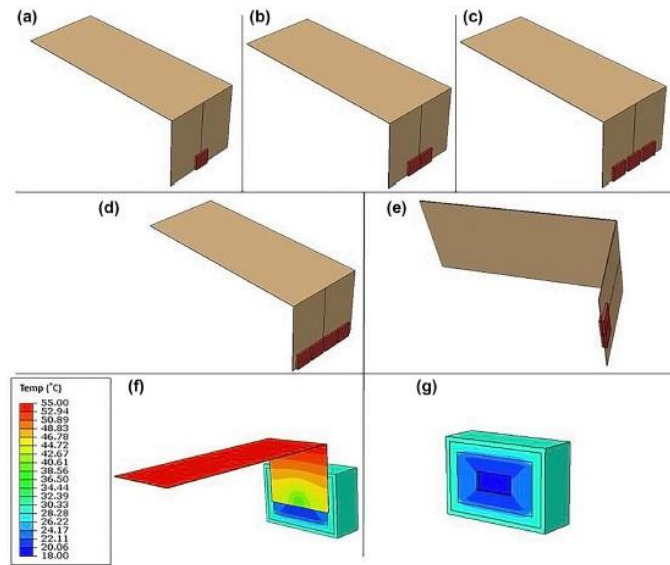
Figure 30. a) 1 module b) 2 modules c) 3 modules d) 4 modules (4x1 distribution) e) 4 modules (2x2 combination) f) Thermal distribution g) Insulation box thermal distribution [27]

The results obtained concluded that an increment in the number of TEG modules decrease the heat absorbed by each TEG module. Table 2 shows the collected results from the finite analysis.

Table 2. TEG temperatures depending on the combination [27]

Model	Temp. at hot side (°C)	Temp. at cold side (°C)	Effective temp. gradient (°C)
1 TEG	34.89	18.63	16.26
2 TEG	31.86	18.75	13.11
3 TEG	29.97	18.80	11.17
4 TEG (one side)	29.12	20.36	8.76
4 TEG (side side)	30.02	18.65	11.37

As mentioned, the experiments were tested in three different temperature ranges: 45ºC, 55ºC and 65ºC. The graphs obtained in the simulations are shown in Figure 31. A summary of the power generated in each simulation is shown in Table 3.
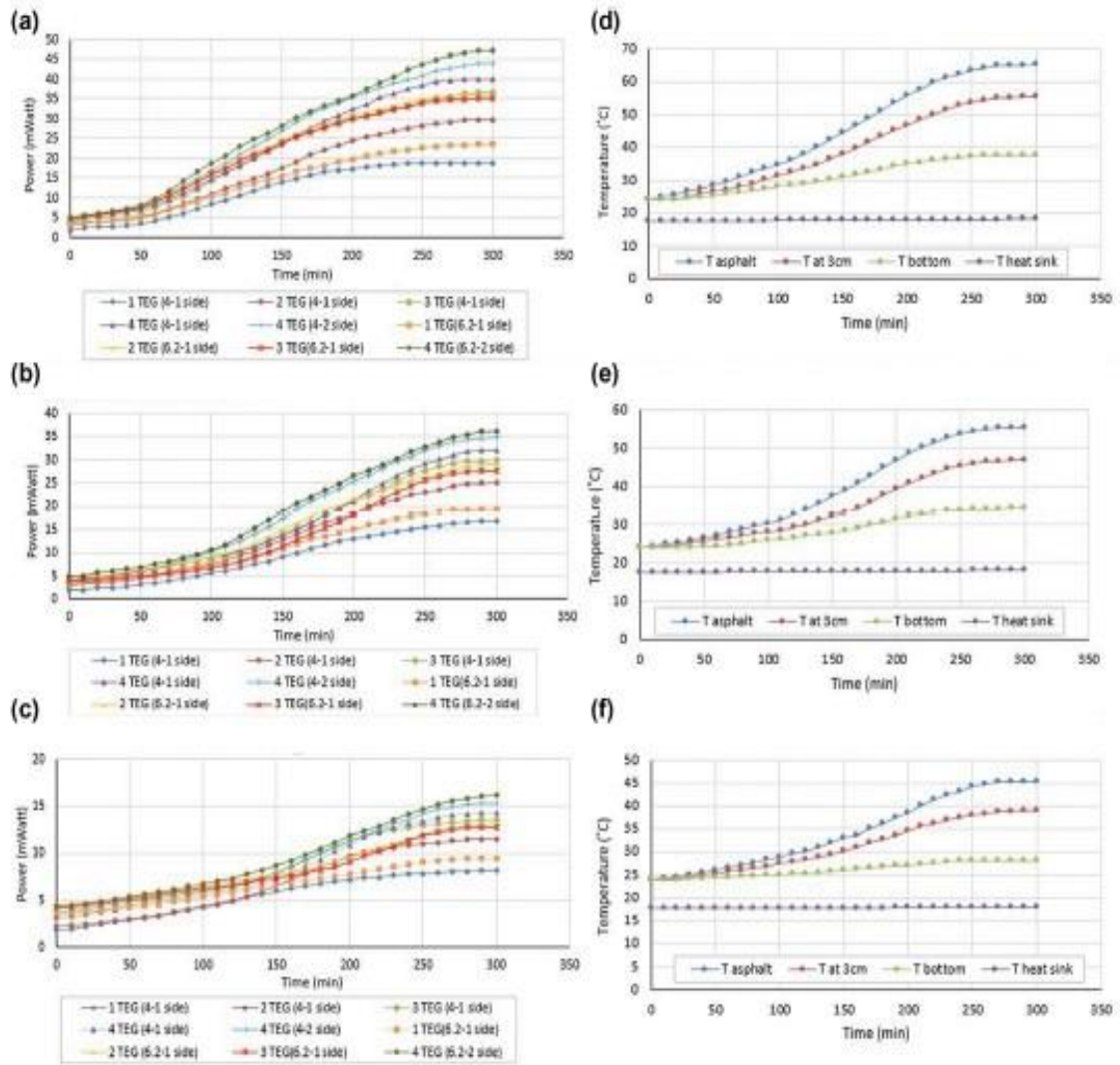
Figure 31. Time vs Power a) 65ºC b) 55ºC c) 45ºC. Time vs Temperature d) 65ºC 65ºC e) 55ºC f) 45ºC [27]

Table 3. Summary of the power generated in each simulation [27]

Prototype	Power (mW) at 45°C	Power (mW) at 55°C	Power (mW) at 65°C
1 TEG (4-1 side)	8.14	16.77	18.9
2 TEG (4-1 side)	11.51	24.95	29.74
3 TEG (4-1 side)	13.05	29.85	36.74
4 TEG (4-1 side)	14.32	32.08	32.35
4 TEG (4-2 side)	15.34	35.07	35.51
1 TEG (6.2-1 side)	9.45	19.14	23.5
2 TEG (6.2-1 side)	12.6	28.7	35.98
3 TEG (6.2-1 side)	12.49	27.96	35.03
4 TEG (6.2-2 side)	16.18	36.16	47.14

29

The results obtained were as expected. The finite element analysis in ABAQUS rightly predicted that less TEG modules get translated into more efficiency. For instance, three TXL-199-02Q TEG modules (40 x 40 mm) at 65ºC produced more power than four because the amount of heat obtained by each module was higher, and consequently, the temperature difference was higher. Also, it was concluded that the combination of 2x2 modules was better than the 4x1. Performing at a temperature of 65ºC, the maximum power generated was with a 2x2 configuration of the TXL.287-03Z TEG modules (62 x 62 mm) obtaining 47.14 mW [27].

It is worth noting that the combination of the aluminum heat sink and the PCM perform perfectly as observed from the time vs temperature graphs (Figure 31d, 31e and 31f). The results were better than expected because the room temperature was around 23-24ºC and the heat sink temperature remained constant all the time at 18ºC, irrespective of the heat source, which was generated by the lamp.

2.4 TEG applications

The thermoelectric effect is a technology that still has a long way to go. The maturity of this technology is very low because it is not really developed. Table 4 [23] represents a comparison of the installed power, conversion efficiency, energy generation and TRL[b] between some renewable energy systems.

- Installed power represents the capacity in general conditions of generating energy. It is measured in W/m^2.
- Conversion efficiency is the relation between the useful output and the energy input.
- Energy generation quantifies the electricity generation under operating conditions. It is measured in W/m^3.
- TRL is a value that evaluates how developed is the technology, where 10 represents a technology which is in its maturity and 1 a technology that is still in its infancy.

Technology	Company/R&D institute	Installed power: W/m^2	Conversion efficiency: %	Energy generation	TRL[b]
Photovoltaic	Solar Roadways	97·3	11·2	NA	4
	TNO	NA	NA	NA	7[c]
TEG	Hasabe *et al.*	NA	NA	38·0 mW/cm^3	3
	Wu and Yu	NA	1·6	2·6 mW/cm^3	3
Piezoelectric	Innowattech	NA	NA	5·8 J/veh m	4
	Genziko	1942·0	NA	40·0 J/veh m	4
Hydraulic	Kinergy	NA	NA	188·0 J/veh m	4
	New Energy Technologies	NA	NA	NA	4
Electromechanical	Waydip	833·0	50·0	680·0 µW/cm^3 180·0 J/veh m	4
	Underground Power	NA	85·0[d]	NA	4
	HES	NA	NA	NA	3
	Energy Intelligence	NA	NA	NA	3

As shown in Table 4, the TEG technology has only a value of 3 in the TRL. For instance, a more developed technology would be photovoltaics on pavements, whose TRL value is 7 [23].

Despite the aforementioned, the thermoelectric effect technology started to be used by the end of the 1950´s for space exploration [28]. Since then, the interest in this technology has gradually increased and more applications have been found. This section will be divided in three parts:

- Electricity generation in extreme environment: the space
- Recovery of heat waste
- Solar TEG: sun as a source of energy

2.4.1 Electricity generation in extreme environment: The space

The use of thermoelectric generators in the space industry is very common, although these devices are different to the commercial ones because they are based on nuclear technology. They are called Radioisotope Thermoelectric Generator (RTG). Figure 32 shows a scheme of the different part that compound a RTG.
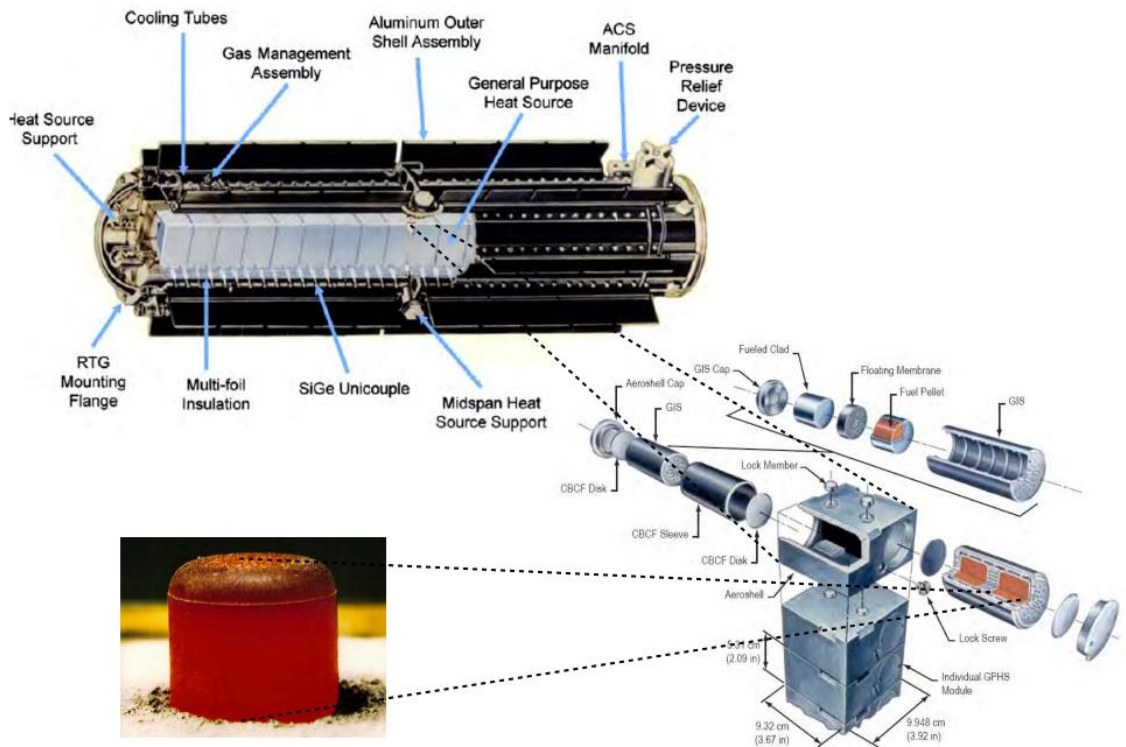
Figure 32. RTG parts (NASA) [29]

The RTG operate using the heat released by radioactive materials, specifically the plutonium-238. This material is the most common due to its long half-life and the little quantity of shield it needs. Its application in space is to provide electricity to the spacecraft, like the solar panels. In distant missions from the sun, these devices are extremely useful because the solar radiation is very low. For instance, in Pluto the solar radiation is 1 W/m^2, compared to 1375 W/m^2 on the outer space of the Earth. In addition, the module life can last for some decades, which makes it a very good choice for long lasting space missions [30]. For example, Cassini-Huygens was a space mission whose task was to study the planet Saturn, that operated for two decades (1997-2017) [31]. Table 5 shows a summary of the different RTG that have been used in the past and that are currently operating, its electrical power generated at the beginning of the mission and its years of operation.

Radioisotope thermoelectric generator RTG	Electric Power at beginning of mission per RTG	Couple	Number of RTG	Mission	Destination	Year	Design lifetime	Lifetime
Space Nuclear Auxiliary Power SNAP-3	2.7 W	PbTe	1	Transit	Navigation satellite	1961		15 years
SNAP-19B RTG	28.2 W	PbTe-Tags	2	Nimbus III	Meteorological satellite	1969		
SNAP-19 RTG	42.6 W	PbTe-Tags	2	Viking 1	Mars landers	1975	90 days	6 years
			2	Viking 2	Mars landers	1975	90 days	4 years
	40.3 W	PbTe-Tags	4	Pioneer 10	Jupiter, asteroid belt	1972	5 years	30 years
			4	Pioneer 11	Jupiter Saturn	1973	5 years	22 years
SNAP-27 RTG	70 W	PbSnTe		Apollo 12, 14, 15, 16, 17	Lunar Surface	1969–72	2 years	5–8 years
Multi-Hundred Watt (MHW) RTG	158 W	SiGe	3	Voyager 1 & 2	Edge of solar system	1977		Still operating over 44 years
General Purpose Heat Source (GPHS) RTG	292 W	SiGe	2	Galileo	Jupiter	1989		14 years
			3	Cassini	Saturn	1997		20 years
			1	Ulysses	Jupiter	1990		21 years
			1	New Horizons	Pluto(12/2014), Kuiper Belt	2006		Still operating after15 years
Multi-Mission Radioisotope Thermoelectric Generator MMRTG	110 W	PbTe-Tags	1	Curiosity	Mars Surface Aug 2012	2011		Expected 14 years

The reason why Table 5 specifies the electrical power at the beginning of the mission is because the radioactive material heat decreases gradually every year and the thermocouples degrade in performance. To conclude, RTGs are a source of electrical energy which have huge advantages such as their reliability and compact design.

2.4.2 Recovery of heat waste

Greenhouse gas emissions is an actual problem that must be solved to reduce the ecological footprint. Besides, the world energy demand continues to increase. TEGs are a good option to reduce the pollution by taking advantage of wasted heat from exhausted gases. The transportation industry including the automotive, aeronautic and maritime sector could adopt this technology [30].

In 2021, less than 1% of the world's cars were electric, and, in 2030, only 13% is expected to be electric [32]. This means that the transition from combustion cars to electric is a slow process. For this reason, something should be done with all of the heat that is wasted from combustion engines. Figure 33 represents the fuel use of a combustion engine.
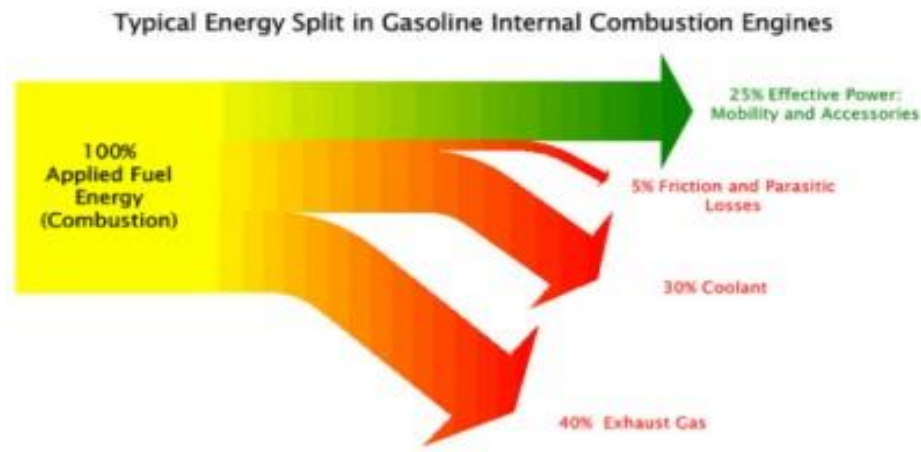
Figure 33. Energy split for internal combustion engines [33]

Gasoline engines waste 40% of their energy in exhaust gas, which could be transformed into electricity. For instance, a diesel car using 50 kW of power fuel, means at least losing 20 kW of heat in exhaust gases. With the use of TEG, assuming a 3 % efficiency (normally it is between 5-8%), around 600 W of power would be generated. According to Fiat Research Centre between 800-1000 W is translated into a reduction of 12-14 g/km CO_2 [30].

Following this information, big companies such as Fiat or BMW are investigating the application of this technology in their cars. In 2012, Fiat Research and Advanced Engineering conducted an experiment where a TEG was installed in a car. The installation of this module is shown in Figure 34.

Figure 34. Illustration of the car with its different parts [33]

As shown, the TEG module was installed in the mid-body of the car through which the exhaust passes. The results obtained in the experiment were satisfactory except for the fact that there was a 70% difference in the power generated when the bypass was closed and opened. The experiments were set with a constant speed of the car of 65 mph and the average exhaust temperature was of 450ºC. With the bypass closed the power generated was of 250 W while when the bypass was opened generated 70 W [33]. Figure 35 shows the graph where all this data is collected.
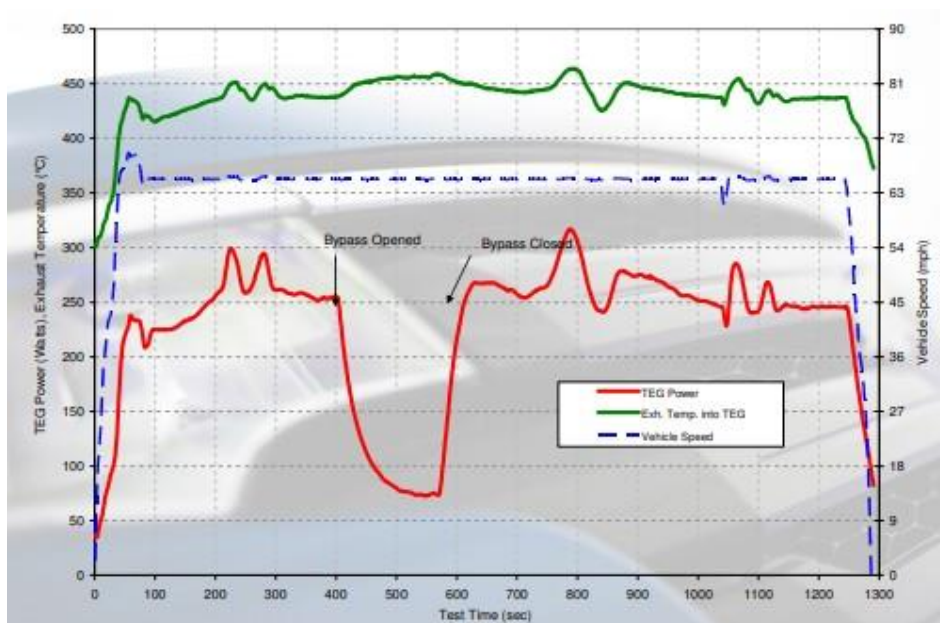
Figure 35. Graph of TEG power generation, temperature, vehicle speed compared with the time [33]

The BMW group has also developed prototypes using this technology. The most recent experiment was carried out in 2012, where a TEG module was installed in a BMW X6 being able to generate 600 W. The vehicle speed was constant of 125 km/h. Even so, the research demonstrated that the automobile application of the TEG is still not feasible. The price of the modules compared with the power generated is not profitable yet.

The engines of planes and helicopters release a significant amount of heat. Boeing Research & Technology conducted an investigation where it was shown that a 0.5% fuel reduction could be reachable with the use of TEG. This reduction means saving $12 M per month for commercial planes. However, another study in turbine nozzles

demonstrated that during real operation conditions a significant amount of electricity was created but not enough when the weight of the cold exchanger was included [30].

In the maritime sector, not many studies have been carried out due to the lack of international regulations against the greenhouse gasses emissions. In fact, three per cent of the global carbon dioxide emissions is produced by ships. This means that ships release nearly 800 million tons of gases into the atmosphere annually [34]. In 2012, Kristiansen carried out a research where the use of TEG in marine waste incinerator could be used to harvest the waste heat. The way of studying the possible application of TEG was with an optimized mathematical model. The results show that when the 850 kW incinerator was operating at maximum power, around 58 kW could be generated at a price of 6.6 $/W. Nevertheless, decreasing the costs, 25 kW could be generated at a price of 2.5 $/W. The combination of both would generate 38 kW at a price of 2.7 $/W [35].

2.4.3 Solar TEG: The sun as a source of energy

In this section, the idea is to analyze the possible applications that the TEGs can have using the sun as a source of energy. As mentioned before, the greater the temperature difference, the more electricity is generated. However, increasing the solar intensity is necessary to create a considerable amount of energy. For this reason, different devices are used to increase the intensity. In 2008, a thermoelectric solar air collector was studied by Lertsatitthanakorn [30]. Flat plate reflectors with its optimum positions were used to increase the solar intensity on the solar air collector. Also, the use of parabolic dish concentrators is now being used to generate energy.

In Argentina, the TEGs have had an enormous acceptance. In 2008, there were around 500 installations in the country [36]. The main applications of this technology in the country are supplying cathodic protection facilities and SCADA (Supervisory Control and Data Acquisition) in wells and pipelines. Moreover, they are used in telecommunication repeaters. Figure 36 shows a TEG installation.

Figure 36. 550 W TEG installation in Argentina [36]

2.5 Literature Review Summary

As discussed in this chapter, many experiments about harvesting energy from the pavements have been conducted. It has been demonstrated that, despite the time of the year, a temperature difference always appears and in turn, electricity is generated. Nevertheless, sometimes the ΔT is not enough. To increase this difference one of the most important things is to cool the cold side of the module as much as possible. In many experiments [27], the water or soil has been used to cool the heat sink that was in contact with the surface of the TEG. However, in this review it has been found that the use of other elements is better. The application of PCM material with a heat sink as a refrigerant has been demonstrated to increase the performance of the TEG significantly.

Furthermore, it is necessary to collect the maximum heat from the sun. To do so, the heat chambers are composed of either aluminum or copper. The way of operating with these plates is to cover as much asphalt as possible for collecting the maximum heat, placing the module on its surface and by conduction transmit the heat. Also, the usage of more modules does not mean more electricity generation. Doing a finite element analysis is recommended to calculate the optimum number of TEG per surface. The best performance combination for placing the modules was proved to be series-parallel configuration.

The use of TEGs is already in existence in niche areas, such as the case of generating electricity in space missions. Furthermore, a number of industries are evaluating the use of TEGs in their products especially in the aviation and automotive sector. However, the

cost is still prohibitive. The use of solar concentrators with TEGs is another are where development is expected in the future.

CHAPTER 3. METHODOLOGY

The methodology is divided into two main parts. The first part consists of the evaluation of the temperature difference (ΔT) on the surface and about 10 centimeters below the surface of three different pavements, namely asphalt concrete and limestone. This will be carried out for sunny, partly cloudy, cloudy, windy, and rainy days during the months of March, April and May 2021.

The second part of the methodology consists of building two laboratory setups to study the behavior of TEG modules under varying temperature gradient. Two GM250 modules, with rated open circuit voltages of 1.9 V and 11.25 V, are used. The modules are rated for a hot side temperature of 250ºC but only temperatures up to around 70ºC will be used, to reflect the expected pavement temperatures. For this purpose, two TEG modules are tested. Both have the same specifications, but different dimensions. The GM250-31-14-10 is a module of 20 mm x 20 mm, while the GM250-161-12-20 module dimensions are 40 mm x 40 mm.

The modules will first be tested under open circuit conditions, where the generated voltage is expected to increase with temperature gradient. The obtained variation will be compared to the datasheet characteristics. In the second experiment, the TEG modules will be loaded using a variable resistor and the output power and voltage will be measured. The test will be repeated with different variable resistor settings to examine the output power variation with load. This allows identification of the maximum power generation under the temperature gradient of interest.

The captured results will be, extrapolated to determine the expected output when the TEG modules are installed on the three different types of pavements.

In so doing, the dissertation will provide a first-hand indication of the potential contribution of TEG modules to power street screens and small warning signs without the need of a grid connection.

3.1 Temperature data collection

A data logger was used to collect temperature data of the three surfaces at the Institute for Sustainable Energy, Marsaxlokk. This is an electronic device that can be programmed

to measure and store any type of data such as temperature, relative humidity, and solar radiation by means of external connected instruments and sensors.

The datalogger that has been used is the Campbell Scientific CR1000 with six thermocouple type T wires (Figure 38). Its interface panel is shown in Figure 37. The thermocouple generates a small voltage due to the difference in the flow of electrons at the junction of the thermocouple. The T-type thermocouple has two wires, the positive element (blue wire), made of copper and the negative element (red wire), made of constantan which is an alloy of copper and nickel. When the union of the two metals is heated or cooled, a voltage difference is generated at the lead that is proportional to the temperature. The range in which it can operate is -180 to +300ºC.

Figure 37. Campbell Scientific CR1000 data logger [37]
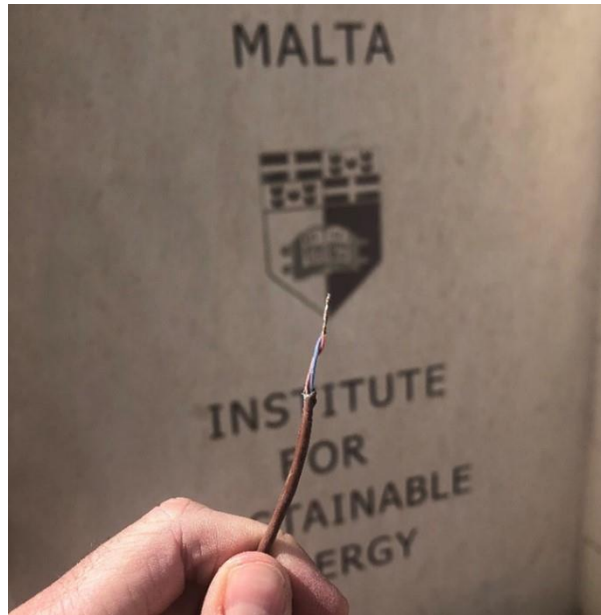
Figure 38. Campbell Scientific CR1000 connected to Type T thermocouples

The data logger is powered by a battery that is charged by a solar photovoltaic panel (Figure 39), thus making the data logger autonomous in its operation.

Figure 41 shows the protective box housing the data logger, which was installed at the Institute for Sustainable Energy of the University of Malta in Marsaxlokk. The six thermocouples (2 for each type of surface) were connected as shown in Figure 40. The surfaces that were tested were asphalt, concrete and limestone (Figure 42).

Figure 39. Solar panel that powers the datalogger´s battery
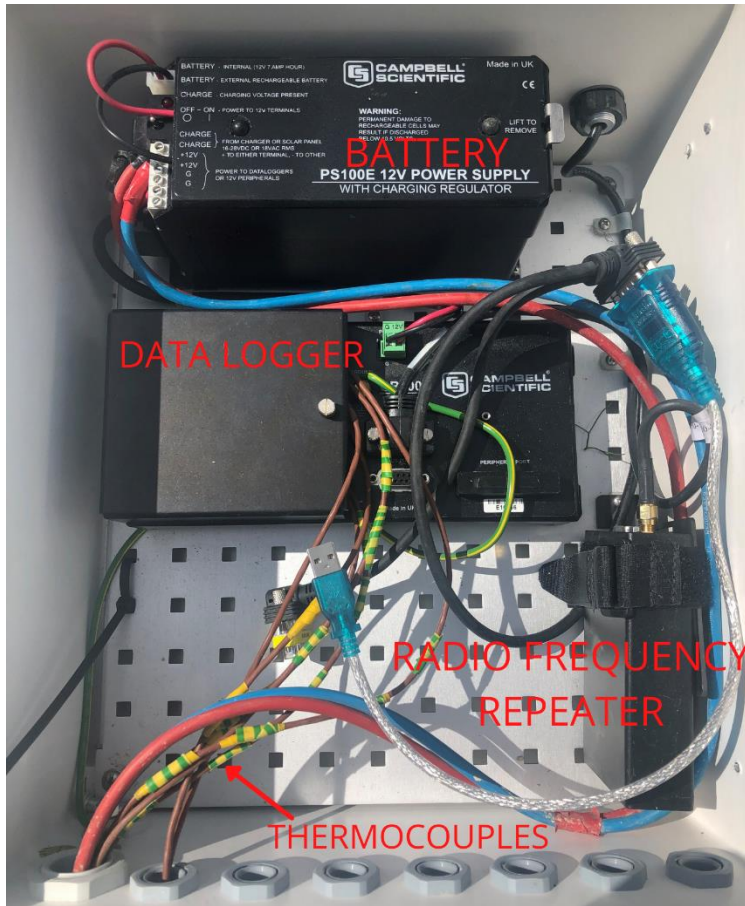
Figure 40. Industrial control panel enclosure
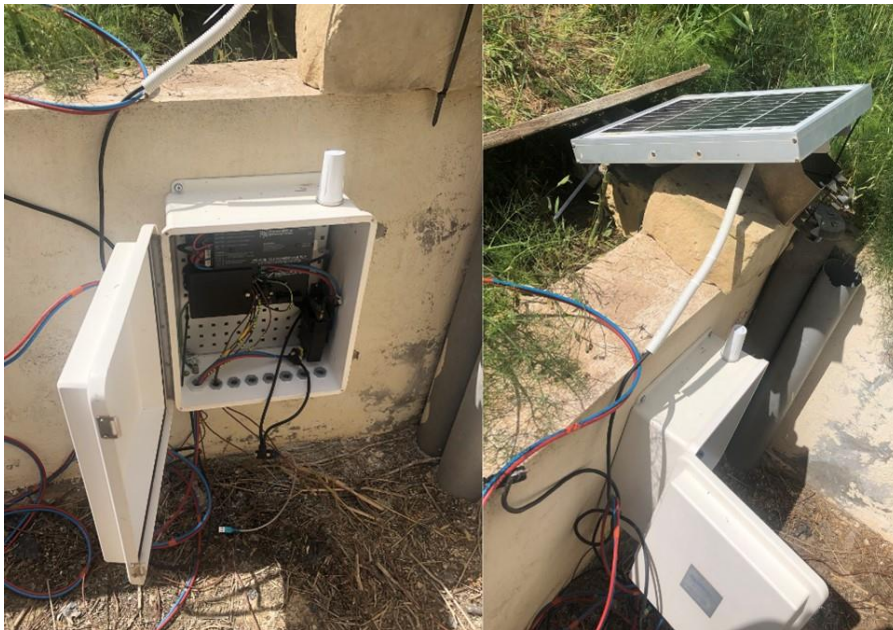
Figure 41. Final installation

Figure 42. From left to right: Asphalt, Concrete and Limestone

Thermocouples number 1 and 2 were situated in the asphalt, nº2 on the top and nº1 at a depth of 10 cm. Number 3 and 4 were situated in concrete, nº4 on the top and nº3 at a depth of 10 cm. The last two thermocouples were used for the limestone temperature. Nº 6 on the top and nº 5 at a depth of 10 cm.

The scope was to monitor the temperature difference through the day for different types of weather. This was carried out for the months of March, April, and May 2021. In this manner it would be possible to identify the expected ΔT between the hot and cold side of a TEG module.

The data logger was set to measure data every 5 seconds and average and store it every 5 minutes. Consequently, every hour there were 12 different temperatures captured by the six thermocouples.

3.2 TEG energy harvesting kit

The main components that have been used to carry out the described experiments on the TEGs consist of an energy harvesting kit ADEH-K-A, which includes the parts shown in Figure 43 [38]; and a separate larger TEG module, which is shown in Figure 44 [39].
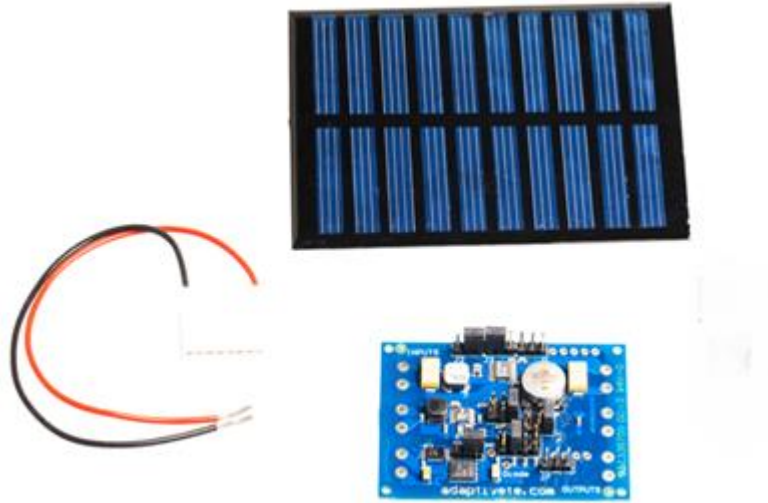
Figure 43. Harvesting kit [38]
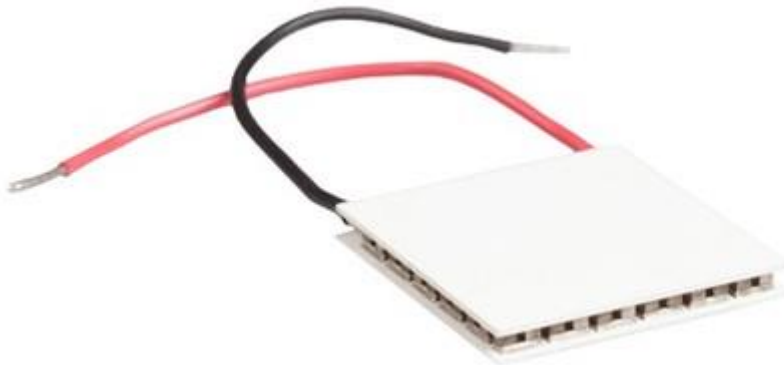
Figure 44. Thermoelectric generator 40x40 mm [39]

The harvesting kit includes the following:

- 1 x Energy Harvesting Board ADEH-P-A
- 1 x Solar Panel ADEH-PD-A
- 1 x TEG Module B ADPD-B (GM250-31-14-10)

The ADEH-P-A board (Figure 45) provides three step-up converter channels, where the first two channels are configured for the TEG and a solar panel, respectively.

It is optimized for either very low input voltage thermoelectric generators (TEG) or small PV modules. In addition, the board implements maximum power point tracking (MPPT) for the PV channel. The ratings of this board are shown in Table 6.

Figure 45. Energy Harvesting Board ADEH-P-A [38]

Table 6. Rating of the Board ADEH-P-A [38]

Input voltage range (TEG harvester)	50mV - 500mV
Output voltage 1 (TEG harvester)	Selectable: 2.35V, 3.3V, 4.1V, 5.0V
Output Current 1 (TEG harvester)	7mA (VOUT = 0V)
Output Voltage 2 (TEG harvester)	LDO 2.2V
Output Current 2 (TEG harvester)	11mA (VLDO = 0V)
Input Voltage Range (Solar harvester)	250mV-5V
Output Voltage (Solar harvester)	Selectable: 1.8V, 3.3V, 5.0V
Output Current (Solar harvester)	500mA
Input Voltage Range (OR-ing controller)	800mV-16.5V
Output Voltage (OR-ing controller)	800mV-16.5V
Output Current (OR-ing controller)	2A

The Output and Input connection map (Figure 46) and the connector and jumper selector map (Figure 47) are important for selecting the desired output voltage [40].
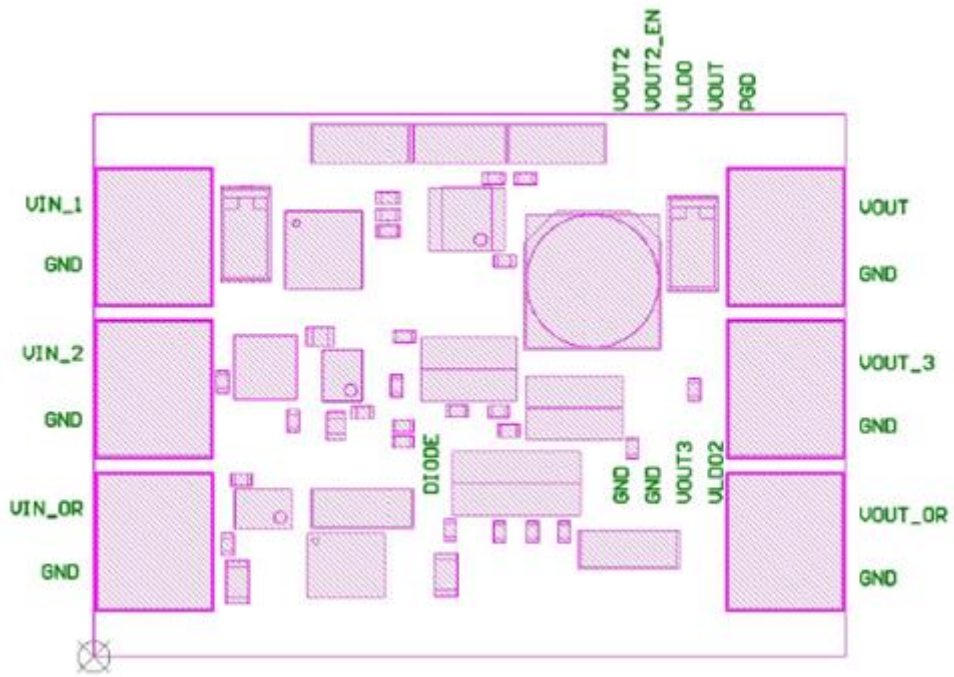
Figure 46.Output and Input connection map [40]
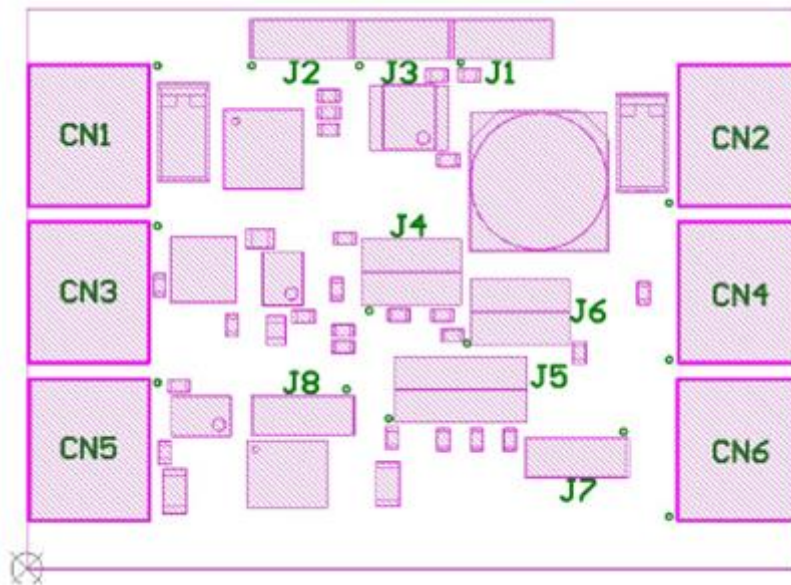
Figure 47. Connector and jumper selector map [40]

The available configurations for the TEG channel are presented in Table 7.

Table 7. TEG part output voltage configurations [40]

JP2	JP3	VOUT (A) Output voltage 1 (TEG harvester)
GND	GND	2.35 V
GND	VAUX	3.3 V
VAUX	GND	4.1 V
VAUX	VAUX	5 V

In this research the focus is on the first two channels of the board where the TEG module must be connected. The first channel represents the TEG harvester diagram and the second the solar harvester diagram. As mentioned in Table 7, depending on the configuration chosen, a different output voltage is obtained.   The circuit diagram of the first channel is shown in Figure 48. The second channel is shown in figure 49.
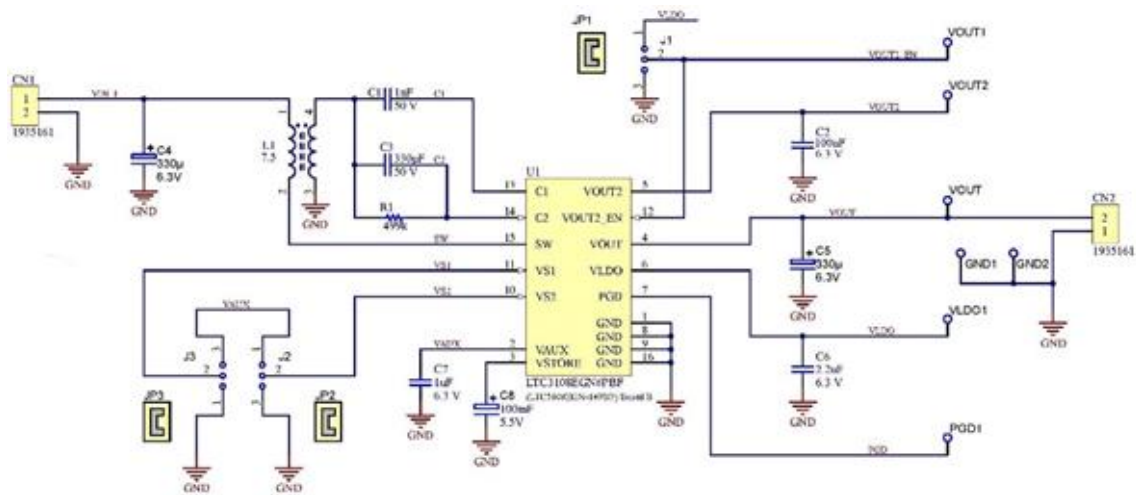
Figure 48. TEG part circuit diagram [40]
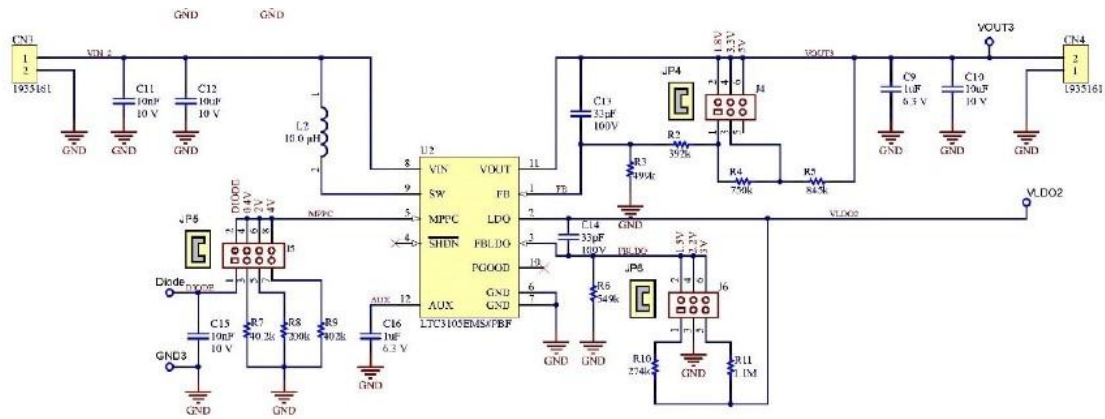
Figure 49. Solar harvester part circuit diagram [40]

The GM250-31-14-10 TEG (Figure 50) module has a compact structure, with reliable performance and, noise-free operation. Its dimensions and the hot and cold sides are identified in Figure 50.
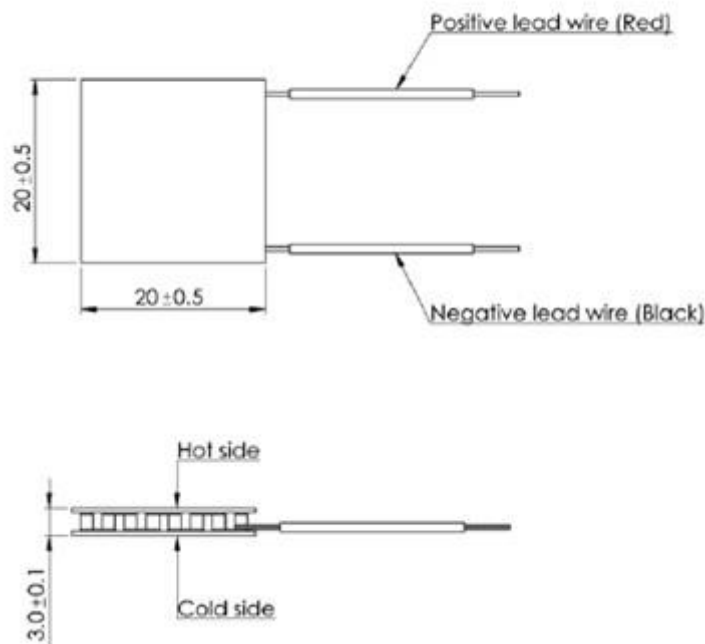
Figure 50. Dimensions of GM250-31-14-10 TEG [41]

The specifications of the TEG for a hot side temperature of 250ºC and a cold side temperature of 30ºC are shown in Table 8.

Matched load output power	2.5W
Matched load resistance	0.36Ω ± 15%
Open circuit voltage	1.9V
Matched load output	2.63A
Matched load output voltage	0.95V
Heat flow through module	~50W
Maximum compress (non-destructive)	1MPa

The GM250-161-12-20 TEG (Figure 51) module has the same features as the previous TEG, but with bigger dimensions, as shown in Table 9.
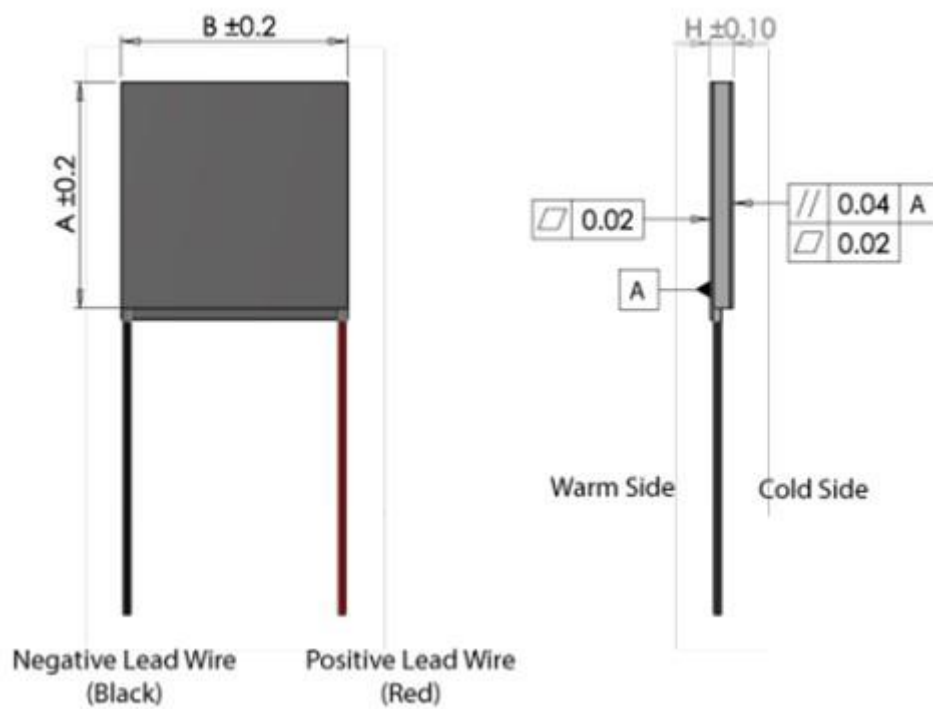
Figure 51. Dimensions of GM250-161-12-20 TEG [42]

Table 9. Geometric dimensions of Figure 3.15 [42]

A	40 mm
B	40 mm
H	5 mm

The specifications of the TEG working parameters with the set temperatures of 250ºC on the hot side and 30ºC on the cold side are available in Table 10.

Table 10.Specifications of GM250-161-12-20 TEG [42]

Matched load output power	3.27W
Matched load resistance	$9.7\Omega \pm 15\%$
Open circuit voltage	11.25V
Matched load output	0.58A
Matched load output voltage	5.6V
Heat flow through module	~65W
Maximum compress (non-destructive)	1 MPa

3.3 TEG modules´ laboratory set-ups

The aim of creating set-ups is to set the desired temperature on both sides of the TEG modules, and in turn, measure the generated output. Later on, these results will be extrapolated to the temperatures monitored by the Campbell Scientific CR1000 data logger installed at the Institute for Sustainable Energy for three different pavements.

Two different set ups have been created, one with the GM250-161-12-20 module and another one with GM250-31-14-10 module. For both set-ups the following devices were used: power resistor/s to generate a heat flow, a heat sink to maintain the cold side temperature close to room temperature, silicone grease, M3 bolts and insulators.

3.3.1 GM250-31-14-10 set-up (Set-up 1)

Given the assumed maximum temperature of 70ºC, the expected heat flow through the TEG at 3A is of 10W. This is calculated by the next formulae:

$$P = I^2 \times R \qquad\qquad (5)$$

In order to generate the required heat dissipation, two HS50 1.2Ω resistors (Figure 52) are used. The value of the resistors was chosen such that together they dissipate a power of 21.6W (each of 10,8W) with a current flow of 3A. The power dissipation from each individual resistor was checked not to exceed the allowed HS50 resistor power dissipation without a heat sink. The latter value was specified in the datasheet as 14W. Also, the required voltage to drive the 3A across the resistors was checked not to exceed 30V.

The HS50 resistor and relevant dimensions are shown in Figure 52 and Table 11.
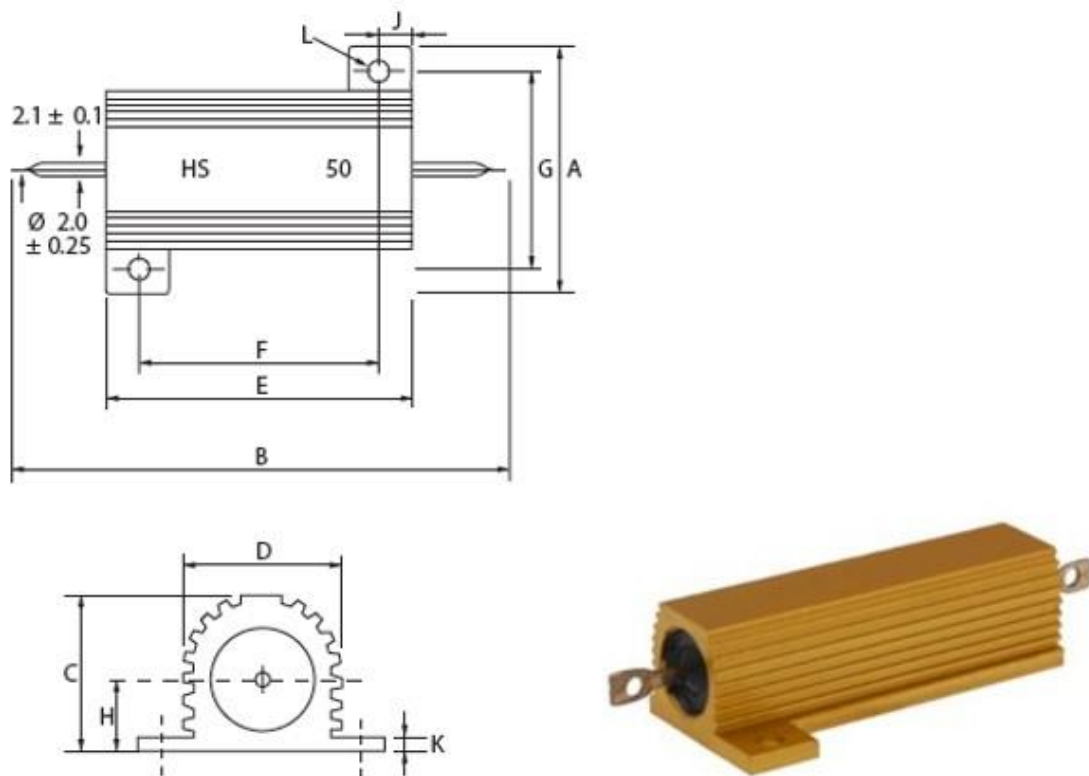
Figure 52. HS50 resistor with dimensions [43]

Size(mm)	A Max	B Max	C Max	D Max	E Max	H Max	K Max
HS50	28	72,5	14,8	14,2	49,1	8,4	2,6

Due to the narrow width of the resistor as compared to the module, two resistors were used to cover its full area. The top view of the designed set-up is shown in Figure 53 while a picture of the actual setup is shown in Figure 54.

Silicon grease was used to increase the conduction between the resistors and the TEG hot side as well as between the bolts securing the resistors to the heat sink to avoid heat flow through the metal bolts. Also, plastic insulators were used with the bolts securing the resistors to the heatsink to avoid heat flow through the metal bolts.
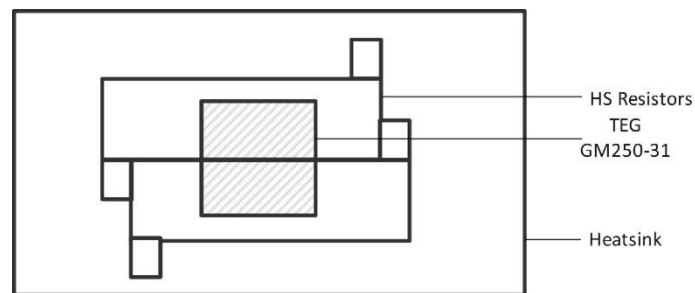
Figure 53. Top view of set-up 1 with TEG module in hatched square
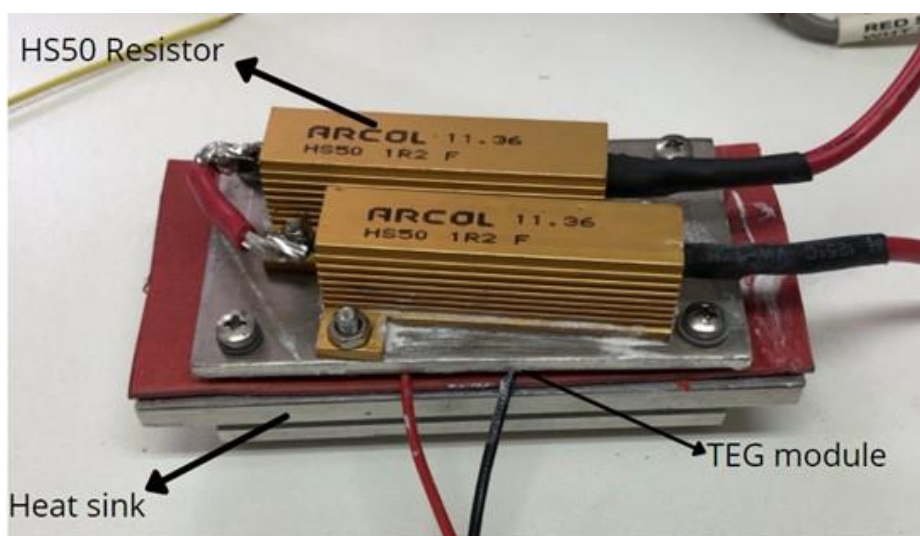
Figure 54. Illustration of set-up 1

3.3.2 GM250-161-12-20 set-up (Set-up 2)

A different resistor - the HS100 (Figure 55) of 2.2 Ω – was used in the set-up 2 (Figure 58), due to the larger size of the GM250-161-12-20 TEG module. The power dissipated by the resistor was of 20W with a current flow of 3A. The value was set not to exceed to allow power dissipation without a heat sink which was of 30W. The voltage across the resistor did not exceed the 30V. The dimensions of the resistor are shown in Table 12.
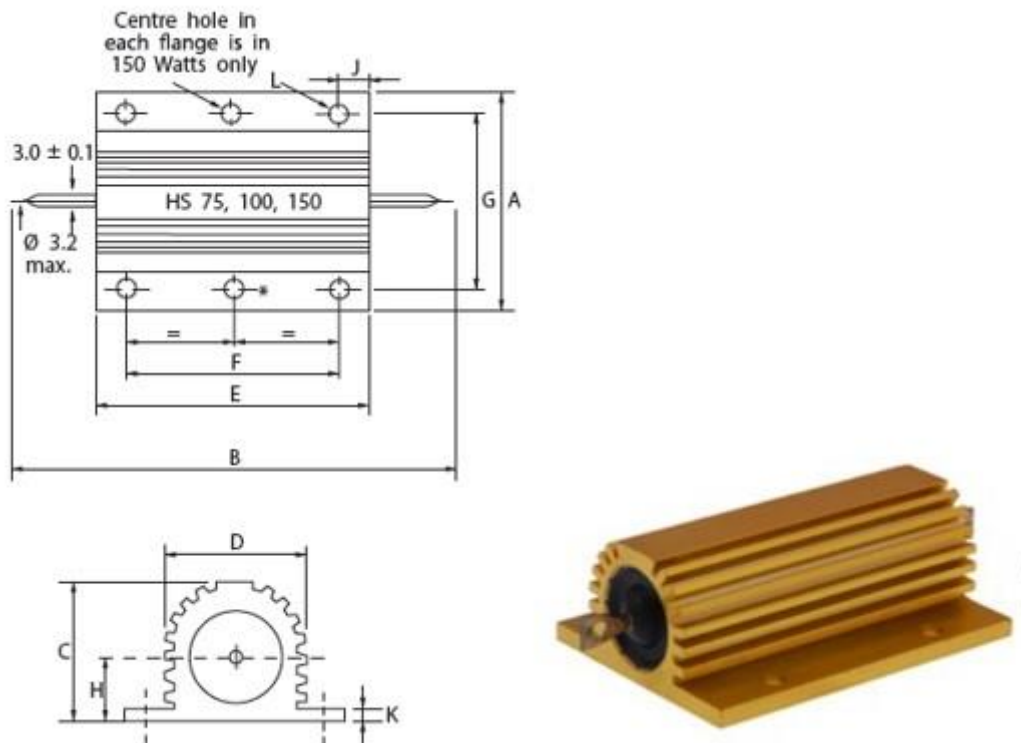
Figure 55. HS100 resistor dimensions [43]

Table 12. Relevant dimensions for HS100 [43]

Size(mm)	A Max	B Max	C Max	D Max	E Max	H Max	K Max
HS100	47.5	88	24.1	27.3	65.2	11.8	3.7

Figures 56 and 57 show the scheme of the set-up 2 seen in different views.
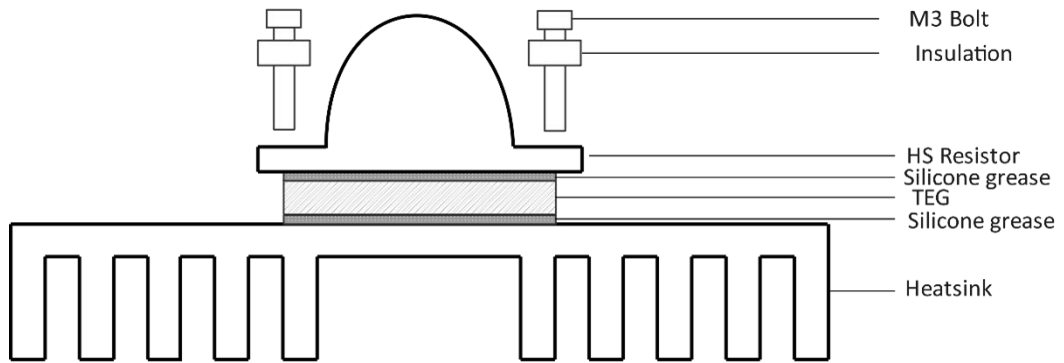
Figure 56. Side view of GM250-161-12-20
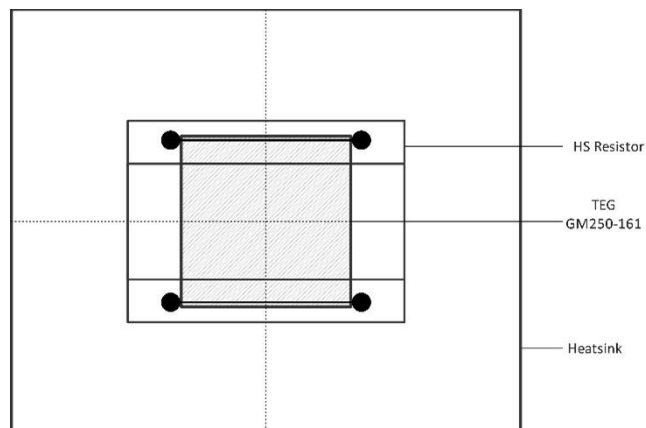
Figure 57. Top view of GM250-161-12-20
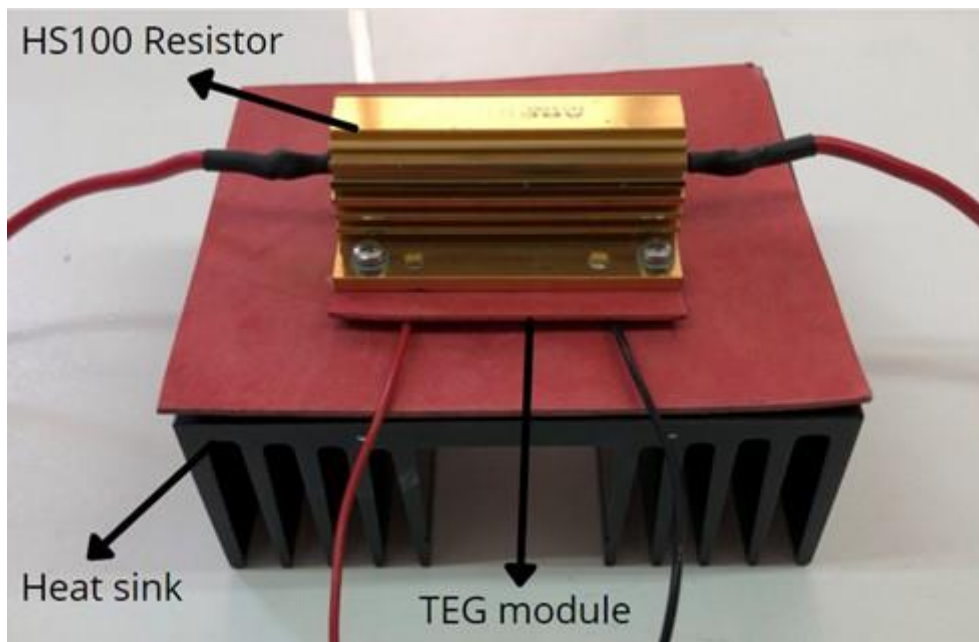
Figure 58. Illustration of set-up 2
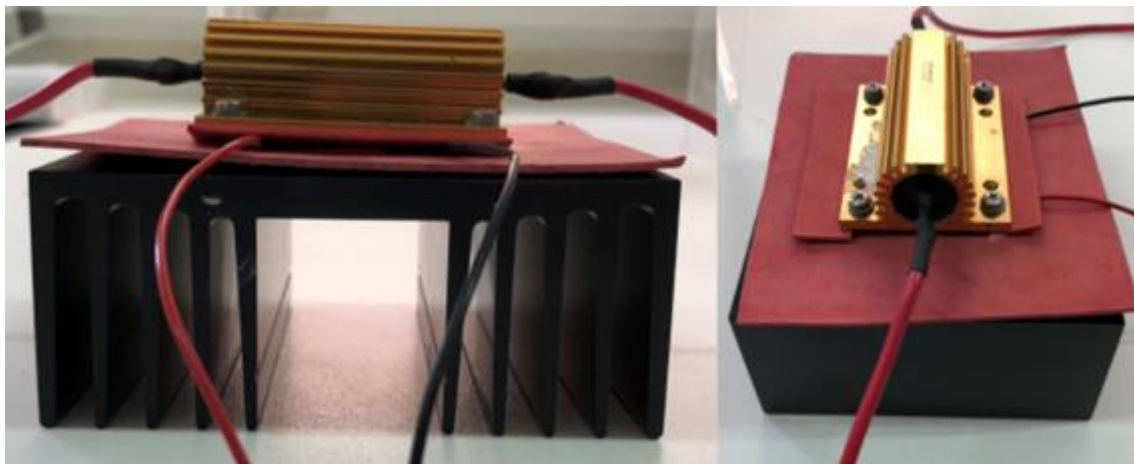
Figure 59. Illustration of side and top view set-up 2

3.3.3 Instrumentation

In order to measure the temperature variation of the hot and cold sides of the TEGs, four different type T thermocouples have been installed. These are shown in Figure 60. The thermocouples number 1 and 2 were placed in the set-up 1, in the hot and cold side,

respectively. The number 3 and 4 collected the set-up 2 temperatures of the hot and cold side of the module.

To log the variation in the temperature and the TEG output, a Campbell Scientific CR1000 data logger similar to the one installed at the ISE, was used. The thermocouples were connected to channels 1 – 4 as shown in Figure 60. The TEG output voltage and the supply voltage are measured through a potential divider to limit the maximum voltage to 5V, so as not to exceed the input voltage range of the logger. The voltage signals are marked as A and B. Therefore, the voltage readings on the logger then multiplied by a factor of two to obtain the actual voltage.
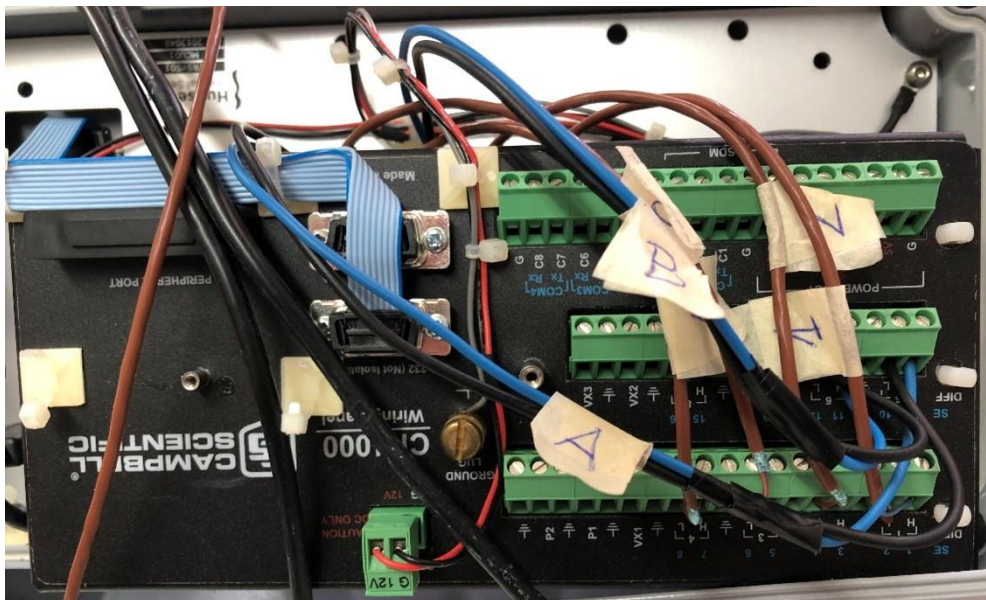
Figure 60. CR1000 Data Logger

One channel of a PL330QMD power supply was used to drive the current of 3A through the power resistors.

The complete setups with the data logger and the power supply are shown in Figure 61.
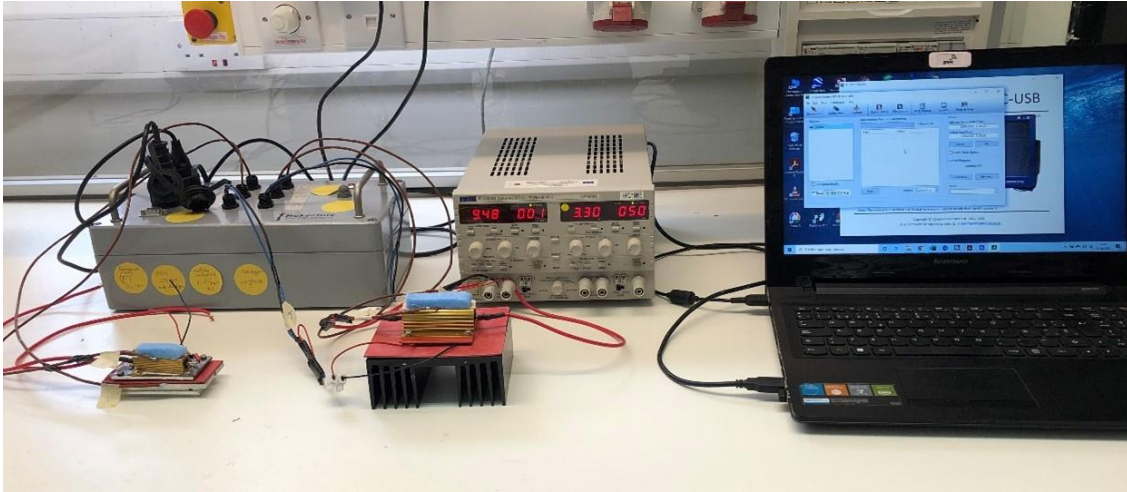
Figure 61. Illustration of set-ups, power supply and data logger

3.4 Experimental tests

As it was mentioned before, the first set of tests was carried out with the TEG module in open circuit. After that, the TEG modules were loaded via a variable resistor to measure the amount of power generated.

3.4.1 Open circuit test

The power supply was set to supply a current of 3A to the power resistors. The open circuit voltage was measured across the TEG terminals and logged every 10s. A small fan was placed to the heatsink to aid the heat dissipation. The hot side temperature was allowed to reach a value of around 70ºC and then the supply was switched off. Each test was run twice.

3.4.2 Test under load

The TEG modules were loaded with a variable resistor and the output voltage was logged at 10s intervals. The matched load resistance for a hot side temperature was extracted

from the datasheet and the variable resistor was varied around this value. Knowledge of the load voltage and the load resistance allowed calculation of the generated power.

For the GM250-31-14-10 module, the matched load resistance was of XXΩ. Due to the low value required, only three tests were carried out with load resistances of 0.218 Ω, 0.248 Ω and 0.309 Ω.

For the GM250-161-12-20 module, the identified matched load resistance was of YYΩ. For this case, six tests were carried out with load resistances of 5.975 Ω, 6.278 Ω, 6.505Ω, 6.789 Ω, 7.015 Ω and 7.210 Ω.

CHAPTER 4. RESULTS AND ANALYSIS

Chapter 4 analyses the results and reliability of two TEGs for a possible application in the pavements to nudge information booths.

This Chapter, as the methodology, is going to be divided in two parts. In the first part, an evaluation of the temperatures collected from the thermocouples in the Institute for Sustainable Energy will be carried out. It will be analysed week by week during the months of March, April and May of 2021. In the second part, the voltage and power generated of two TEG modules will be analysed while a ΔT is being applied.

4.1 Pavement temperature data collection

In this section, the goal is to analyse the data collected for the temperatures of different pavements when operating in a number of months in spring during the time of conducting this dissertation. The temperature difference between the surface and about 10 cm below the surface of three different pavement materials is analysed, namely, limestone, asphalt and concrete. This would be the expected temperature difference that a TEG installation would experience in spring. Also, weather information classified as sunny, partly cloudy, cloudy, windy and rainy, and the maximum and minimum daily temperature of each week are provided to have a scenario of the ambient conditions that the thermocouples were exposed to during that day.

It is important to mention that during the temperature collection a problem arose with the thermocouple that was situated at the top of the limestone surface. This happened between the April 26th and May 10th, so during these days the temperatures were not correctly recorded due to a disconnected wire for the limestone top surface pavement. For this reason, the weeks number 6 and 7 will not contain the temperatures of the limestone. For week number 8, the first day will not contain the limestone data either. Another aspect to consider, is that the asphalt and concrete were sometimes covered by some shadow from the nearby soil, which was at a higher level. This occurred mainly in the afternoon, so lower temperatures would be registered for the two surfaces.

In the next subsections, which are divided by weeks, the graphs represent the time of the day on the x-axis and the temperature difference (ΔT) between the top and bottom levels, on the y-axis, for each of the three materials.

4.1.1 Week 1: 22 March- 28 March

Table 13 shows the maximum and minimum air temperature and weather conditions for different days.

Table 13.Week 1 maximum and minimum temperature and weather [44]

WEEK 1	22	23	24	25	26	27	28
Tmax (ºC)	16	15	16	15	16	20	17
Tmin (ºC)	12	9	10	11	9	11	11
Weather	Cloudy	Cloudy	Partly cloudy	Partly cloudy	Partly cloudy	Partly cloudy	Partly cloudy
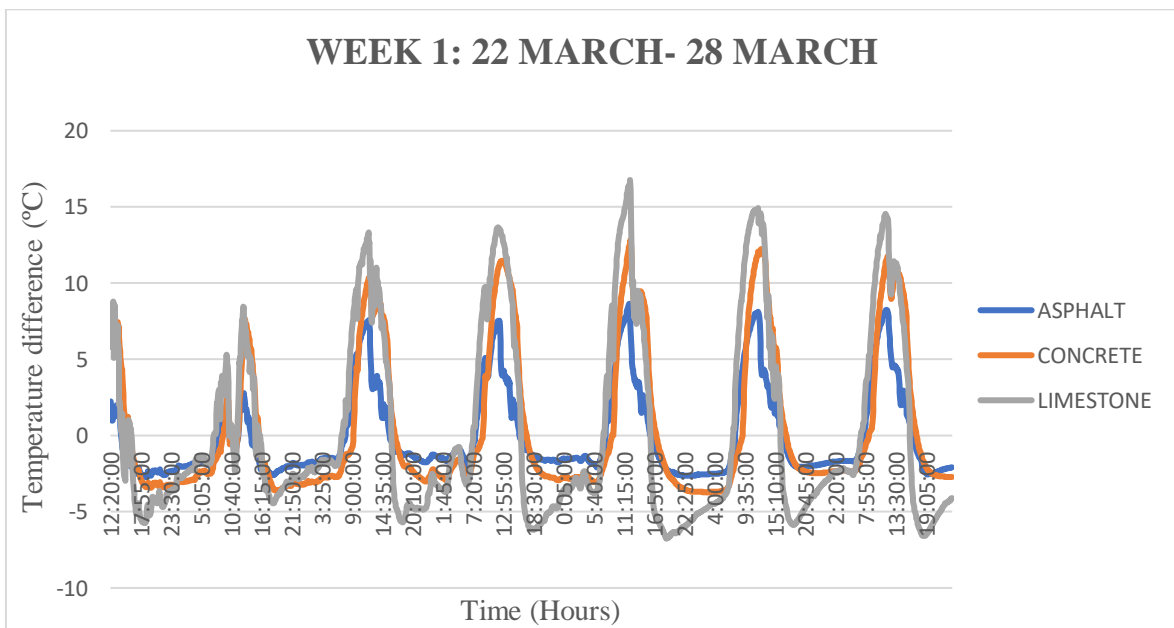
Figure 62. Temperature difference vs time representation of the 3 materials during week 1

During the first week of collecting data, it can be observed that in Figure 62 the first two days did not reach 10ºC of temperature difference due to the clouds, but this improved for the next two days when the conditions became partly cloudy, even though the air temperature remained similar to those in the cloudy days before. The peak during this week was reached by the limestone material with a ΔT of 17ºC followed by the concrete at 14ºC and the asphalt, which did not exceed 10ºC throughout the whole week. During the night, the ΔT becomes negative because the thermocouple of the surfaces got colder, while the ground would still be warm due to thermal inertia.

4.1.2 Week 2: 29 March- 4 April

Table 14 shows the maximum and minimum air temperature and weather conditions for different days.

Table 14. Week 2 maximum and minimum temperature and weather [44]

WEEK 2	29	30	31	1	2	3	4
Tmax (ºC)	19	20	21	20	19	25	18
Tmin (ºC)	12	10	11	11	12	14	14
Weather	Sunny	Partly cloudy	Partly cloudy	Sunny	Sunny	Partly cloudy	Rainy
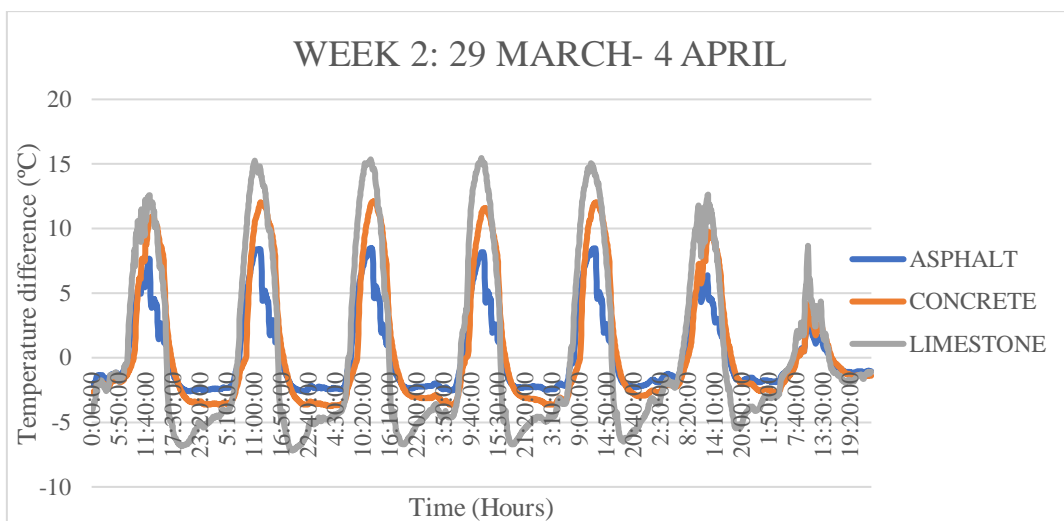
Figure 63. Temperature difference vs time representation of the 3 materials during week 2

During the second week, four days registered more than 15ºC of ΔT in limestone surface. The concrete was over 10ºC of ΔT for the whole week except for the las day because of the rain. The asphalt did not reach 10ºC of ΔT as yet. It is striking in Figure 63 that despite of having on April 4th a temperature of 18/14ºC, there was an enormous drop in the ΔT because of the rain.

4.1.3 Week 3: 5 April- 11 April

Table 15 shows the maximum and minimum air temperature and weather conditions for different days.

Table 15. Week 3 maximum and minimum temperature and weather [44]

WEEK 3	5	6	7	8	9	10	11
Tmax (ºC)	15	19	20	16	16	18	19
Tmin (ºC)	12	11	13	10	10	9	12
Weather	Rainy	Cloudy	Partly Cloudy	Cloudy	Partly Cloudy	Partly cloudy	Partly cloudy
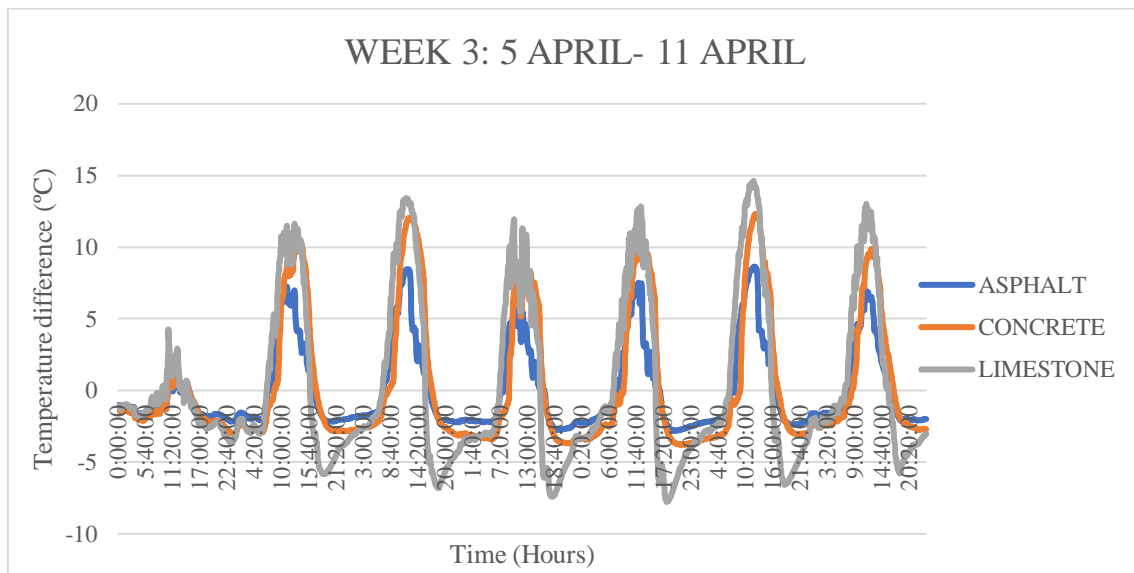
Figure 64. Temperature difference vs time representation of the 3 materials during week 3

As shown in Figure 64, no temperatures over 15ºC of ΔT were registered during the third week. Most of the week was cloudy so lower ΔT were obtained. Due to the rain on April 5 the ΔT did not reach 5ºC of ΔT in any of the surfaces. It should be noted that during the night the ΔT of the limestone decreases much more than the ΔT asphalt and concrete, given that limestone absorbs more water than asphalt or concrete and due to evaporation the temperature drops faster. The lowest ΔT during the night was of -7ºC while in the other two surfaces it was around 2/3ºC.

4.1.4 Week 4: 12 April- 18 April

Table 16 shows the maximum and minimum air temperature and weather conditions for different days.

Table 16. Week 4 maximum and minimum temperature and weather [44]

WEEK 4	12	13	14	15	16	17	18
Tmax (ºC)	15	19	20	16	16	18	19
Tmin (ºC)	12	11	13	10	10	9	12
Weather	Rainy	Windy	Sunny	Cloudy	Cloudy and Windy	Partly cloudy	Sunny
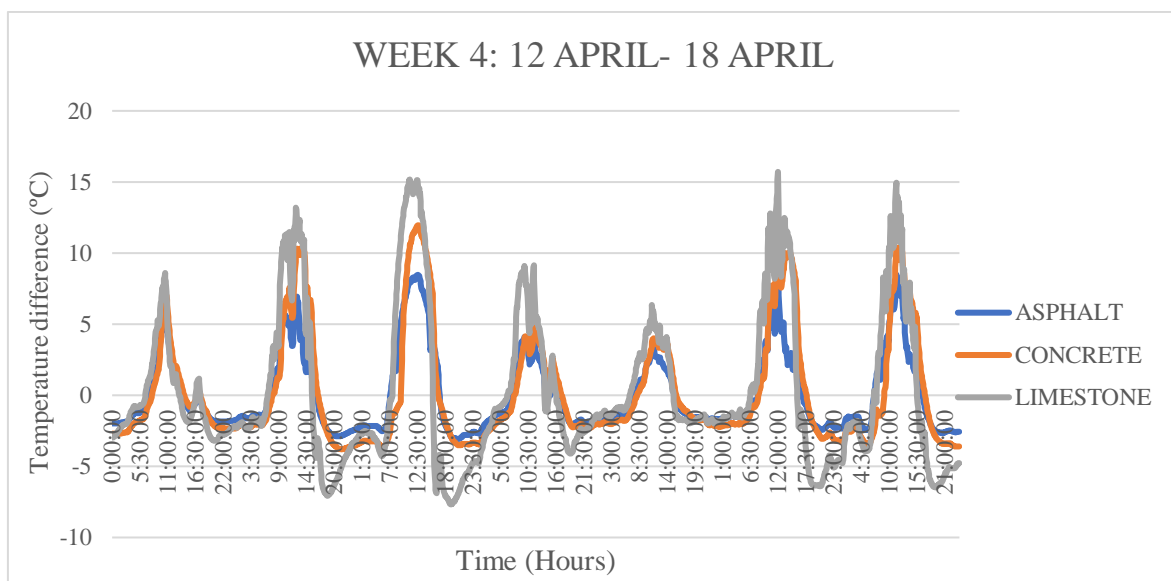
Figure 65. Temperature difference vs time representation of the 3 materials during week 4

In the fourth week, three of the seven days did not reach the 10ºC of ΔT due to the climate conditions (rain, wind, and clouds). On the other hand, in four days the limestone peak was 15ºC of ΔT as shown in Figure 65. The asphalt and concrete during these days reached between 5 and 12ºC of ΔT. It has to be noticed that these results effectively means that the time that potentially support energy generation from the TEGs is only during the day, between sunrise around 7-8 am and 3-4 pm.

4.1.5 Week 5: 19 April- 25 April

Table 17 shows the maximum and minimum air temperature and weather conditions for different days.

Table 17. Week 5 maximum and minimum temperature and weather [44]

WEEK 5	19	20	21	22	23	24	25
Tmax (ºC)	18	19	19	18	17	18	19
Tmin (ºC)	14	12	10	12	14	13	12
Weather	Cloudy	Sunny	Partly cloudy	Partly cloudy	Rainy	Sunny	Sunny
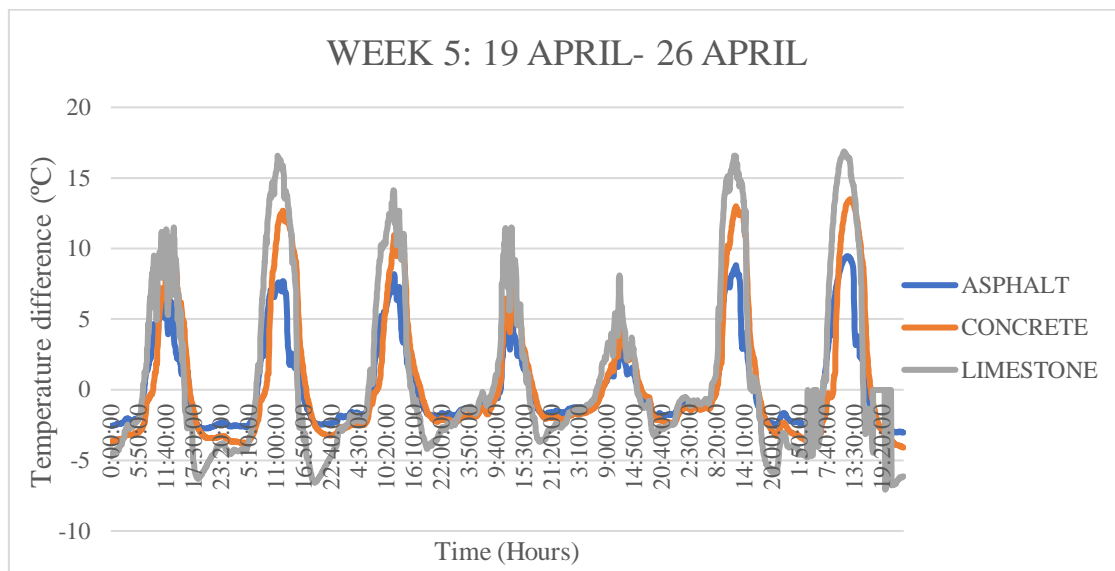
Figure 66. Temperature difference vs time representation of the 3 materials during week 5

In Figure 66, shows that the days with cloudy or rainy weather have an impact on a low ΔT while the days that were sunny and partly cloudy favoured a higher generation of ΔT between 10 and 15ºC for the three surfaces.

4.1.6 Week 6: 26 April- 2 May

Table 18 shows the maximum and minimum air temperature and weather conditions for different days.

Table 18. Week 6 maximum and minimum temperature and weather [44]

WEEK 6	26	27	28	29	30	1	2
Tmax (ºC)	17	19	20	21	18	21	20
Tmin (ºC)	12	11	12	16	15	14	11
Weather	Partly cloudy	Partly cloudy	Sunny	Partly cloudy	Partly cloudy	Cloudy	Partly cloudy
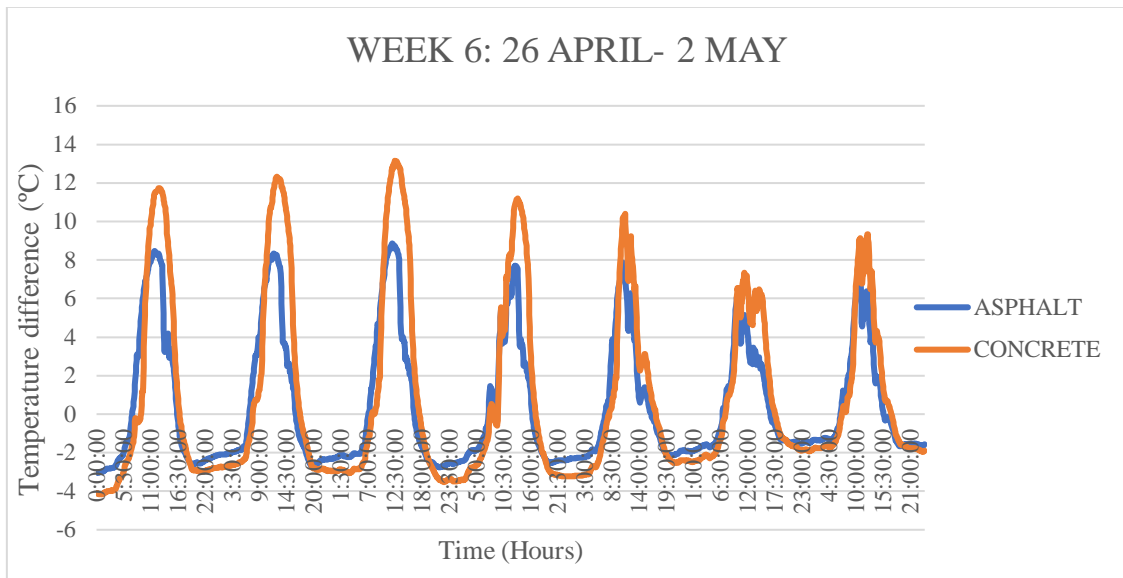
Figure 67. Temperature difference vs time representation of the 3 materials during week 6

As explained before, in Figure 67 the limestone ΔT does not appear because of the thermocouple connection problem on the surface. For the other two surfaces relatively high ΔT were obtained. The last three days of the week had a lower ΔT, as a consequence of the weather.

4.1.7 Week 7: 3 May- 9 May

Table 19 shows the maximum and minimum air temperature and weather conditions for different days.

Table 19. Week 7 maximum and minimum temperature and weather [44]

WEEK 7	3	4	5	6	7	8	9
Tmax (ºC)	20	23	26	25	24	24	27
Tmin (ºC)	12	15	15	15	16	17	18
Weather	Partly cloudy	Sunny	Rainy	Cloudy	Sunny	Sunny	Sunny
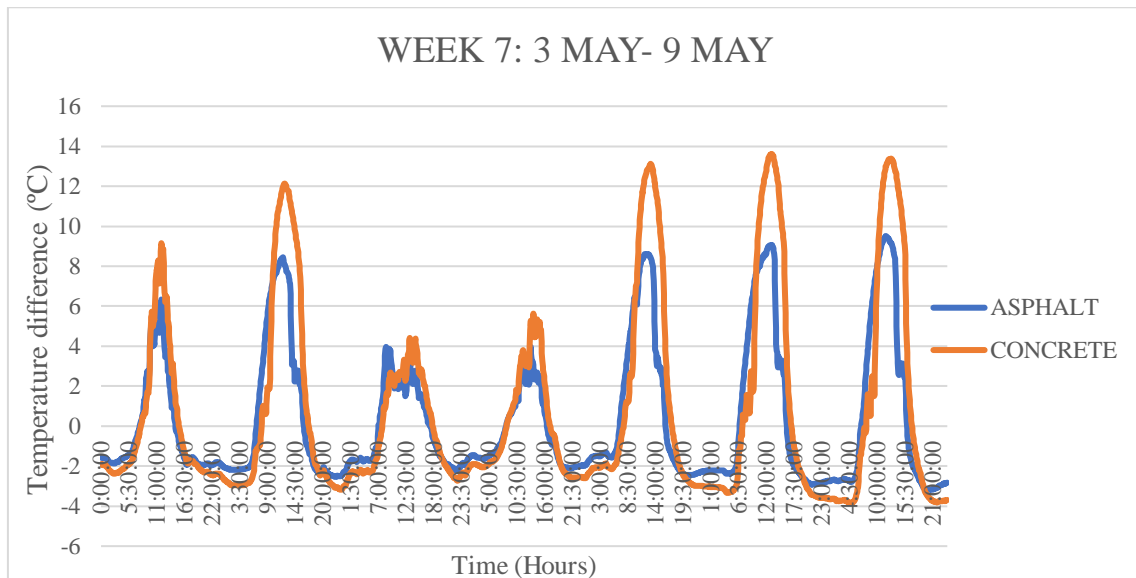
Figure 68. Temperature difference vs time representation of the 3 materials during week 7

During this week, the limestone ΔT is not shown. In Figure 68 draws attention that on May 5th despite being the hottest day of the week, the less ΔT was created. This was because of the rain of that day. The rest of the days perform normally reaching a ΔT of 14ºC and 9ºC for concrete and asphalt, respectively.

4.1.8 Week 8: 10 May- 16 May

Table 20 shows the maximum and minimum air temperature and weather conditions for different days.

Table 20. Week 8 maximum and minimum temperature and weather [44]

WEEK 8	10	11	12	13	14	15	16
Tmax (ºC)	23	23	22	22	26	26	24
Tmin (ºC)	16	15	16	16	16	16	14
Weather	Partly cloudy	Partly cloudy	Partly cloudy	Sunny	Sunny	Partly cloudy	Sunny
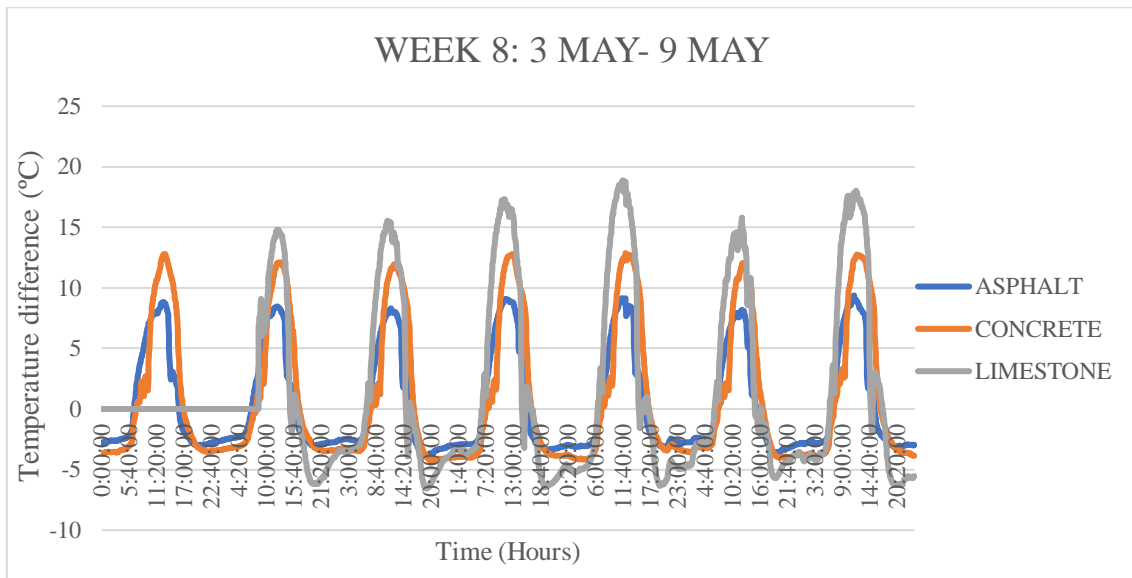
Figure 69. Temperature difference vs time representation of the 3 materials during week 8

During this week, as we can see in Table 20 the maximum temperatures were always over 20ºC as the seventh week. The limestone data since the second day is shown again as the problem was fixed. Due to the time of the year, mid-May temperatures started increasing (Figure 69). For example, the limestone was able to reach a ΔT of 15ºC every day.

4.1.9 Week 9: 17 May- 23 May

Table 21 shows the maximum and minimum air temperature and weather conditions for different days.

Table 21. Week 9 maximum and minimum temperature and weather [44]

WEEK 9	17	18	19	20	21	22	23
Tmax (ºC)	23	24	23	23	24	22	26
Tmin (ºC)	15	17	15	14	14	16	15
Weather	Sunny	Sunny	Sunny	Partly cloudy	Partly cloudy	Sunny	Sunny
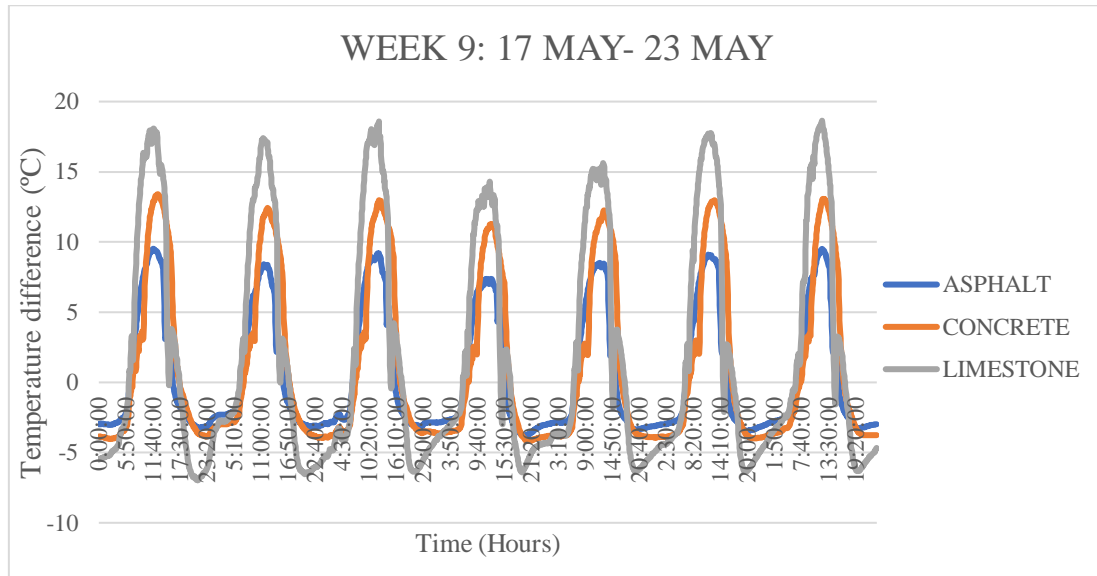
Figure 70. Temperature difference vs time representation of the 3 materials during week 9

In the last week, higher ΔT started being recorded. For limestone readings exceeding 15ºC became norm, also asphalt and concrete started to have higher temperatures. The weather during this whole week was mostly sunny with some clouds as shown in Table 21.

4.1.10 Week 10: 24 May- 30 May

Table 15 shows the maximum and minimum air temperature and weather conditions for different days.

Table 22. Week 10 maximum and minimum temperature and weather [44]

WEEK 10	24	25	26	27	28	29	30
Tmax (ºC)	25	28	27	28	27	26	29
Tmin (ºC)	17	16	18	18	19	18	17
Weather	Partly cloudy	Sunny	Sunny	Partly cloudy	Partly cloudy	Partly cloudy	Sunny
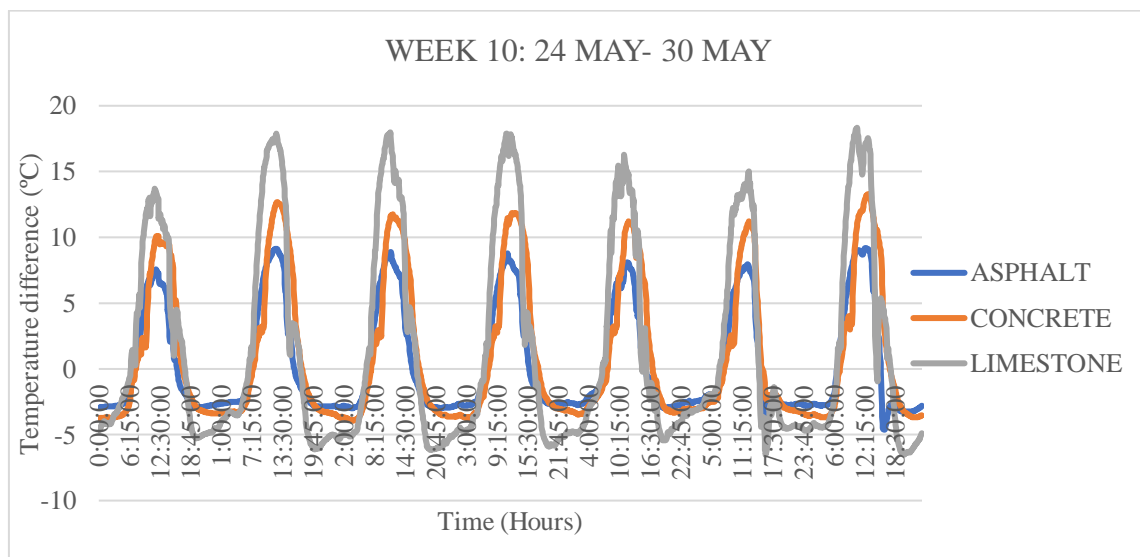
Figure 71. Temperature difference vs time representation of the 3 materials during week 10

The last week of May registered the highest temperatures by the time of writing. However, due to the clouds during this week the ΔT were not as high as expected. Even so, the limestone ΔT exceeded 15ºC for most of the week, the ΔT for concrete exceeded the 10ºC and the asphalt maintained its ΔT around the 8/9ºC during the week.

4.1.11 Analysis of the temperature data

This section analyses all the data obtained and compares the results with other similar experiments that have been carried out.

From the data obtained during these 10 weeks it can be seen that positive ΔT is generated for around 9 or 10 hours per day (the month of May was observed to have more hours than March and April as it is closer to summer). However, during these 9 or 10 hours per day the effective time is reduced further because a minimum threshold of ΔT above 5ºC is needed for the TEG to start generating a voltage. So, the real effective time that the modules had during most of the weeks was: in the asphalt around 3 or 4 hours (the shadow influenced this result), the concrete around 4 or 5 hours (also influenced by some shadows) and the limestone around 6 hours (which had no shadows).

The maximum and minimum air temperature of the day has influenced the ΔT but not as much as the direct solar incidence. It has been noticed that the clouds and rain have a huge impact on the generation of ΔT between the two surfaces of the TEG module. A 60% decrease in voltage generation happens when there is this kind of weather.

Asphalt, concrete and limestone have been the materials tested. Asphalt, as shown in Figures 62 to 71 is the one that created the lowest ΔT. This could be due to the fact that during the afternoon the nearby shadows affected the exposure of the asphalt to direct sunshine. Indeed, the same happened to concrete but in spite of this, its temperature was higher than asphalt so it can be concluded that this last material absorbs more heat than the asphalt. The third material tested was limestone, which had the best performance in creating a ΔT reaching a maximum of 18.37ºC on May 19th.

As mentioned in Chapter 2, in the city of Xi´an (2016) [12] a similar experiment was carried out in which the temperatures were tested in asphalt during two different days (August 23rd and December 27th). A thermocouple was placed 9 cm below the surface

(very similar to our experiment which was at 10 cm below the surface) and another thermocouple measuring the surface temperature. In August, the maximum ΔT was of 9ºC and in December the highest ΔT was of 5.7ºC. These results are very similar to ours in the asphalt material. However, if our temperature data collection would be in August in Malta more ΔT would be expected. Also, in Xi'an in August around 5 pm and in December around 4 pm the surface temperature started to be lower than the underneath one, and consequently, the ΔT was negative. This is the same situation that happened in our experiment. In the Xi'an experiment, the effective time when positive ΔT over 5ºC was created was of 5 hours in August and 2 hours in December.

4.2 TEG modules' experimental test

In this section, the results obtained in the laboratory will be compared with research studies that have been carried out in the past. However, many factors affect the power generation as it depends on the hot and cold side temperatures of the modules. In some experiments, the thermocouples for measuring the temperature were placed on the surface of the modules while in others, they were placed some millimeters or centimeters away from them. In our case, the thermocouple that measures the hot side was placed on top of the resistor that heated the module, and the other thermocouple was placed on the heat sink next to the cold side of the module as shown in Figure 72.
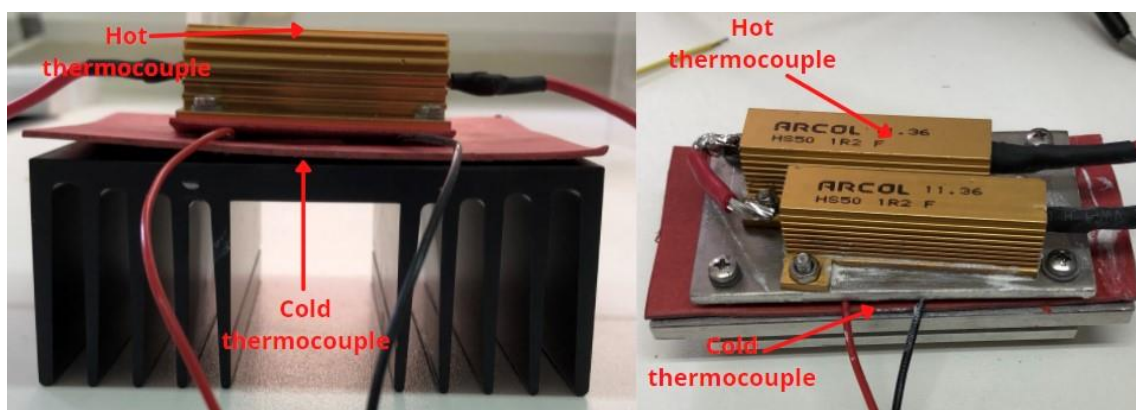
Figure 72. Illustration pointing out the thermocouples placement

4.2.1 Setup 1 tests (GM250-31-14-10 module)

The first set-up was utilized with the GM250-31-14-10 TEG module. In the first test, the module was operated under open circuit conditions to check the module's open circuit voltage generation. The results will be analysed and compared with the manufacturer´s specifications. For the rest of the tests, a variable resistor was applied to load the TEG modules, where the output voltage was measured.

4.2.1.1 Open circuit test

For this test, two runs were conducted to check the consistency in the module operation. Figure 73 shows the open circuit voltage generated plotted against the temperature gradient.
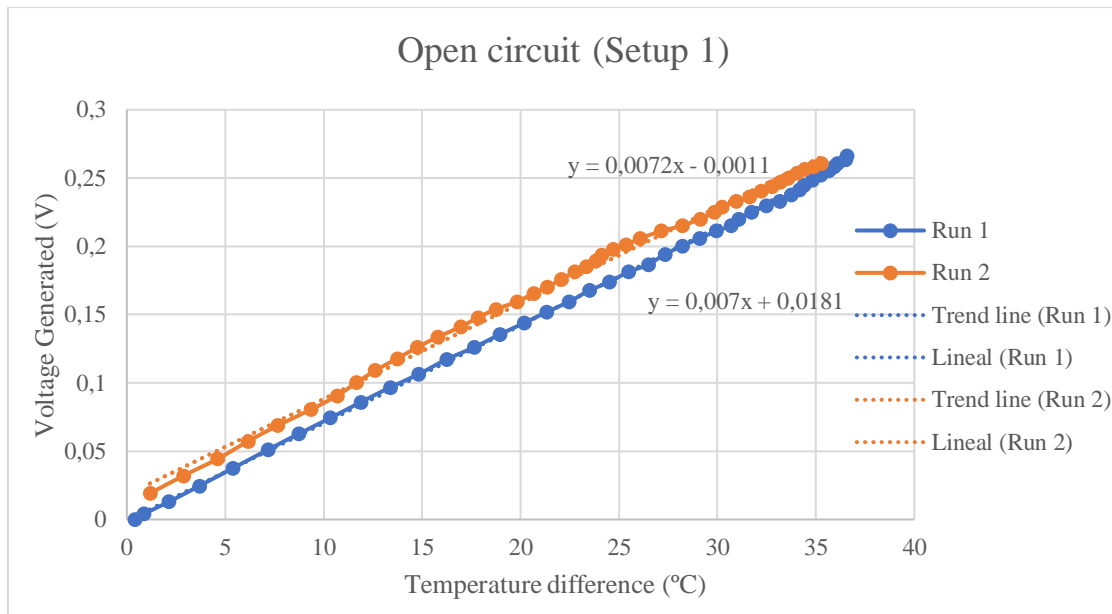
Figure 73. Voltage generated vs Temperature difference in open circuit voltage for setup 1.

As can be seen in Figure 73, the open circuit voltage varies linearly with the ΔT. The voltage generated (U) as a function of ΔT can be expressed by (6) and (7) for the run 1 and 2. It can be seen that the obtained ΔT coefficients are very close.

$$U_1 = 0.0072 \times \Delta T - 0.0011 \qquad (6)$$

$$U_2 = 0.007 \times \Delta T + 0.0181 \qquad (7)$$

Where U is the voltage generated (V); ΔT is the temperature difference (K);

The maximum ΔT reached was of 36.57 K and for that value the U was of 0.266V. For a ΔT of 30 K the manufacturer specifies a U of 0.23 V, and the U we obtained was of 0.21V. The result is very close. A possible explanation of the discrepancy could be from the temperature readings as the thermocouples are not measuring directly at the surface of the modules. Despite that, it can be concluded that the results obtained in the test were right [41].

4.2.1.2 Test under load

As mentioned before, different resistance values were applied to load the module. The blue, orange and grey colors-represent a resistance of 0.218 Ω, 0.248 Ω and 0.309 Ω respectively. The output voltage plotted against the ΔT is shown in Figure 74.
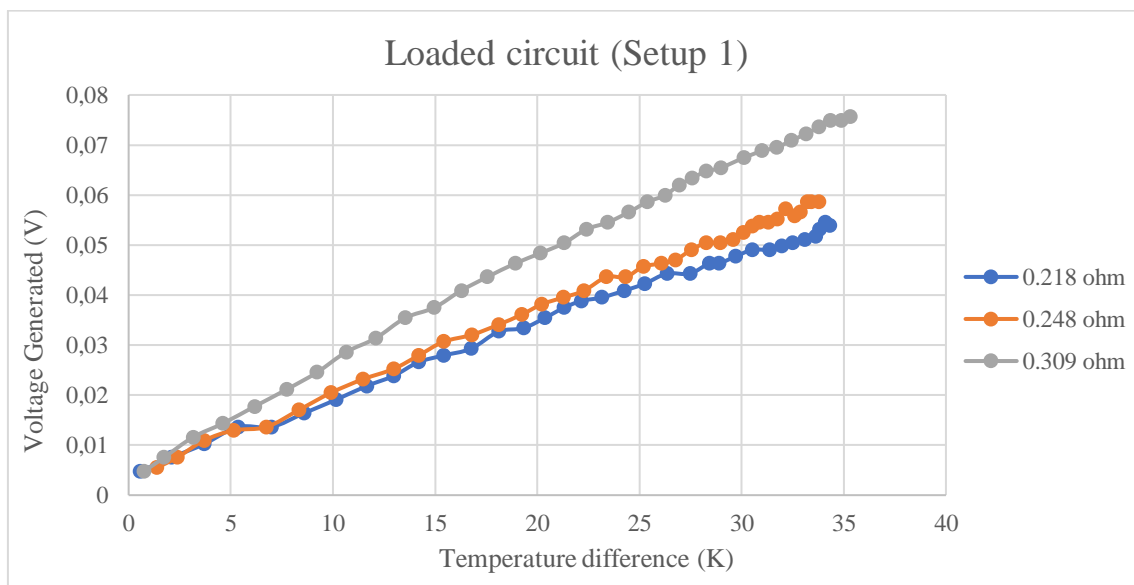
Figure 74. Output voltage vs Temperature difference in loaded circuit for setup 1

As expected, in Figure 74 the U is less than in the open circuit test. The highest voltage generated was of 0.075 V at a ΔT of ΔT 35 K when a 0.309 Ω resistance was being applied. For the 0.218 Ω and 0.248 Ω resistances the maximum U was of 0.055 V and 0.059 V, respectively. The best performance of the TEG module occurred when the 0.309Ω resistance was used. Comparing the results with the manufacturer's datasheet [41], reveals a discrepancy. The matched load voltage for a 30 K of ΔT is given at 0.13 V while in our case, the maximum U obtained was 0.067 V. This implies that the load resistance was different for the two cases. This can be attributed to the difficulty in setting the low resistance value precisely.

In a past experiment explained in Chapter 2, a single TEC1-12710 module was tested. For a ΔT of 35K the U varied between 0.25 V and 0.45 V when a resistance between 1 and 10 Ω was being applied. It has to be taken into account that our TEG module dimensions are 20x20x3 mm while the article´s dimensions are 40x40x3 mm, so the U expected was lower [15].

Figure 75 shows the power generated (P) vs the ΔT. The P was calculated through the set value of the load resistance using (8).

$$P = \frac{U^2}{R}$$ (8)

Where P is the power (W); R is the resistance applied (Ω); U is the output voltage (V);
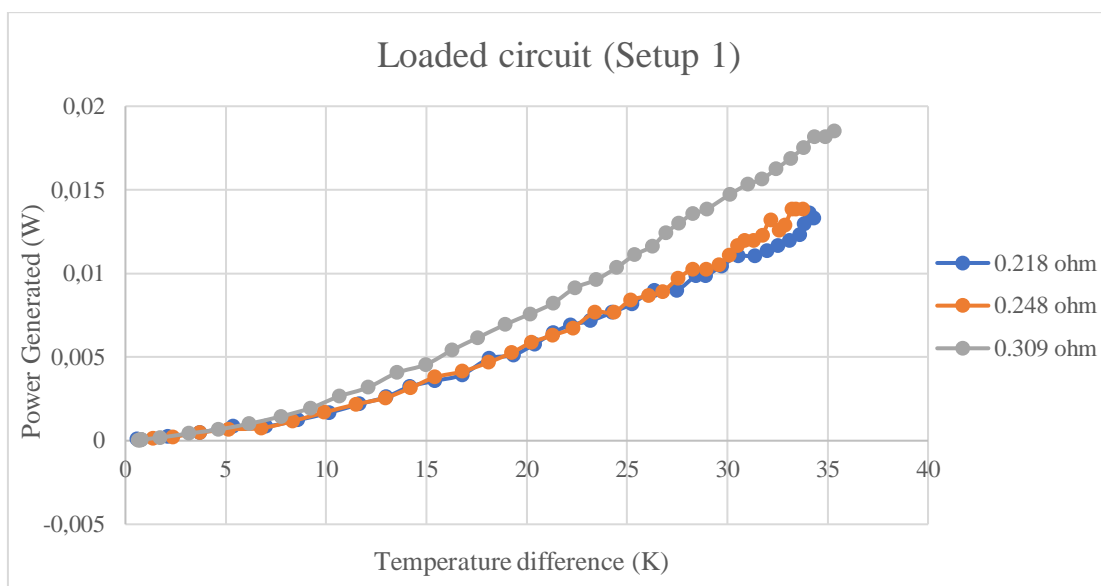
Figure 75. Power generated vs Temperature difference in loaded circuit for setup

Figure 75 shows a clearer distinction for the run with the resistance of 0.309 Ω. The module generated a power of 0.0181 W for a ΔT of 35 K. Operation with the other resistance values yielded similar power variation reaching around 0.0138 W for a ΔT of 33.76 K. The datasheet provided by the manufacturer specified a power output of 0.015 W for a ΔT of 30 K [41].

Comparing the results with the experiment mentioned before, the power generated was lower for the same reason as before. For a ΔT of 30 K the TEC1-12710 generated between 0.01 and 0.06 W [15].

Figure 76 shows the power generated plotted against the voltage output.
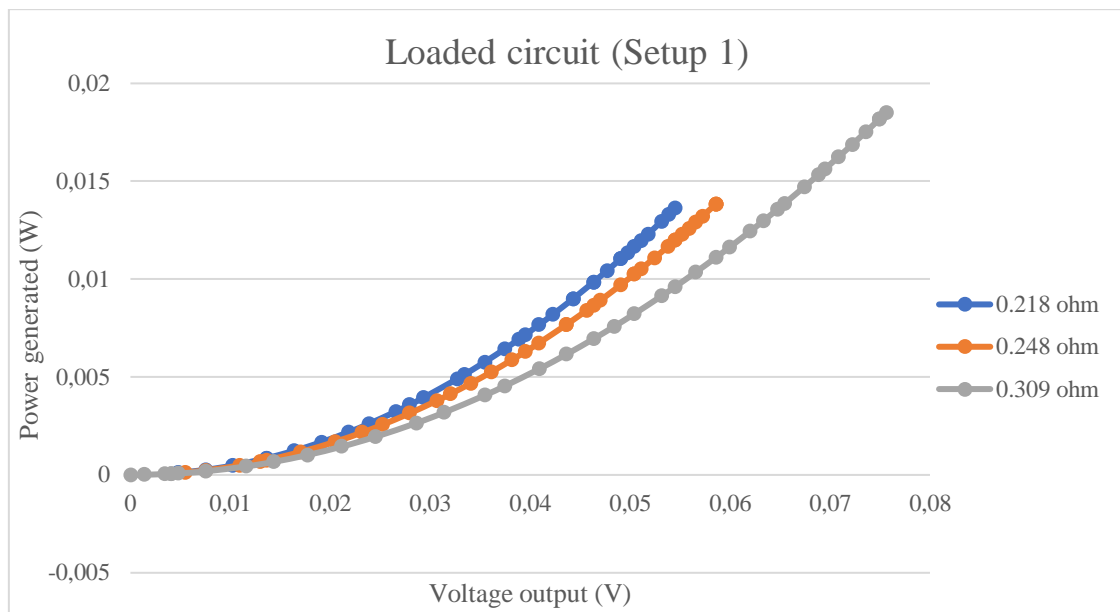
Figure 76. Power generated vs Voltage output in loaded circuit for setup 1.

The trend line in Figure 76 represents a potential function. The U peak is reached at a value of 0.0756 V with a P of 0.0185 W when a resistance of 0.309 Ω was applied.

4.2.2 Setup 2 tests (GM250-161-12-20 module)

The second set-up utilised the GM250-12-20 TEG module. Similar tests to those carried out in Setup 1 were carried out. Since this is a larger version of the same technology, higher voltage and power generation are expected.

4.2.1.1 Open circuit test

In this simulation, three runs were carried out. Figure 77 shows the open circuit voltage vs the temperature difference (ΔT).
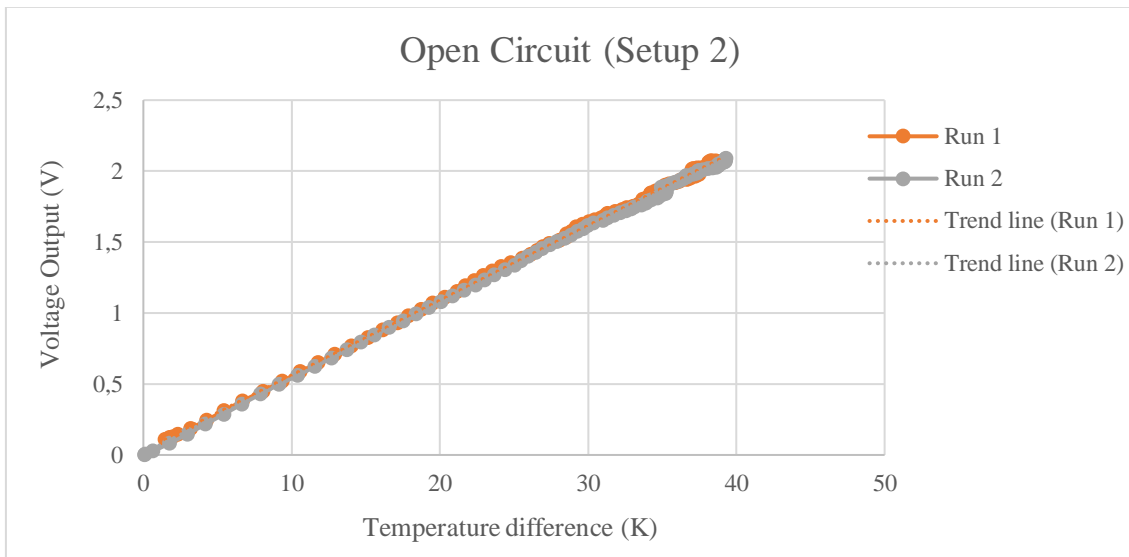
Figure 77. Voltage generated vs Temperature difference in open circuit voltage for setup 2.

It can be observed from Figure 77 that the two runs yielded very close values of open circuit voltage. This reached a maximum value of 2.06 V at a ΔT of 38.64 K. The following equations represent the two runs:

$$U_2 = 0.0527 \times \Delta T + 0.0334 \qquad (9)$$

$$U_3 = 0.0529 \times \Delta T + 0.0099 \qquad (10)$$

The voltage generated when the ΔT was 35 K was of 1.886 V. In the parameters given by the manufacturer the necessary ΔT to generate 2V is 35K, so the results were very similar [42]. The differences could be because the thermocouples installed for measuring the temperature were not in the surface of the modules.

4.2.2.2 Test under load

As mentioned in Chapter 3, different resistance values were applied load the 40x40 mm TEG module. In total 6 resistance setting with the following values were used: 5.975Ω, 6.278Ω, 6.505Ω, 6.789Ω, 7.015Ω and 7.210Ω. However, the plots will only present the three of values, which will be shown in a blue color the 5.795Ω resistance, in an orange color the 6.278 Ω and in yellow color the 6.789 Ω. T

In Figure 78 shows the voltage generated against the temperature difference of the second setup. The plots should be lineal equations as the should increase proportionally with the ΔT.
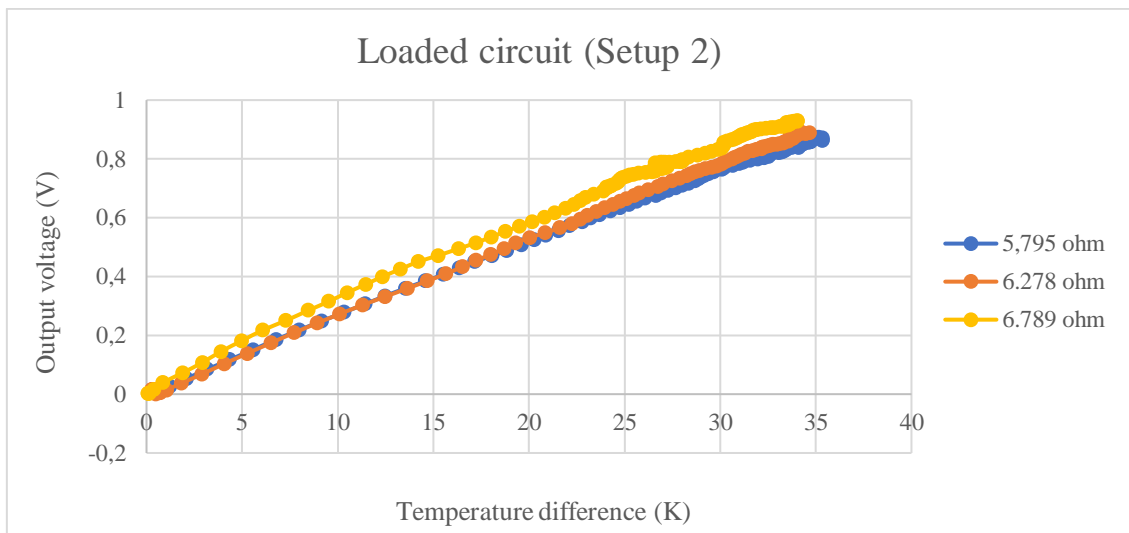
Figure 78. Voltage generated vs Temperature difference in loaded circuit for setup 2.

As for the case of setup 1, the maximum U obtained is less than in the open circuit test. The highest voltage generated was of 0.928 V for 34 K of ΔT when the 6.789 Ω resistance was being applied. A similar voltage of 0.875 V was reached with a resistance of 5.795 Ω resistance but with a higher ΔT of 35 K.

Comparing a past experiment result where a module with same dimensions but different parameters was used, the results obtained were much better than expected. For a 30K of ΔT the maximum value they were able to obtain was of 0.45V while our module was generating more than the double, 0.928 V [15].

The manufacturer's datasheet specified a voltage output of 0.85 V for a ΔT of 30 K. In our case, the highest value for 30 K of ΔT was 0.863 V. So effectively the results agree.

Figure 79 shows the generated power against the temperature difference as calculated from the equation (8). For the test, a ΔT of 35 K was reached as shown in Figure 79. At that temperature, the highest value was very similar for the three resistances with a value was of 0.125 V.
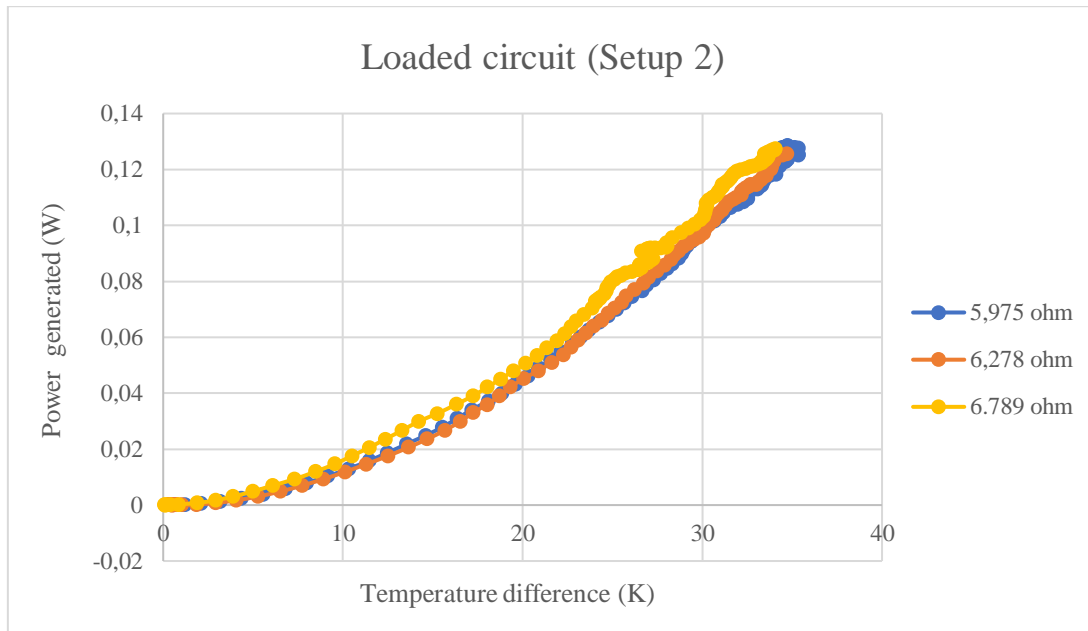
Figure 79. Power generated vs Temperature difference in loaded circuit for setup 2.

In the datasheet, 0.1 W were expected to be obtained with a ΔT of 30 K, which is the same value we obtained [42].

Figure 80 shows the power generated against the output voltage of the three resistances.
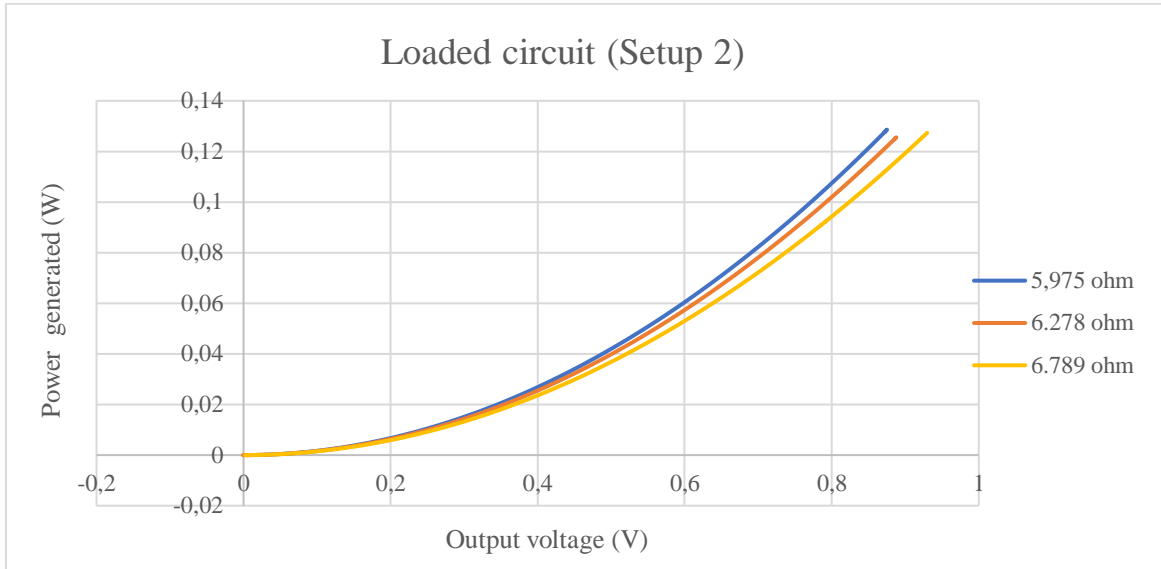
Figure 80. Power generated vs Temperature difference in loaded circuit for setup 2.

In the plots it can be observed that for the same power generation, the 6.789 Ω resistance needs the highest output voltage. For example, for generate 0.12 W the 6.789 Ω needs a U of 0.9 V while the 5.795 Ω needs 0.84 V.

4.3 ADEH-P-A board testing

As mentioned in Chapter 3, a board was used with the GM250-31-14-10 TEG modules to test the output voltage obtained. As the material used was a TEG harvester, the device was connected to the first channel of the board. The output voltage configurations set were the jumper nº2 connected as a VAUX and the jumper nº3 in the GND. All the possible configurations are shown in Table 7 in the methodology. The output voltage expected was of 3.3 V. Figure 81 shows the output voltage and the temperature of the hot side of the module against the time.
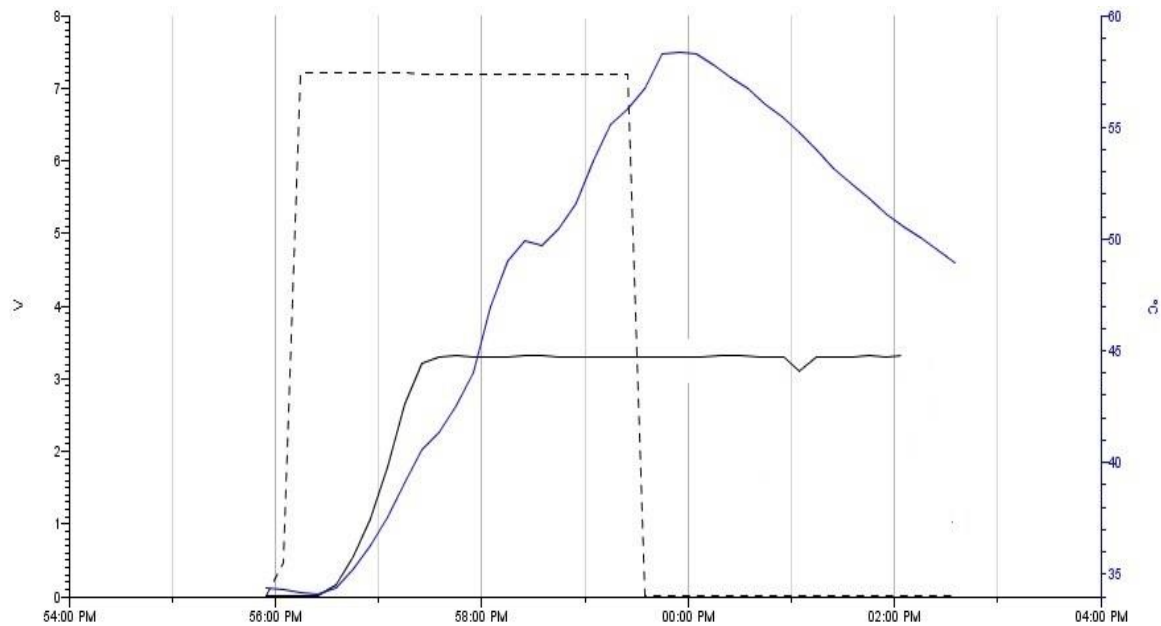
Figure 81. Voltage output and hot side temperature against time with ADH board

As shown in Figure 81, the temperature difference is not indicated. For this case is supposed that the cold side of the module remains constant at 22 ºC (the ambient temperature of the room) to anaylse behavior. It can be observed that the U increased gradually with the temperature difference until reaching the 3.3 V. At that time the board had sufficient charge to maintain the output voltage at the set value. The temperature difference kept increasing while the output voltage remained constant at 3.3V.

Afterwards, a small LED was powered by the GM250-31-14-10 TEG module. It was connected in the Vout pin of the channel one board. The module was able to light up the LED once a temperature difference of 23ºC was reached. Figure 82 shows the energy harvesting board ADEH-P-A and the red LED lighted up.

80
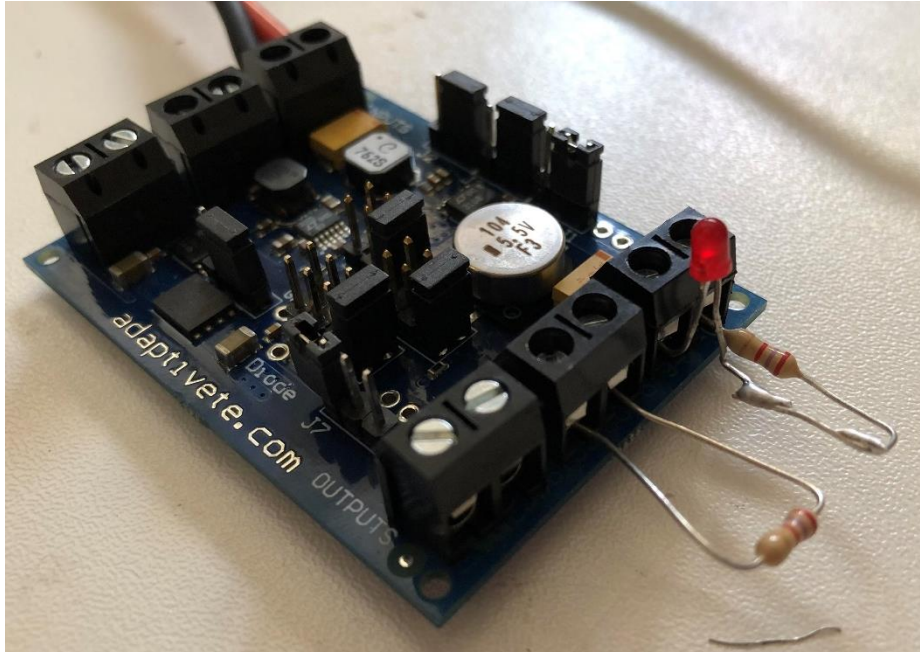
Figure 82. ADEH-P-A board and LED lighted up

4.4 Application to power booths

The power generated with these modules, can potentially be used to power street screens and small warning sign without the need of a grid connection. Figure 82 represents a prototype of a smart pole that could be installed in the streets for different applications. The screen could be used to provide information to pedestrians about public buses information or information for active travelers (such as pedestrians and cyclists) to identify routes that they can be used to encourage in engaging in sustainable mobility. Also, the power generated could be used to supply electricity to lights or security cameras, which provide a sense of safety and security to different mode users.

Figure 83. Smart pole prototype [45]

The typical estimated power demand for a LCD screen of 17' is about 35 W and of an sleeping monitor (when is not turned on) between 0-15 W [46]. In order to save energy, a motion sensor could be installed to turn on the screen only when a pedestrian is nearby. The demand of this device is around 0.5 W [47]. Based on the results obtained in the lab tests supposing a 10ºC of temperature difference between both sides, the power generated per TEG would be 0.018W. If the mean of the screen demand (supposing that it is decreased with the aid of the motion sensor) is about 15W, the number of necessary TEG modules needed would be around 833. As the number of modules to be installed is very high, part of the energy demand of smart poles could be also supplied by a photovoltaic panel on the top of the prototype.

In the case of a LED light with a power between 75 and 100 lumens per watt the demand is around 5-9 W [48]. Supposing the same situation as before, 277 TEG modules should

be installed. For an IP security camera, the energy demand of this device is between 4 and 7 W [49]. 222 modules should be installed to supply the energy demand.

Apart from these devices, smaller screens with E-Ink technology incorporated could be used. This technology decrease significantly the screens power demand compared with the LCD [50].

All of these hypothetic situations are estimated from the data obtained from the experiments. Sometimes the power generated will be more than what it has been estimated and sometimes the opposite.

CHAPTER 5. CONCLUSIONS

The purpose of this dissertation was to evaluate the potential of power generation from a TEG module. The research started at first with a review of past similar experiments in order to know the materials used in the prototypes, the different ways of cooling the cold side of the module and finally the voltage and power expected as a function of the temperature difference. Furthermore, temperature characteristics of three different surface materials were investigated to know the real conditions the TEG were going to be exposed to.

The temperature gradient between the surface and 10 cm underneath of the three materials was gathered by a data logger. The village of Marsaxlokk, in Malta proved to have the necessary conditions to generate a significant temperature gradient. Nevertheless, the results demonstrated that the effective time when a significant temperature difference was created, was only for 4-5 hours a day under our conditions (depending on the place, the material tested and the period of the year).

As mentioned in Chapter 4, the asphalt and concrete materials results were influenced by a shadow during the day. Still, the average of the temperature gradient for the asphalt was between 5ºC and 9 ºC during most of the days. The concrete, which had a greater temperature gradient than the asphalt, stayed between the 10ºC and 14ºC. The limestone had the best performance of the three materials. During the three months when the tests were carried out the material always exceeded the 10ºC of temperature difference. In May, it was normal for the limestone to exceed the 15ºC of temperature gradient. The highest ΔT registered by the thermocouples installed in the Institute for Sustainable Energy was of 18.37 ºC. The tests were carried out during the season of spring, so higher results would be expected during the summer.

During the tests it was also noticed that the characteristic that influenced the most in obtaining a high ΔT was not the ambient temperature but the daily weather. The rain or very cloudy weather significantly decreases ΔT.

In the laboratory, two different setups were prepared to test the TEG modules. Each of them contained a heat sink to dissipate the heat provided by the HS resistor. The biggest challenge during the simulations was to maintain the temperature difference as high as possible. The laboratory modules were tested until a ΔT of 35 ºC was reached between

both sides of the module. However, such value of temperature gradient was not obtained from the materials tested.

In the case of asphalt, with a mean of 5-9 ºC of ΔT the voltage generated would be between 0.0185-0.31 V and the power generated of 0.0049-0.014 W if the 6.789 Ω resistance is applied.

The concrete, which normally performed between the 10-14ºC of ΔT the voltage generated would be 0.335-0.45 V and the power generated of 0.0176-0.0298 W if the 6.789 Ω resistance would be applied.

In the limestone the highest results would be obtained. Its normal ΔT has been between 12-16ºC. At those conditions, the voltage generated would be 0.388-0.49 V and the power generated of 0.0228-0.035 W if the 6.789 Ω resistance would be applied.

As discussed in Chapter 4, using the TEG technology to supply an entire smart pole is not feasible because of the number of modules that have to be installed. However, they can be use as an aid to PV panels for supplying booths that are powered by renewable energy.

To sum up, this is still a technology (TRL 3) that needs further research. All the energy wasted from the sun on pavements should be used in one way or another and TEGs are a great solution to this problem. However, it has still a very low energy conversion efficiency. Even so, many companies are starting to compete between each other investigating this technology. Coupled with other technologies such as PV pavements it can be beneficial to use for outlets with low power requirements, such as, displays with information that can be used in nudging to nudge people for sustainable mobility as presented in this dissertation.

5.1 Further studies and recommendations

This dissertation has shown the performance of a single TEG. It would be interesting to create a setup with some modules and embed them on the surface of a pavement. Then, study the real voltage and power that can be generated due to overheating by the sun.

Also, the use of different TEGs rated at a lower temperature are recommended as the ones we used were rated at 250ºC and that temperature will never be reached by the asphalt.

On the other hand, it would be interesting to keep recording the temperature data for the three pavements for at least one year to get to know the ΔT that can be generated during the months, especially for summer.

REFERENCES

[1] "La energía en el 2040 - Energía para el Futuro." https://blogs.iadb.org/energia/es/la-energia-en-el-2040/ (accessed May 24, 2021).

[2] "EIA projects 28% increase in world energy use by 2040 - Today in Energy - U.S. Energy Information Administration (EIA)." https://www.eia.gov/todayinenergy/detail.php?id=32912 (accessed May 24, 2021).

[3] "Malta's first solar pavement to be installed in Rabat - TVM News." https://www.tvm.com.mt/en/news/maltas-first-solar-pavement-to-be-installed-in-rabat/ (accessed Jun. 04, 2021).

[4] "Cuáles son las fuentes de energía más utilizadas en el mundo." https://www.ecologiaverde.com/cuales-son-las-fuentes-de-energia-mas-utilizadas-en-el-mundo-1426.html (accessed May 17, 2021).

[5] "Climate change consequences | Climate Action." https://ec.europa.eu/clima/change/consequences_en (accessed May 17, 2021).

[6] "Global annual mean temperature difference from preindustrial conditions... | Download Scientific Diagram." https://www.researchgate.net/figure/Global-annual-mean-temperature-difference-from-preindustrial-conditions-1850-1900-The_fig1_340135130 (accessed May 08, 2021).

[7] "Malta's 2030 National Energy and Climate Plan," 2019.

[8] "Strategies, Policies & Actions National Transport Strategy and Transport Master Plan - Transport Malta." https://www.transport.gov.mt/strategies/strategies-policies-actions/national-transport-strategy-and-transport-master-plan-1343 (accessed May 30, 2021).

[9] "Two-thirds of land built up since 1990 was outside development zones." https://timesofmalta.com/articles/view/two-thirds-of-land-built-up-since-1990-was-outside-development-zones.680851 (accessed May 19, 2021).

[10] M. Attard, "Mobility justice in urban transport-the case of Malta," *Transp. Res. Procedia*, vol. 45, no. 2019, pp. 352–359, 2020, doi: 10.1016/j.trpro.2020.03.026.

[11] "File: Malta Luftbild.jpg - Wikipedia." https://de.wikipedia.org/wiki/Datei:Malta_Luftbild.jpg#globalusage (accessed May 19, 2021).

[12] R. This, C. C. Attribution-noncommercial-noderivs, C. C. By-nc-nd, T. If, and W. Rose, "This is a repository copy of Energy harvesting from asphalt pavement using thermoelectric White Rose Research Online URL for this paper : Version : Accepted Version Article : Jiang , W , Yuan , D , Xu , S et al . (4 more authors) (2017) Energy harvest," 2017.

[13] "Introducción a la Termoelectricidad." http://www.unavarra.es/ets02/Introduccion a TE(c).htm (accessed May 18, 2021).

[14] "a) The representation of seebeck effect. (b) The representation of... | Download Scientific Diagram." https://www.researchgate.net/figure/a-The-representation-of-seebeck-effect-b-The-representation-of-peltier-effect_fig1_325813385 (accessed May 19, 2021).

[15] S. Ouitrakul, "Preliminary Experiment for Electricity Generation using Peltier Modules," pp. 26–30, 2014.

[16] "Diy thermoelectric generator | Thermoelectric generator, Renewable energy projects, Alternative energy." https://www.pinterest.es/pin/510032726530977142/?autologin=true (accessed May 19, 2021).

[17] "Thermoelectric materials - Wikipedia." https://en.wikipedia.org/wiki/Thermoelectric_materials (accessed May 19, 2021).

[18] "Thermoelectric figure of merit (ZT) versus temperature in bulk... | Download Scientific Diagram." https://www.researchgate.net/figure/Thermoelectric-figure-of-merit-ZT-versus-temperature-in-bulk-thermoelectric-materials_fig8_275546016 (accessed May 19, 2021).

[19] H. S. Kim, W. Liu, and Z. Ren, "Efficiency and output power of thermoelectric module by taking into account corrected Joule and Thomson heat," *J. Appl. Phys.*, vol. 118, no. 11, 2015, doi: 10.1063/1.4930869.

[20] H. Zhao, J. Yu, and J. Ling, "Finite element analysis of Cymbal piezoelectric

transducers for harvesting energy from asphalt pavement," *J. Ceram. Soc. Japan*, vol. 118, no. 1382, pp. 909–915, 2010, doi: 10.2109/jcersj2.118.909.

[21]   N. G. Elvin and A. A. Elvin, "An experimentally validated electromagnetic energy harvester," *J. Sound Vib.*, vol. 330, no. 10, pp. 2314–2324, 2011, doi: 10.1016/j.jsv.2010.11.024.

[22]   B. C. Kok, S. Gareh, H. H. Goh, and C. Uttraphan, "Electromechanical-Traffic Model of Compression-Based Piezoelectric Energy Harvesting," *MATEC Web Conf.*, vol. 70, 2016, doi: 10.1051/matecconf/20167010007.

[23]   F. Duarte and A. Ferreira, "Energy harvesting on road pavements: State of the art," *Proc. Inst. Civ. Eng. Energy*, vol. 169, no. 2, pp. 79–90, 2016, doi: 10.1680/jener.15.00005.

[24]   "World Weather Information Service." https://worldweather.wmo.int/en/city.html?cityId=42 (accessed May 28, 2021).

[25]   "Detailed map of Annual Average Temperature around the World : MapPorn." https://www.reddit.com/r/MapPorn/comments/9sc1a8/detailed_map_of_annual_a verage_temperature_around/ (accessed May 19, 2021).

[26]   . P. G., "Generating Electricity From Pavement," *Int. J. Res. Eng. Technol.*, vol. 05, no. 26, pp. 36–41, 2016, doi: 10.15623/ijret.2016.0526008.

[27]   S. A. Tahami, M. Gholikhani, and S. Dessouky, "Thermoelectric Energy Harvesting System for Roadway Sustainability," *Transp. Res. Rec.*, vol. 2674, no. 2, pp. 135–145, 2020, doi: 10.1177/0361198120905575.

[28]   B. C. Blanke, J. H. Birden, K. C. Jordan, and E. L. Murphy, "Nuclear battery-thetmocouple type summary report," *United States At. Energy Comm.*, 1962.

[29]   "Por qué Philae no lleva un generador de radioisótopos - Eureka." https://danielmarin.naukas.com/2014/12/04/por-que-philae-no-lleva-un-generador-de-radioisotopos/ (accessed May 21, 2021).

[30]   D. Champier, "Thermoelectric generators: A review of applications," *Energy Convers. Manag.*, vol. 140, pp. 167–181, 2017, doi: 10.1016/j.enconman.2017.02.070.

[31] "Generador termoeléctrico de radioisótopos." https://www.etsist.upm.es/estaticos/ingeniatic/index.php/tecnologias/item/466-generador-termoeléctrico-de-radioisótopos.html (accessed May 21, 2021).

[32] "Electric Car Statistics and Facts 2021 | Policy Advice." https://policyadvice.net/insurance/insights/electric-car-statistics/ (accessed Jun. 04, 2021).

[33] C. W. Maranville, "Thermoelectric opportunities in light-duty vehicles," *Glob. Powertrain Congr. 2009, GPC 2009 Troy - Proc.*, vol. 54, pp. 91–107, 2009.

[34] "Contaminación por la Industria Naval | Oceana Europe." https://europe.oceana.org/es/contaminacion-por-la-industria-naval-0 (accessed May 22, 2021).

[35] N. R. Kristiansen, G. J. Snyder, H. K. Nielsen, and L. Rosendahl, "Waste heat recovery from a marine waste incinerator using a thermoelectric generator," *J. Electron. Mater.*, vol. 41, no. 6, pp. 1024–1029, 2012, doi: 10.1007/s11664-012-2009-6.

[36] E. Bollati, "Generadores termoeléctricos, Generación de energía sin partes móviles," *Petrotecnica*, pp. 84–90, 2007.

[37] "CR1000X: Measurement and Control Datalogger." https://www.campbellsci.eu/cr1000x (accessed May 25, 2021).

[38] T. Blocks, "Energy Harvesting Kit Energy Harvesting Kit," vol. 44, no. 0, pp. 2–3, 2017.

[39] M. Thermoelectric and G. Module, "MGM250-97-10-16 Mini Thermoelectric Generator Module MGM250-97-10-16 Mini Thermoelectric Generator Module," vol. 44, no. 0, pp. 3–5, 2017.

[40] L. Power, W. Transceivers, and E. H. Sensors, "Pinout Block Diagram Applications Electrical Characteristics (25 ° C)," pp. 1–5, 2016.

[41] T. G. Module, "GM250-127-28-10 Thermoelectric Generator Module GM250-127-28-10 Thermoelectric Generator generator Module," vol. 44, no. 0, pp. 1–3, 2017.

[42] European Thermodynamics Limited, "Thermo Electric Generation Module GM250-49-45-25," vol. 44, no. 0, pp. 1–6.

[43] Arcol, "HS Aluminium Housed Resistors," pp. 11–12, 1872.

[44] "Tiempo mensual en La Valeta, Valletta, Malta | AccuWeather." https://www.accuweather.com/es/mt/valletta/233779/may-weather/233779?year=2021 (accessed May 31, 2021).

[45] "Hefei Ming energy-saving Technology Co., Ltd. - PRODUCT - Smart Pole." http://www.fitbright.com/en/info.asp?base_id=3&second_id=3006 (accessed Jun. 07, 2021).

[46] "Power Management Statistics: Information Technology - Northwestern University." https://www.it.northwestern.edu/hardware/eco/stats.html (accessed Jun. 07, 2021).

[47] "Ahorra energía con los sensores de movimiento | Endesa." https://www.endesa.com/es/blog/blog-de-endesa/otros/Ahorro-sensores-movimiento (accessed Jun. 07, 2021).

[48] "kW vs. kWh: How much energy is my lighting using? [Calculator]." https://insights.regencylighting.com/kw-vs-kwh-how-much-energy-is-my-lighting-using (accessed Jun. 07, 2021).

[49] "PoE para videovigilancia – key Business Process Solutions." https://www.keybps.com/poe-para-videovigilancia (accessed Jun. 07, 2021).

[50] "E-Ink: What Is It and How Does It Work?" https://www.lifewire.com/what-is-e-ink-2740879 (accessed Jun. 07, 2021).